DI Robert Tratnig

RELIABILITY OF NEW FIBRILLATION DETECTION ALGORITHMS FOR AUTOMATED EXTERNAL DEFIBRILLATORS (AEDs)

Dissertation

zur Erlangung des akademischen Grades
Doktor der Technischen Wissenschaften
eingereicht an der
Fakultät für Technische Mathematik und Technische Physik

Technische Universität Graz

Betreuer:
Prof. (FH) DI Dr. Univ.- Doz. Karl Unterkofler
Institut für Theoretische Physik - Computational Physics
Technische Universität Graz

2. Begutachter:
Ao. Univ.- Prof. DI Dr. Ferdinand Schürrer
Institut für Theoretische Physik - Computational Physics
Technische Universität Graz

Dornbirn, am 17. Jänner 2005

E-mail: rtratnig@sbox.tugraz.at

Abstract

A central component in automated external defibrillators (AEDs) is the detection of ventricular fibrillation (VF) in the electrocardiogram (ECG) by means of appropriate detection algorithms. In the scientific literature there exists a wide variety of methods and ideas for handling this task. This methods should have a high detection quality and also be able to work properly in the presence of different disturbances, like electric noise, artifacts of motion, cardiopulmonary reanimation (CPR) artifacts, interspersion of electrical fields. Furthermore, the algorithm should be easily implementable in any kind of computer language, and should work in real time in an AED.

To test the quality of an algorithm for ECG analysis, it is essential to do this with a large amount of annotated data under equal conditions. For our investigation we used the complete BIH-MIT and CU data banks, and the files 7001 - 8210 of the AHA data bank ([16], [17], [2]). No preselection of certain ECG episodes was made since this equals the situation of a bystander more accurately.

In this work different fibrillation detection algorithms are evaluated. Some are taken from the scientific literature, some are new. They are based on different mathematical methods: Fourier transform, autocorrelation, wavelet transform, Hilbert transform, etc. We calculate the sensitivity and specificity and compare the different algorithms by their IROC value. Furthermore, we investigate the positive predictivity and accuracy. Surprisingly, very simple algorithms show very good results compared to quite involved techniques. The best three algorithms are new.

Key words: fibrillation detection, automated external defibrillator (AED), ventricular fibrillation (VT), cardiopulmonary reanimation (CPR), sinus rhythm (SR), ECG analysis.

Verlässlichkeit von Flimmererkennungsalgorithmen für automatisierte externe Defibrillatoren(AEDs)

Zusammenfassung

Eine wesentliche Aufgabe von automatisierten externen Defibrillatoren (AEDs) ist die Erkennung von ventrikulärem Flimmern (VF) aus dem Elektrokardiogramm (EKG) des Patienten mittels geeigneter Erkennungsalgorithmen. In der Fachliteratur existiert ein breites Spektrum von Methoden und Ideen, um diese Aufgabe durchführen zu können. Diese Methoden sollen eine hohe Erkennungsqualität aufweisen und selbst dann richtig arbeiten, wenn dem Signal, das durch die elektrische Aktivität des Herzens entsteht, unterschiedliche Störungen überlagert sind, wie z.B. elektrisches Rauschen, Bewegungsartefakte, Artefakte durch kardiopulmonare Reanimation (CPR, mechanische Wiederbelebung), Einstreuung elektrischer Felder. Weiters sollen die Algorithmen gut implementierbar sein und in AEDs in Echtzeit arbeiten.

Um die Qualität eines Algorithmus für die EKG-Analyse zu untersuchen, ist es wesentlich, dies mit einer grossen annotierten Datenmenge unter gleichen Bedingungen zu tun. In dieser Arbeit wurden die gesamte BIH-MIT und CU Datenbank, sowie die Dateien 7001 - 8210 der AHA Datenbank ([16], [17], [2]) verwendet. Um die Situation eines Laien möglichst realitätsnah zu simulieren, wurde keine Vorselektion der EKG - Episoden vorgenommen.

Einige der untersuchten Flimmererkennungsalgorithmen stammen aus der Fachliteratur, andere sind neu. Sie basieren auf verschiedensten mathematischen Methoden: Fourieranalyse, Autokorrelation, Wavelettransformation, Hilberttransformation, etc. Es werden für alle Algorithmen die Sensitivität und die Spezifität berechnet und die IROC Werte (integrated receiver operator characteristic) verglichen. Auch die positive Vorhersagbarkeit sowie die Genauigkeit werden berechnet. Überraschenderweise liefern gerade sehr einfach zu programmierende Algorithmen die besten Ergebnisse. Die drei mit Abstand besten Algorithmen wurden von uns neu entwickelt.

Schlüsselwörter: Flimmererkennung, automatisierter externer Defibrillator(AED), ventrikuläres Flimmern (VF), kardiopulmonare Reanimation (CPR), Sinusrhythmus (SR), EKG-Analyse.

Contents

Introduction

In Austria every year approximately 15 000 people die from sudden cardiac arrest. Of this number 40% to 50% exhibit ventricular fibrillation, and approximately one third could survive with a timely employment of a defibrillator. Beside the manual defibrillation by an emergency physician in recent years, bystander defibrillation with semi-automated external defibrillators (AEDs) has been recommended for resuscitation. These devices analyze the electrocardiogram (ECG) of the patient and recognize whether a shock should be delivered or not, like in the case of ventricular fibrillation (VF). The survival rate with sudden cardiac arrest in Austria is at present below 10%. In Las Vegas, in the context of a study, the survival rate has increased with AEDs by 57%. The bystander defibrillation is already firmly established in the first aid training in the USA. It is of vital importance that the ECG analysis algorithms used by AEDs possibly differentiate well between VF and a stable but fast sinus rhythm. For example, an AED should not deliver a shock, if the patient has collapsed not due to cardiac arrest, on the other hand a successfully defibrillated patient should not due to an analysis error be defibrillated again, which would possibly bring him back into cardiac arrest. Commercial AEDs use different, partly published, partly company-owned analysis algorithms. Despite or because of these different analysis algorithms, ECG classification errors are frequently reported in use.

In this thesis, 10 different algorithms well known from the literature as well as 5 new algorithms for the recognition of VF were implemented in MATLAB under a user-friendly interface. These were evaluated on the basis of annotated ECG databases, whereby our algorithms produced the best three results. As a single quality parameter we used the integrated receiver operator characteristic (IROC).

In Chapter 1 some general problems in the task of arrhythmia detection are described, that occur in practice. International recommendations for AEDs are presented. Rhythms to be defibrillated versus such which should not are discussed. The problem of external influences on ECG analysis is mentioned and the important quality parameters for a quantification of fibrillation detection algorithms are introduced. Furthermore, the process taking place in all investigated algorithms, is shown. Also different types of ECGs and methods to analyze them are described.

Chapter 2 describes some already well known algorithms from the scientific

literature. The used techniques are shortly described for each investigated algorithm. Some of the techniques are illustrated more detailed in Chapter 3. Chapter 4 deals with existing QRS detectors, which are originally destined to search for and find QRS complexes rather than VF. We use them as VF detectors. Chapter 5 deals with some new approaches and describes the ideas and justifications. Chapter 6 shows the results of our evaluations in tables. The quality of the algorithms used both as VF detectors and QRS detectors are presented. Chapter 7 represents the results in plots and Chapter 8 discusses the results and further ideas for future work. The Appendix A presents some MATLAB code for our filter preprocessing.

Chapter 1

General Problems of Arrhythmia Detection

Electrocardiograms (ECGs) provide a record of the heart's electrical activity. This simple test records any abnormal findings in the heart's electrical impulses. Electrodes are placed on the arms and chest to monitor electrical activity, which is recorded on graph paper or displayed on a screen. Information can be obtained during rest or exercise.

An AED should be able to detect life-threatening ECG rhythms like ventricular fibrillation and deliver user instructions to carry out a defibrillation in an easy to understand way. In an ideal case it should also perform a fibrillation scoring. This means an evaluation of the probability of the success for a defibrillation, and an evaluation of the CPR with a feedback to the emergency physician. Furthermore, the ideal time of a defibrillation should be determined.

The defibrillation should be optimal in a way that it is specific to the patient, should have the proper energy and give an exponential biphasic defibrillation pulse [22].

Many of the mentioned wishes are not fulfilled in common defibrillators.

1.1 Medical facts

An AED should be able to detect life-threatening ECG rhythms and deliver user instructions. In 1999, the American Heart association [2] published a number of recommendations for AEDs as Public Access Devices (PAD)[11].

(1) Rhythms to be defibrillated: rough ventricular fibrillation (> 0.2mV), fast ventricular tachycardia (no specification of threshold frequency)

(2) Intermediate rhythms: fine ventricular fibrillation (small amplitude and low frequency), other ventricular tachycardia

(3) Rhythms not to be defibrillated: normal sinus rhythm, supraventricular tachycardia, sinus bradycardia, premature ventricular contractions, atrial fibrillation/flutter, AV block (II, III degree), asystoles,...

The most important rhythm to be detected is ventricular fibrillation.

Ventricular fibrillation (VF) is a very fast, chaotic electrical heart activity in the lower chambers of the heart, resulting from multiple areas of the ventricles attempting to control the heart's rhythm. Ventricular fibrillation can occur spontaneously (generally caused by heart disease) or when ventricular tachycardia has persisted too long. When the ventricles fibrillate, they do not contract normally, so they cannot pump blood effectively. The instant VF begins, effective blood pumping stops. VF quickly becomes more erratic, resulting in sudden cardiac arrest. This arrhythmia must be corrected immediately via a shock from an external defibrillator or an implantable cardioverter defibrillator (ICD). The defibrillator stops the chaotic electrical activity and restores normal heart rhythm.

1.2 External influences on AEDs

An AED has to make its decision on the basis of an ECG, obtained by only 2 electrodes with variable positioning and quality of the electrode contacts. The electrode contacts are positioned at the chest of the patient. There is only the ECG as a basis of the decision, no information about pulse or respiration is fed into the device. Therefore, the majority of influences and disturbances on an AED and its algorithm is of electrical nature.

(1) Artifacts: CPR, transport, respiration, motion of AED user, etc.

(2) Electric disturbances: Electrical fields (interspersion of mains frequency, electric fields from railway power systems), radio communication, noise, implanted pace makers, etc.

A possible result of external influences can be a false ECG interpretation. Therefore, the algorithm should be able to filter artifacts. If the ECG data have been changed by artifacts, e.g., various strong electrical noises or artifacts caused by cardiopulmonary reanimation (CPR), it is interesting to find out how well the algorithms still work. In real applications of defibrillators these kinds of artifacts occur frequently, but they should not affect the results of the analysis. The aim of good fibrillation detection algorithms is the possibility of performing an analysis during CPR with suppression of artifacts of motion. By the use of such algorithms the reanimation could be applied up to a few seconds in advance of the defibrillation. Moreover, the analysis of the ECG to test for the necessity of defibrillation could be carried out without interrupting the manual reanimation.

1.3 Quality parameters

In this test we analyzed 15 different fibrillation detection algorithms. The results are expressed in the quality parameters *Sensitivity*, *Specificity*, *Positive Predictivity*, *Accuracy* and the *Integrated Receiver Operator Characteristic*. Furthermore, we investigated the *calculation time* of the different algorithms.

Sensitivity is the ability (probability) to detect ventricular fibrillation. It is given by the quotient

$$\frac{\text{detected cases of VF}}{\text{all cases of VF}} = \frac{TP}{TP+FN}, \tag{1.1}$$

with TP being the number of true positive decisions, and FN is the number of false negative decisions.

Specificity is the probability to identify "no VF" correctly.

It is given by the quotient

$$\frac{\text{detected cases of "no VF"}}{\text{all cases of "no VF"}} = \frac{TN}{TN+FP}, \tag{1.2}$$

where TN is the number of true negative decisions, and FP is the number of false positive decisions.

This means that if a defibrillator has a sensitivity of 90 % and a specificity of 99 %, it is able 90 % of the time to detect a rhythm that should be defibrillated, and 99 % of the time to recommend not shocking when defibrillation is not indicated.

Furthermore, we calculated the *Positive Predictivity* and the *Accuracy* of the investigated algorithms.

Positive predictivity is defined by

$$\frac{\text{detected cases of "VF"}}{\text{all cases classified by the algorithm as "VF"}} = \frac{TP}{TP+FP}. \tag{1.3}$$

Positive predictivity is the probability, that classified VF is really VF:

Accuracy is defined by

$$\frac{\text{all true decisions of "VF" and "no VF"}}{\text{all decisions}} = \frac{TP+TN}{TP+FP+TN+FN}. \tag{1.4}$$

Accuracy is the probability to obtain a correct decision.

Also the calculation time, compared to the time of the real data, was calculated for the different algorithms. The values in per cent of the real data time can be seen in the tables. They were obtained by analyzing the CU data bank only.

The quality parameters are obtained by comparing the decisions suggested by the algorithm with the annotated decisions suggested by cardiologists. The cardiologists' decisions are considered as true. We distinguish only between ventricular fibrillation and no ventricular fibrillation, since the annotations in the used data banks do not include a differentiation between ventricular fibrillation and ventricular tachycardia. The closer the quality parameters are to 1, the better the algorithm works.

To represent the quality of an algorithm by its sensitivity and specificity bears some problems. A special algorithm can have a high sensitivity, but a not so high specificity, whereas another algorithm can have a high specificity, but a

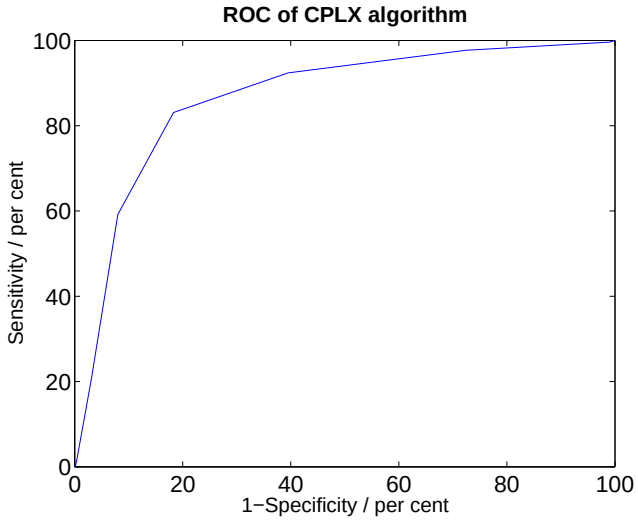

Figure 1.1: *ROC curve for the algorithm CPLX described in Section 2.5, for a window length of* 8 *s. The parameter, which is varied to obtain the curve, is* C*. The calculated value for the area under the curve, IROC, is 0.867.*

not so high sensitivity. Which one is better? To come to a common and single quality parameter, the receiver operator characteristic (ROC) can be investigated. The sensitivity is plotted in dependence of (1-specificity), where different points in the plot are obtained by varying the critical threshold parameter in the decision stage of the algorithm. By calculating the area under the ROC curve (we call the obtained value "integrated receiver operator characteristic", and denote it by IROC), it is possible to compare different algorithms by one single quality value. Figure 1.1 shows an example for a ROC curve.

To gain insight into the quality of algorithms for ECG analysis, it is essential to test the algorithms under equal conditions with a large amount of data, which are already commented by qualified cardiologists. We used the complete BIH-MIT and CU data banks, and the files 7001 - 8210 of the AHA data bank ([16], [17], [2]). No preselection of certain ECG episodes was made since this equals the situation of a bystander more accurately.

The parameters generally used to describe the reliability of fibrillation detection algorithms are their sensitivity and specificity. These values should be 1 in the ideal case and should not differ much in an AED application. Since the annotation of ECG data may not always be completely correct, experienced cardiologists should inspect the discrepancies between the results of the analysis and the annotations of the data in order to ascertain whether the results of the algorithm are perhaps also justified.

1.4 Process used in all implemented algorithms

In this thesis, we use the same procedure when testing different algorithms. This is important to make the different methods comparable.

(1) The process in the algorithm **reads** the data according to the specified window length and signal time. In an AED application, the window length has to be specified as well.

(2) A **signal modification** is carried out to simulate real applications. This includes an optional adding of artificial CPR, noise and external mains electricity fields.

(3) A **preprocessing** is carried out. This includes a filtering process described in Appendix A and a CPR filter, that can optionally be applied to the detection process.

(4) The **analysis** is performed. This is the main part of each algorithm and characterizes its behavior. Each algorithm uses another method.

(5) A **storage or output** of the results, i.e., the results are saved into a file and/or displayed on the screen.

This process is displayed in the following block diagram:

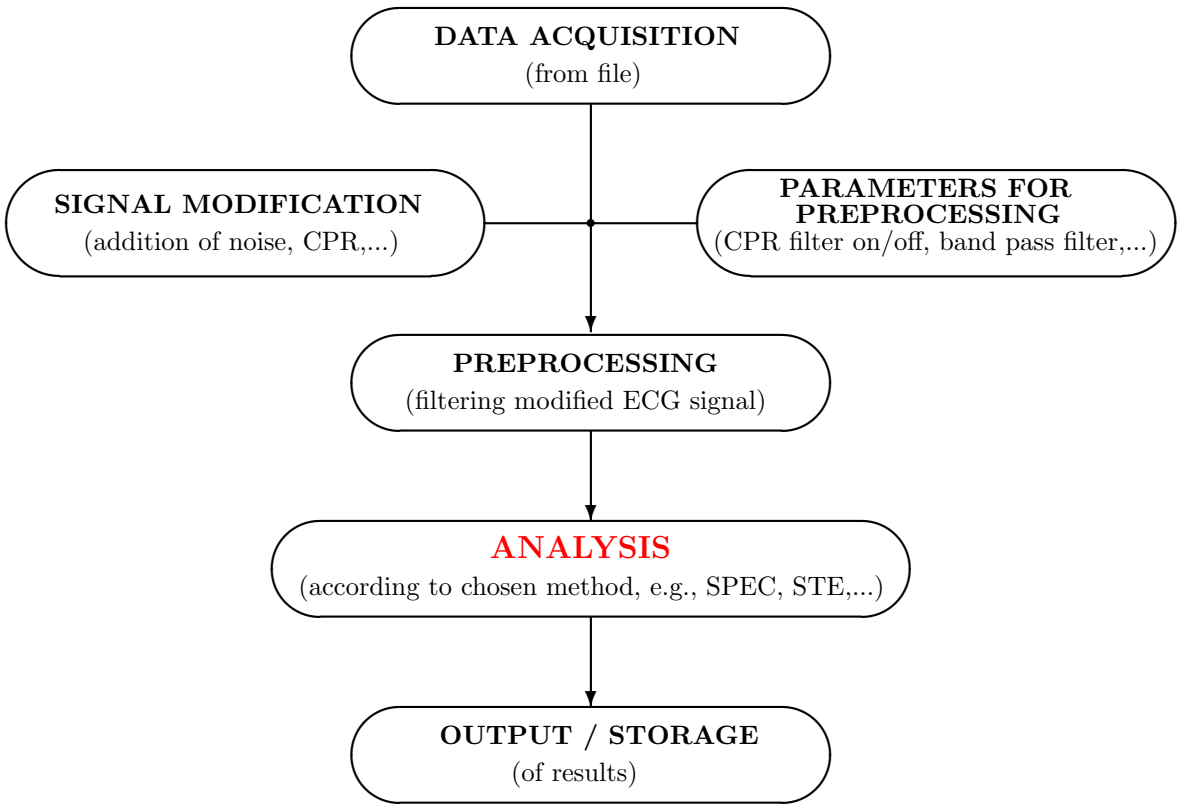

All algorithms are implemented in MATLAB.

1.5 Characteristic types of ECGs

Principally, an AED has to make a decision whether an ECG episode is shockable or not. According to Section 1.1, certain ECG episodes should be considered as not shockable. A healthy heart shows a typical ECG form, called sinus rhythm. It basically consists of P-, Q-, R-, S-, and T- waves ([7], page 18). A small bunch of heart cells called the sinoatrial node controls the rhythm. The typical average fundamental frequency of a healthy heart lies in the region of 60 - 80 beats per minute. The signal is called sinus rhythm (SR). It shows regularly occurring spikes called QRS-complexes.

Below, Figure 1.2 shows a healthy heart with sinus rhythm. The ECG episode from $t = 148\,s$ until $t = 156\,s$ in the file cu01 from the CU database [17] contains parts with sinus rhythm:

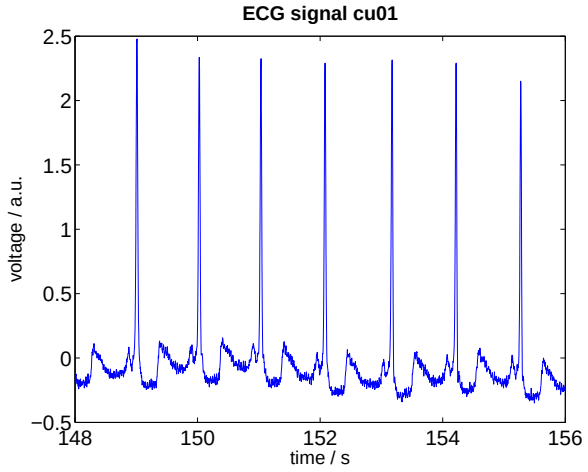

Figure 1.2: *Sinus rhythm in file cu01 from the CU database [17].*

A completely irregular electric activity of the heart is called ventricular fibrillation (VF). The heart is not able to pump blood through the arteries any more, the body (particularly the brain) cannot be supplied with oxygen. This is a life-threatening situation and has to be treated immediately. A heart suffering ventricular fibrillation shows an irregular cosine like structure. The fundamental frequency is much higher than in the case of sinus rhythm. In the case of ventricular fibrillation it has values higher than 200 beats per minute.

VF is often immediately observed whenever a person collapses suddenly. Usually, there is no pulse or heartbeat detected on initial examination.

A heart suffering ventricular fibrillation shows a typical ECG form like in Figure 1.3. The ECG episode is taken from the CU data bank (cu21, from $t = 0\,s$ until $t = 8\,s$)

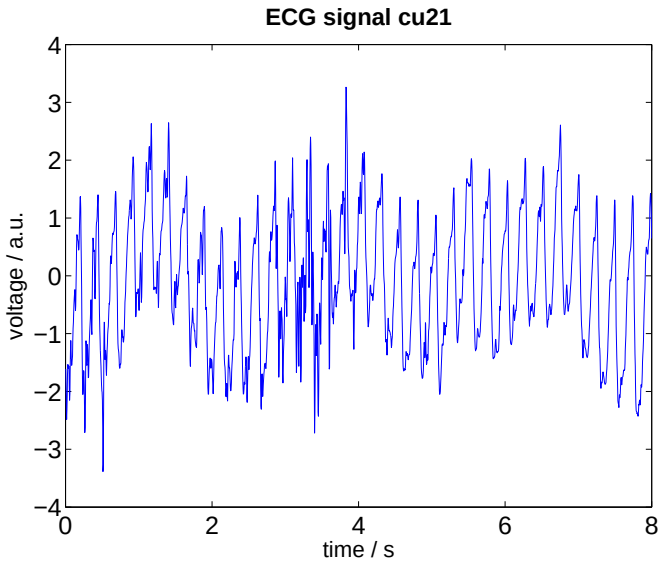

Figure 1.3: *Ventricular fibrillation in file cu21 from the CU database [17].*

1.6 Techniques for the analysis

The fibrillation detection algorithms should recognize certain features of a signal. To this aim, the signal can be changed by any kind of transformation into another signal, which allows to find the searched features more easily. The transformation can use different methods known from signal processing and applied mathematics. We can divide the possible methods for fibrillation detection analysis into two principally different kinds:

Time domain analysis: The signal is treated with the help of suitably set thresholds [21], by means of autocorrelation functions [4], by a complexity measure [23], or by signal comparison. No transformation of the signal into the frequency domain has to be carried out. This can save computational time.

Frequency domain analysis: The signal is transformed into the frequency domain by means of Fourier transform. Spectral filters and thresholds are applied to the signal, e.g., in [3], [12]. The advantage is, that in the frequency domain high frequency noise can be removed easily from well known ECG frequencies. Also, frequency dependent features of SR or VF can be treated easily. The continuous Fourier transform is carried out as follows:

(1) **periodic signals, time period T:**

$$\hat{f}_k = \frac{1}{T}\int_0^T f(x)\exp(-\frac{2\pi ikx}{T})dx, \qquad k \in \mathbb{Z}, \tag{1.5}$$

$$f(x) = \sum_{k=-\infty}^{\infty} \hat{f}_k \exp(+\frac{2\pi ikx}{T}), \tag{1.6}$$

$$T = \frac{1}{\nu}, \tag{1.7}$$

ν being the fundamental frequency of the period T. Here, the Fourier transform yields a discrete spectrum.

(2) **non-periodic signals:**

$$\hat{f}(k) = \frac{1}{\sqrt{2\pi}}\int_{-\infty}^{\infty} f(x)\exp(-ikx)dx, \tag{1.8}$$

$$f(x) = \frac{1}{\sqrt{2\pi}}\int_{-\infty}^{\infty} \hat{f}(k)\exp(+ikx)dk. \tag{1.9}$$

In this case the Fourier transform yields a continuous spectrum. In signal processing applications, like ECG analysis, the discrete Fourier transform of a signal x of length N is carried out:

$$\hat{f}_k = \frac{1}{N}\sum_{j=1}^{N} x_j \exp(-\frac{2\pi i(j-1)(k-1)}{N}), \qquad 1 \le k \le N, \tag{1.10}$$

$$x_j = \sum_{k=1}^{N} \hat{f}_k \exp(+\frac{2\pi i(j-1)(k-1)}{N}), \tag{1.11}$$

where $\hat{f}_1$ gives the mean value of the signal x and corresponds to the frequency 0.

Combined methods: An example for a combined method are wavelet based algorithms, since they can be considered as to work both in the time and frequency domain. Combinations of more methods are possible. The computation effort is usually higher than in the techniques mentioned above.

Chapter 2

Existing Methods for VF Detection

The fibrillation detection algorithms considered here are partly taken from the scientific literature, some of them are not published so far. The algorithms are fed with the ECG signal and deliver a decision, whether the rhythm should be defibrillated or not.

2.1 TCI algorithm

The threshold crossing intervals algorithm (TCI) [21] operates in the time domain. Decisions are based on the number and position of signal crossings through a certain threshold.

A binary signal is generated from the preprocessed ECG data according to the position of the signal above or below a given threshold. The threshold value is set to 20% of the maximum value within each one second segment S and recalculated every second. Subsequent data analysis takes place over successive one second stages. The ECG signal may cross the detection threshold one or more times, and the number of pulses is counted. For each stage, the threshold crossing interval TCI, this is the average interval between threshold crossings, is calculated as follows

$$TCI = \frac{1000}{(N-1) + \frac{t_2}{t_1+t_2} + \frac{t_3}{t_3+t_4}} \ [ms]. \tag{2.1}$$

Figure 2.1 illustrates the situation.

Here, N is the number of pulses in S. t_1 is the time interval from the beginning of S back to the falling edge of the preceding pulse. t_2 is the time interval from the beginning of S to the start of the next pulse. t_3 is the interval between the end of the last pulse and the end of S and t_4 is the time from the end of S to the start of the next pulse.

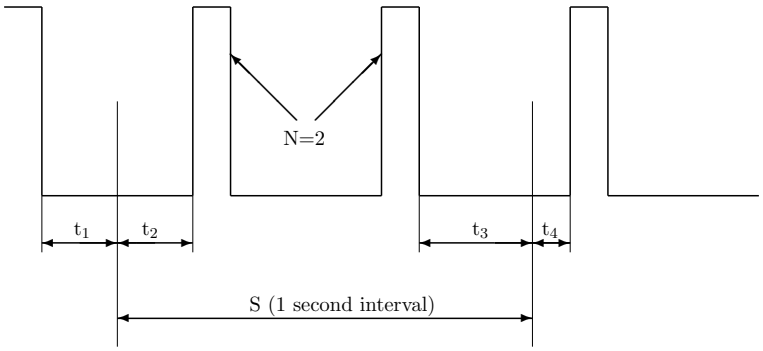

Figure 2.1: *Signal analysis in TCI algorithm.*

If $TCI \geq TCI_0 = 400ms$, sinus rhythm (SR) is diagnosed. Otherwise sequential hypothesis testing [21] is used to separate ventricular tachycardia (VT) from ventricular fibrillation (VF).

As stated above, the original algorithm works with single one second time segments, (see [21], page 841). In this study additionally 2 to 8 consecutive one second episodes were selected. The final SR or VF decision is taken if diagnosed in more than half of the segments.

The critical threshold parameter to obtain the ROC is TCI_0.

2.2 ACF algorithm

The autocorrelation algorithms (ACF_{95}[1] and ACF_{99}[2]) [4] analyze the periodicities within the ECG. Autocorrelation is a signal processing technique which can be used to distinguish between periodic and non-periodic signals. Given a discrete signal $x(m)$ the short-term ACF of $x(m)$ with a rectangular window is calculated by

$$R(k) = \sum_{m=0}^{N-1-k} x(m)x(m+k), \qquad k = 0, 1, 2, \ldots, N-1. \tag{2.2}$$

Here, this technique is used to separate VT and SR from VF. It is assumed that VF signals are more or less aperiodic and SR signals are approximately periodic.

There exist an interesting context between the autocorrelation function and the Fourier transform. The autocorrelation function $C(t)$ of a function $E(t)$ is defined by

[1] Probability of 95% in the Fisher distribution $\rightarrow \alpha = 0.05$ in $F(\alpha, k_1, k_2)$ with $k_1 = 1, k_2 = 5$

[2] Probability of 99% in the Fisher distribution $\rightarrow \alpha = 0.01$ in $F(\alpha, k_1, k_2)$ with $k_1 = 1, k_2 = 5$

$$C(t) = \int_{-\infty}^{\infty} \bar{E}(\tau)E(t+\tau)d\tau, \tag{2.3}$$

with $\bar{E}(t)$ being the complex conjugated of E(t). The Fourier transform of $E(t)$ is defined by

$$E(\tau) = \int_{-\infty}^{\infty} E_\nu \exp(-2\pi i\nu\tau)d\nu. \tag{2.4}$$

Then, the autocorrelation is simply given by the Fourier transform of the absolute square of $E(\nu)$,

$$C(t) = \mathcal{F}_\nu[|E_\nu|^2](t). \tag{2.5}$$

This theorem is called "Wiener Khinchin Theorem".

The detection algorithm performs a linear regression analysis of ACF peaks. An order number i is given to each peak according to its amplitude. So, the highest peak is called P_0, etc., ranged by decreasing amplitudes. In a SR signal, which is considered to be periodic or nearly periodic, a linear relationship should exist between the peaks lag and their index number. No such relationship should exist in VF signals. The linear regression equation of the peak order and its corresponding lag of m peaks in the ACF is described as

$$y_i = a + bx_i \tag{2.6}$$

where x_i is the peak number (from 0 to $(m-1)$), and y_i is the lag of P_i.

$$a = \bar{y} - b\bar{x}, \qquad b = \sum_{i=1}^{m}(x_i - \bar{x})y_i \left(\sum_{i=1}^{m}(x_i - \bar{x})^2\right)^{-1}, \tag{2.7}$$

$$\bar{x} = \frac{1}{m}\sum_{i=1}^{m} x_i, \qquad \bar{y} = \frac{1}{m}\sum_{i=1}^{m} y_i. \tag{2.8}$$

In this study, $m = 7$. The variance ratio VR is defined by

$$VR = \frac{b\sum_{i=1}^{m}(x_i - \bar{x})y_i}{R/(m-2)}, \tag{2.9}$$

where

$$R = \sum_{i=1}^{m}\left(y_i - \bar{y} - b(x_i - \bar{x})\right)^2. \tag{2.10}$$

If $VR \geq VR_0$ is greater than the Fisher statistics for degrees of freedom $k_1 = 1$ and $k_2 = m - 2$ with 95%(99%) probability, the rhythm is classified to be SR; otherwise it is VF. $VR_0 = 6.61(16.3)$ for 95%(99%) probability.

The critical threshold parameter to obtain the ROC is VR_0.

2.3 VF filter algorithm

The VF filter algorithm (VF) [12] applies a narrow band elimination filter in the region of the mean frequency of the considered ECG signal.

After preprocessing, a narrow band-stop filter is applied to the signal, with central frequency being equivalent to the mean signal frequency f_m, $f_m = 1/T_m$. Its calculated output is the VF filter leakage. The VF signal is considered to be of quasi-sinusoidal waveform.

The number N of data points in an average half period $T_m/2$ is given by

$$N = \lfloor \pi \left(\sum_{i=1}^{m} |V_i| \right) \left(\sum_{i=1}^{m} |V_i - V_{i-1}| \right)^{-1} + \frac{1}{2} \rfloor, \tag{2.11}$$

where V_i are the signal samples, m is the number of data points in one mean period, and $\lfloor \ldots \rfloor$ denotes the floor function. The narrow band-stop filter is simulated by combining the ECG data with a copy of the data shifted by a half period. The VF-filter leakage is computed as

$$leakage = \left(\sum_{i=1}^{m} |V_i + V_{i-N}| \right) \left(\sum_{i=1}^{m} (|V_i| + |V_{i-N}|) \right)^{-1}. \tag{2.12}$$

In the original paper [12] this algorithm is invoked only if no QRS complexes or beats are detected. Since we employ no prior QRS detection, we use the thresholds suggested by [6].

If the signal is higher than a third of the amplitude of the last detected QRS (in a previous segment) and the leakage is smaller than $l_0 = 0.406$, VF is identified. Otherwise the leakage must be smaller than $l_0 = 0.625$ in order to be classified as VF.

The critical threshold parameter to obtain the ROC is the leakage l_0.

2.4 Spectral algorithm

The spectral algorithm (SPEC) [3] works in the frequency domain and analyses the energy content in different frequency bands by means of Fourier analysis.

The ECG of most normal heart rhythms is a broadband signal with major harmonics up to about 25 Hz. During VF, the ECG becomes concentrated in a narrow band of frequencies between 4 and 7 Hz ([5], [18]).

After preprocessing, each data segment is multiplied by a Hamming window and then the ECG signal is transformed into the frequency domain by fast Fourier transform (FFT). The amplitude is approximated in accordance with [3] by the sum of the absolute value of the real and imaginary parts of the complex coefficients. Let Ω be the frequency of the component with the largest

amplitude (called the peak frequency) in the range $0.5-9$ Hz. Then frequences with amplitudes whose value is less than 5 % of the amplitude of Ω are set to zero. Four spectrum parameters are calculated, the normalized first spectral moment M

$$M = \frac{1}{\Omega} \frac{\sum_{j=1}^{j_{max}} a_j \omega_j}{\sum_{j=1}^{j_{max}} a_j}, \tag{2.13}$$

j_{max} being the index of the highest investigated frequency, and A_1, A_2, A_3. Here ω_j denotes the j-th frequency in the FFT between 0 Hz and the minimum of $(20\,\Omega\,, 100$ Hz) and a_j is the corresponding amplitude. A_1 is the sum of amplitudes between 0.5 Hz and $\Omega/2$, divided by the sum of amplitudes between 0.5 Hz and the minimum of $(20\,\Omega\,, 100$ Hz). A_2 is the sum of amplitudes between $0.7\,\Omega$ and $1.4\,\Omega$ divided by the sum of amplitudes between 0.5 Hz and the minimum of $(20\,\Omega\,, 100$ Hz). A_3 is the sum of amplitudes in 0.6 Hz bands around the second to eighth harmonics $(2\,\Omega - 8\,\Omega)$, divided by the sum of amplitudes in the range of 0.5 Hz to the minimum of $(20\,\Omega\,, 100$ Hz).

VF is detected if $M \leq M_0 = 1.55,\ A_1 < A_{1,0} = 0.19,\ A_2 \geq A_{2,0} = 0.45$, and $A_3 \leq A_{3,0} = 0.09$.

The critical threshold parameter to obtain the ROC is $A_{2,0}$, where the other threshold parameters ($A_{1,0}$, $A_{3,0}$, M_0) being kept constant.

2.5 Complexity measure algorithm

The complexity measure algorithm (CPLX) [23] transforms the ECG signal into a binary sequence and searches for repeating patterns.

Lempel and Ziv [13] have introduced a complexity measure $c(n)$, which quantitatively characterizes the complexity of a dynamical system.

After preprocessing, a $0-1$ string is generated by comparing the ECG data x_i ($i = 1...n$, n being the number of data points) to a suitably selected threshold. The mean value x_m of the signal in the selected window is calculated. Then x_m is subtracted from each signal sample x_i. The positive peak value V_p, and the negative peak value V_n of the data are sought out.

By counting, the quantities P_c and N_c are obtained. P_c represents the number of data x_i with range $0 < x_i < 0.1V_p$ and N_c the number of data x_i with range $0.1V_n < x_i < 0$. If $(P_c + N_c) < 0.4n$, then the threshold is selected as $T_d = 0$. Else, if $P_c < N_c$, then $T_d = 0.2V_p$, otherwise $T_d = 0.2V_n$. Finally, x_i is compared with the threshold T_d to turn the ECG data into a $0-1$ string $s_1 s_2 s_3 \ldots s_n$. If $x_i < T_d$, then $s_i = 0$, otherwise $s_i = 1$. Now, from this string a complexity measure $c(n)$ is calculated by the following method, according to [13].

If S and Q represent two strings then SQ is their concatenation. $SQ\pi$ is the string SQ when the last element is deleted. Let $v(SQ\pi)$ denote the vocabulary of all different substrings of $SQ\pi$. At the beginning, $c(n) = 1$, $S = s_1$, $Q = s_2$,

and therefore $SQ\pi = s_1$. For generalization, now suppose $S = s_1 s_2 \dots s_r$ and $Q = s_{r+1}$. If $Q \in v(SQ\pi)$, then s_{r+1} is a substring of $s_1 s_2 \dots s_r$, therefore S does not change. Q has to be renewed to be $s_{r+1}s_{r+2}$. Then it has to be judged if Q belongs to $v(SQ\pi)$ or not. This procedure has to be carried out until $Q \notin v(SQ\pi)$, now $Q = s_{r+1}s_{r+2} \dots s_{r+i}$, which is not a substring of $s_1 s_2 \dots s_r s_{r+1} \dots s_{r+i-1}$, thus $c(n)$ is increased by one. Thereafter S is combined with Q, and S is renewed to be $S = s_1 s_2 \dots s_r s_{r+1} \dots s_{r+i}$, and at the same time Q has to be renewed to be $Q = s_{r+i+1}$. The above procedures are repeated until Q contains the last character. At this time the number of different substrings of $s_1, s_2, \dots, s_n$ is $c(n)$, i.e. the measure of complexity, which reflects the rate of new pattern arising with the increase of the pattern length n.

The normalized $C(n)$ is computed:

$$C(n) = \frac{c(n)}{b(n)}, \tag{2.14}$$

where $b(n)$ gives the asymptotic behavior of $c(n)$ for a random string:

$$b(n) = \frac{n}{\log_2 n}. \tag{2.15}$$

Evidently, $0 \leq C(n) \leq 1$. In order to obtain results that are independent of n, n must be larger than 1000.

Since n is given by window length WL times sampling rate SR, we choose $WL = 8s$.

If $C < C_0 = 0.173$, the ECG is classified as SR, if $C > C_1 = 0.426$, the ECG is classified as VF. Otherwise the ECG is classified as VT.

Since in our investigation VT is treated like VF, the critical threshold parameter to obtain the ROC is C_0.

2.6 Autoregressive modeling algorithm

The autoregressive modeling algorithm (AAR_{50}, AAR_{100}, AAR_{250}) [8] uses Burg's algorithm of order 4 to compute AR coefficients in a generalized linear model (GLM) based algorithm. The algorithm implemented here is a simplification of [8].

Here, only a distinction of SR and VF is performed, whereas the original work executes a separation into more different groups of arrhythmias. After preprocessing, the ECG signal is sampled down to a frequency of $250\,Hz$ by linear interpolation. AR coefficients are used to classify cardiac arrhythmias. A GLM based classification model is used to distinguish VF from SR. A GLM is given by

$$\hat{Y} = A\beta + \epsilon, \tag{2.16}$$

where $\hat{Y} = (y_1, y_2, ..., y_N)^T$ is an N-dimensional vector of observed responses, $\beta = (\beta_0, \beta_1, ..., \beta_P)^T$ is a $P+1$ dimensional vector of unknown parameters, A is a $N \times (P+1)$ matrix of known predictors (AR coefficients) and $\epsilon = (\epsilon_1, \epsilon_2, ..., \epsilon_N)^T$ is an N dimensional error vector. As mentioned above, $P = 4$ and the number N of ECG segments in the training set is 120 (60 SR episodes and 60 VF episodes). The least squares estimator is given by

$$\beta = (A^T A)^{-1} A^T \hat{Y} \tag{2.17}$$

A generalized linear model based classification is performed to differentiate between SR and VF. First, a training phase is performed, i.e., the estimator β is computed based on known classes of ECG segments that form the training set. Several episodes of SR and VF from the CU database were used as a training set (cu01, cu06, cu12, cu21, cu23, cu29). Each observed segment i of this training set was either SR or VF. If the segment was SR, $\hat{Y}_i$ was set to 1, otherwise $\hat{Y}_i$ was set to -1. The autoregressive coefficients matrix or observation matrix A was calculated from the ECG episodes from the training set by Burg's algorithm. The observation matrix $A = (I, A_2, A_3, A_4, ..., A_{P+1})$ consists of the AR coefficients of all training ECG segments, where I is an identity vector and the column vectors $A_2, A_3, A_4, ..., A_{P+1}$ consist of AR coefficients $a(2), a(3), a(4), ..., a(P+1)$, that are obtained from the ECG segments of the training set. This calculation was carried out only once in order to obtain β.

In the analyzing process, the algorithm works as follows: The AR coefficients of the ECG segment to be analyzed and the previously estimated β are used to compute the correct response for the classification. The AR coefficients $C = (a(2), a(3), a(4), ..., a(P+1))$ of a particular ECG segment are mapped to a response r by $r = C\beta^T$. A threshold value of zero is used to classify the ECG segment to be SR of VF. If $r > r_0 = 1$, the ECG segment is classified as SR, otherwise the analyzed ECG segment is classified as VF.

In [8], the sample frequency is $250\,Hz$. Additionally, we use sample frequencies of $50\,Hz$ and $100\,Hz$ (see AAR_{50}, AAR_{100} and AAR_{250} in the tables in Chapter 6), since this approach improves the quality of the detection considerably.

The critical threshold parameter to obtain the ROC is r_0.

2.7 Standard exponential algorithm

The standard exponential (STE) algorithm counts the number of crossing points of the ECG signal with an exponential curve decreasing on both sides. The decision for the defibrillation is made by counting the number of crossings.

The ECG signal is investigated in the time domain. First, the absolute maximum value of the investigated sequence of the signal is searched. An exponential like function $E_s(t)$ is put through this point. This function is decreasing in both

directions. Hence, it has the representation:

$$E_s(t) = M \exp\left(-\frac{|t - t_m|}{\tau}\right). \tag{2.18}$$

Here, M is the value of the signal maximum, t_m is the corresponding time, τ is a time constant. In our investigation, τ is set to 3 seconds. The number of intersections n of this curve with the ECG signal is counted and a number N is calculated by

$$N = \frac{n}{T}, \tag{2.19}$$

where T is the time length of the investigated signal part. If $N > N_0 = 250$ crossings per minute (cpm), VF is identified. If $N < N_1 = 180$ cpm, SR is identified.

Otherwise the signal is classified as VT. Figure 2.2 illustrates the situation.

Since in our investigation VT is treated like VF, the critical threshold parameter to obtain the ROC is N_1.

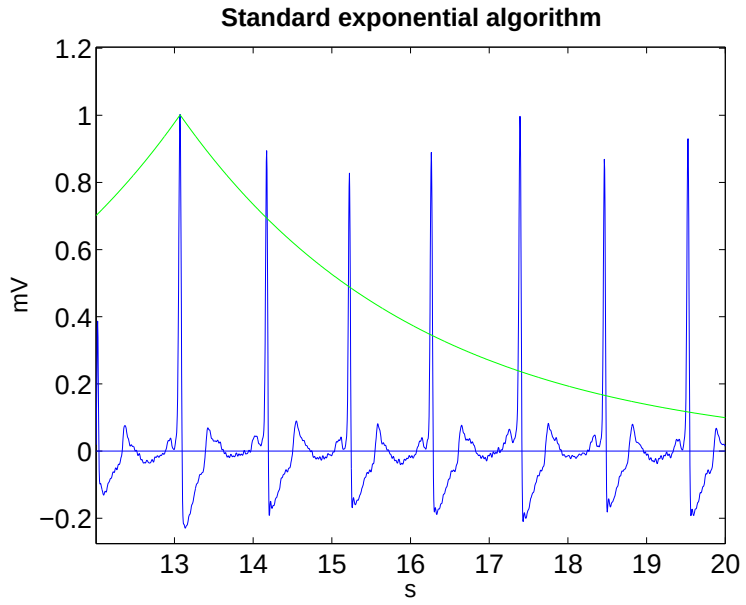

Figure 2.2: *ECG signal cu01 from the CU database considered with the standard exponential algorithm.*

2.8 Modified exponential algorithm

A modified version of STE, called MEA, lifts the decreasing exponential curve at the crossing points onto the following relative maximum. This modification gives rise to better detection results.

This algorithm works in the time domain. First, the first relative maximum value of the investigated sequence of the signal is searched and an exponential like function $E_{n,1}(t)$ is put through this point. Here, it has the representation:

$$E_{n,j}(t) = \begin{cases} M_j \exp\left(-\frac{t-t_{m,j}}{\tau}\right) & t_{m,j} \leq t \leq t_{c,j} \\ \text{given ECG signal} & t_{c,j} \leq t \leq t_{m,j+1} \end{cases} \tag{2.20}$$

with M_j being the value of the j-th relative maximum of the signal, $t_{m,j}$ the corresponding time and τ the time constant. Here, τ is set to 0.2 seconds. $t_{c,j}$ is the time value, where the exponential function crosses the ECG signal.

As one can see, the exponent does not contain the absolute value of $t - t_m$ any more, but rather its unchanged value. Therefore, this function is decreasing if $t > t_m$. Moreover, the difference to (STE) is, that here the function does not have the above representation over the whole investigated signal part, but only in the region from the first relative maximum to the first intersection with the ECG signal. Then, the function $E_{n,j}(t)$ coincides with the ECG signal until it reaches a new relative maximum. In some way one can say that the function $MEA(t)$ is lifted here from a lower value to a peak. From that peak on it has again the above representation with M being the value of the next relative maximum. This is done until the curve reaches the end of the investigated ECG sequence.

The number of the liftings n of this curve with the ECG signal is counted and a number N is calculated by

$$N = \frac{n}{T}, \tag{2.21}$$

where T is the time length of the investigated signal part. If $N > N_0 = 230$ crossings per minute (cpm), VF is identified. If $N < N_1 = 180$ cpm, SR is identified. Otherwise the signal is classified as VT. Figure 2.3 illustrates the situation.

Since in our investigation VT is treated like VF, the critical threshold parameter to obtain the ROC is N_1.

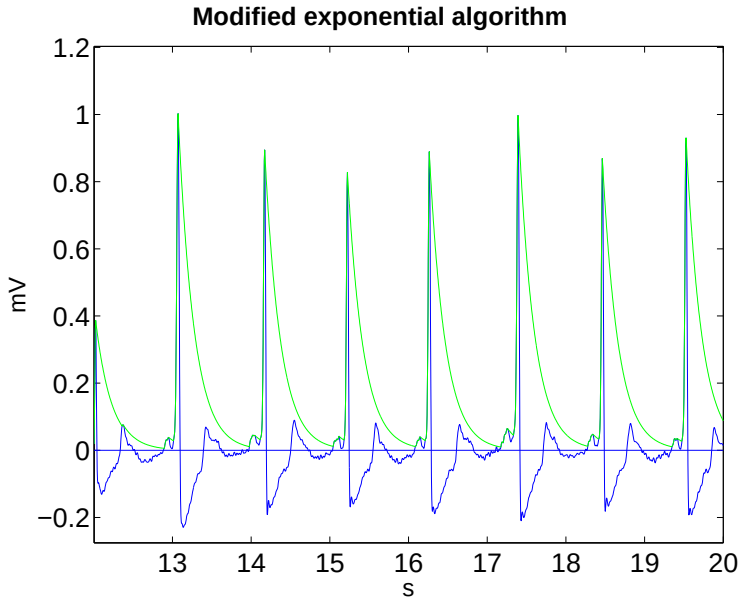

Figure 2.3: *ECG signal cu01 from the CU database considered with the modified exponential algorithm.*

Chapter 3

Illustration of detection techniques of some existing algorithms

An example for the technique used in the SPEC algorithm is illustrated in the following figure. Here, the ECG shows sinus rhythm.

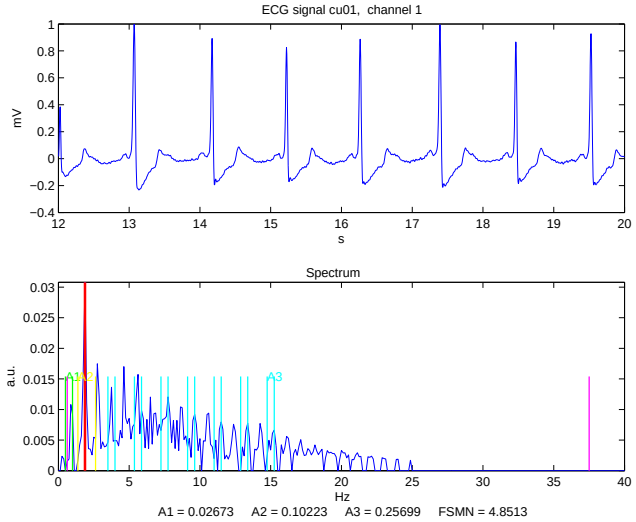

Figure 3.1: *Sinus rhythm with according spectrum, parameters for the SPEC algorithm. Typical band structure in the spectrum, i.e. many harmonics and a low fundamental frequency. (red vertical line = fundamental frequency)*

The following figure again shows the technique of the SPEC algorithm. Here, the ECG shows ventricular fibrillation.

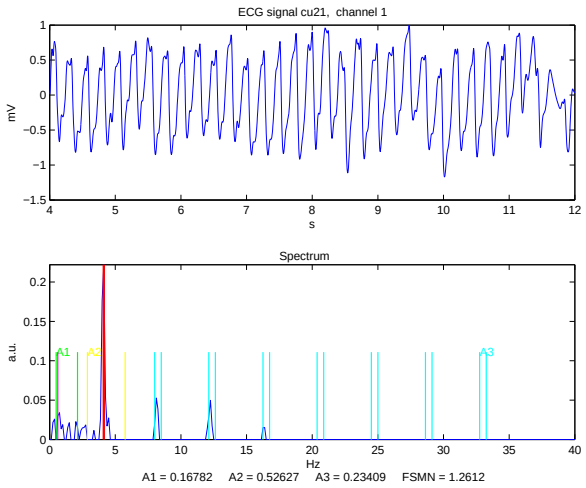

Figure 3.2: *Ventricular fibrillation with according spectrum, SPEC algorithm. No distinct band structure visible, few harmonics, a relatively high fundamental frequency. (red line = fundamental frequency)*

Description of Figure 3.1 and Figure 3.2:
top plot: ECG signal
bottom plot: continuous line: spectrum of ECG signal (dark blue)
after filtering, from 0 to 40 Hz.
vertical lines: characteristic points and limits in the
ECG spectrum, calculated with SPEC algorithm:
red line: frequency with maximum spectrum value between 0.5 Hz and 9 Hz,
i.e. peak frequency, f_m.
magenta lines: limits for calculation of AA, 0.5 Hz - $\min(40, 20f_m)$ Hz.
cyan lines: 0.6 Hz bands around multiples of f_m (= 2^{nd} to 8^{th} harmonics),
at most 7 bands.
green lines: limits for calculation of A_1.
yellow lines: limits for calculation of A_2.

AUS = area under spectrum
AA = AUS between magenta lines
A_{100} = AUS between 0 and 100 Hz
A_1 = (AUS between green lines)/ AA
A_2 = (AUS between yellow lines)/ AA
A_3 = (AUS in bands limited by cyan lines)/ AA
$FSMN$=$(1/f_m)$ * (area under (spectrum * frequency))/A_{100}
(= normalized first spectral moment).
Decision: **VF** is detected if $FSMN < 1.55,\ A_1 < 0.19,\ A_2 > 0.45,\ A_3 < 0.09$.

The next figure illustrates the method, that is used by the ACF algorithm. Ventricular fibrillation is investigated, but not recognized.

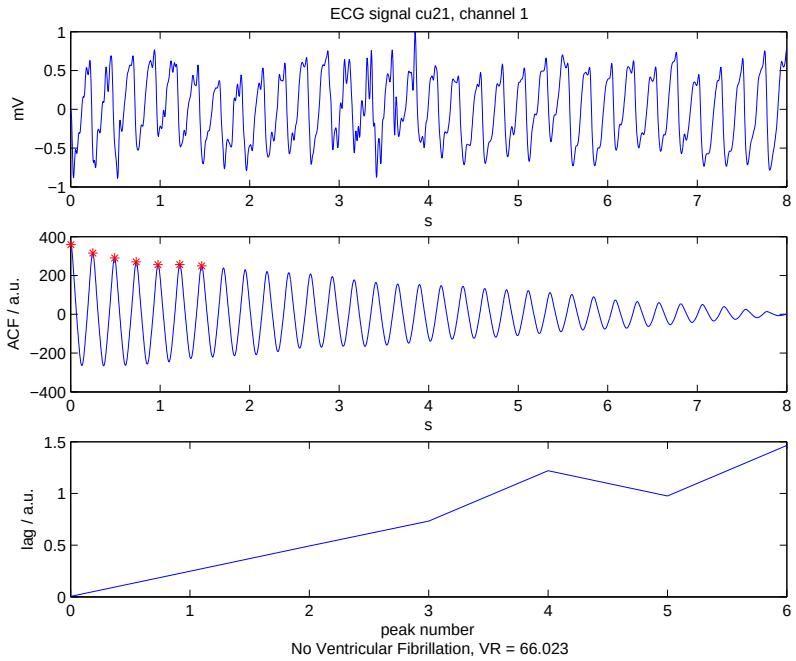

Figure 3.3: *Ventricular fibrillation with parameters from the ACF algorithm. Searches for similar signal episodes with autocorrelation. Assumes high correlation in sinus rhythm due to regular signal. Problem: also ventricular fibrillation can be regular* $\rightarrow$ *no good results.*

Description of Figure 3.3:
top plot: ECG signal (here: VF)
middle plot: autocorrelation function with the seven highest peaks
bottom plot: x-axis: index number of peaks
(highest peak = 0, lowest peak = 6)
y-axis: time lag (= x distance from t = 0 in middle plot)

Decision: **VF** is detected if $VR \geq F$, where $F \approx 10 \ldots 100$,
according to Fisher distribution.
VR = variance ratio (statistical measure,
obtained by linear regression).

Here, the method used by the TCI algorithm is illustrated. Sinus rhythm is investigated.

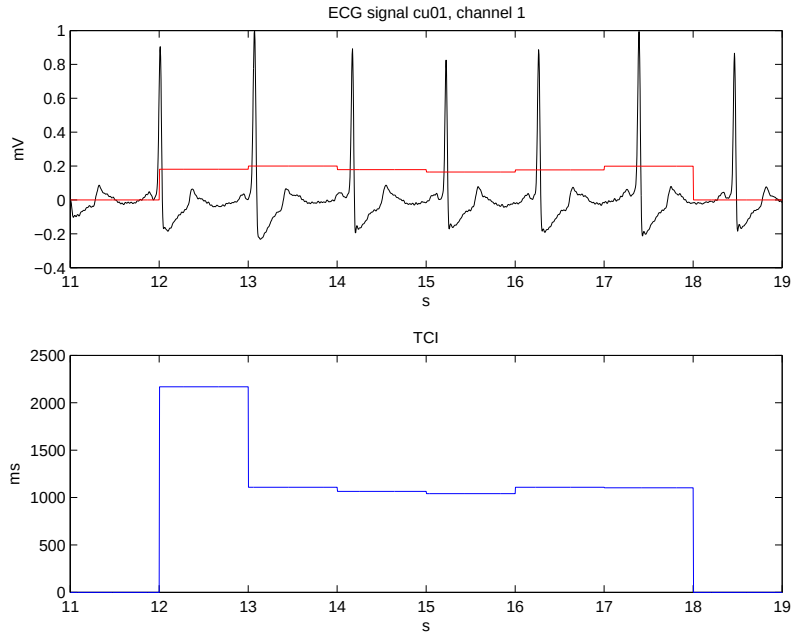

Figure 3.4: *Sinus rhythm with parameters analyzed with the TCI algorithm. A threshold T is set to 20% of the maximum signal value within the investigated episode.*

Description of Figure 3.4:
top plot: black curve: ECG signal (here: SR)
red curve: calculated threshold T,
$T = 0.2 \cdot \max(1 \text{ second ECG signal episode})$.
bottom plot: TCI, Threshold crossing interval.
Decision: **VF** is detected if $TCI < 400$ms.

Chapter 4

Existing Methods for QRS Detection

The algorithms described in this chapter had been developed for QRS detection and not for VF detection. Still we want to use them as VF detectors by classifying a rhythm containing no QRS complexes as VF. The results show, that this kinds of algorithms are not able to work as VF detectors.

4.1 Li algorithm

This algorithm (LI) is described in [14]. It works on the basis of a wavelet transformation.

The wavelet transforms of the ECG signal are calculated using the following equations:

$$S_{2^j} f(n) = \sum_{k \in \mathbb{Z}} h_k S_{2^{j-1}} f(n - 2^{j-1}k) \tag{4.1}$$

$$W_{2^j} f(n) = \sum_{k \in \mathbb{Z}} g_k S_{2^{j-1}} f(n - 2^{j-1}k) \tag{4.2}$$

Here, S_{2^j} is a smoothing operator and $S_{2^0} f(n) = d_n$, d_n being the ECG signal. h_k and g_k are coefficients of a lowpass filter $H(\omega)$ and a highpass filter $G(\omega)$. Scales 2^1 to 2^4 are selected to carry out the search for QRS complexes. QRS complexes are found by comparing energies from the ECG signal in the scale 2^3 with the energies in the scale 2^4. Redundant modulus maximum lines are eliminated and the R peaks detected. Different methods from [9] are used to improve the detection quality:

Method 1: Blanking, where events immediately following a QRS detection are ignored for a period of $200ms$.

Method 2: Searching back, where previously rejected events are reevaluated when a significant time has passed without finding a QRS complex. If no QRS

complex was detected within 150% of the latest average RR interval, then the modulus maxima are detected again at scale 2^3 with a new threshold.

Here, two different approaches of this algorithm are analyzed: First, the algorithm is implemented exactly like described in [14]. The corresponding results in the tables of Chapter 6 are named "LI". One must keep in mind that this algorithm was originally written as a QRS detection algorithm and not as a VF detection algorithm. Here, it is analyzed, how it works as a VF detection algorithm, so the results are not expected to be very good.

Second, some parameters are changed, since they improve the results, when the algorithm is used as a VF detection algorithm:

The pre factor for ϵ in the investigation of the maxima and minima of the dyadic Wavelet transform is changed from 0.3 to 0.1 (See section "Detection methods" in [14]).

The calculation of α_1 and α_2 (See section "Detection methods" in [14]) is changed into the following assignment: if $W_3 > W_4$ and $W_3 > 1.2W_5$, W_i being the values of the expected QRS complexes in the Wavelet transform, then α_1 and α_2 are set from 0 to -1. The corresponding results in the tables of Chapter 6 are named "LI_m".

If the number of found QRS complexes is 0 or higher than 5 times the window length in seconds, the ECG segment is classified as VF.

The critical threshold parameter to obtain the ROC is the number of found QRS complexes .

4.2 Tompkins algorithm

This algorithm is based on a QRS complex search (TOMP) [20]. It uses slope, amplitude and width information to carry out this task.

After preprocessing, the ECG signal is band filtered by a low pass filter and a high pass filter to reduce interference and high frequency noise. Then, the signal is differentiated to provide the QRS complex slope information. The difference equation for the slope $y(j)$ of the ECG data $x(j)$ reads

$$y(nT) = \frac{1}{8T}\Big(-x(nT-2T)-2x(nT-T)+2x(nT+T)+x(nT+2T)\Big), \quad (4.3)$$

where T is the sampling period of the ECG signal. Afterwards the signal is squared to make all data points positive. A moving window integration with a window width of $150ms$ (e.g., 54 points at a sampling rate of $360Hz$) is applied. Thresholds are set up to detect QRS complexes.

This algorithm uses a dual threshold technique and a searchback for missed beats. If the number of found QRS complexes is smaller than 0.25 times the window length or higher than 4 times the window length, the ECG segment is classified as VF.

The critical threshold parameter to obtain the ROC is the number of found QRS complexes.

Chapter 5

New Methods

Dealing with existing methods of VF detection, ideas for new approaches had occurred. The following techniques explain this ideas.

5.1 Modified Spectral algorithm

The modified spectral algorithm (SPEC_m) works like SPEC [3] in the frequency domain and analyses the energy content in different frequency bands by means of Fourier analysis. It is a slight modification of SPEC.

As in SPEC, after preprocessing, each data segment is multiplied by a Hamming window and then the ECG signal is transformed into the frequency domain by fast Fourier transform (FFT). Here, the amplitude is not approximated by the sum of the absolute value of the real and imaginary parts of the complex coefficients (like in SPEC), but it is first calculated exactly, and then squared. So "amplitude" means here the sum of the squared imaginary part and the squared real part of the FFT. Since the ECG signal is measured in Volts, it means that the amplitude calculated in the above described way is the energy density of the signal.

Here, Ω is the frequency of the component with the largest amplitude (called the peak frequency) in the range $0.5 - 7$ Hz. No frequency parts are set to zero.

The further procedure is equal to the technique in the SPEC algorithm. Four spectrum parameters are calculated, the normalized first spectral moment M

$$M = \frac{1}{\Omega} \frac{\sum_{j=1}^{j_{max}} a_j \omega_j}{\sum_{j=1}^{j_{max}} a_j}, \tag{5.1}$$

j_{max} being the index of the highest investigated frequency, and A_1, A_2, A_3. Here ω_j denotes the j-th frequency in the FFT between 0 Hz and the minimum of $(20\,\Omega\,, 100$ Hz) and a_j is the corresponding amplitude. A_1 is the sum of

amplitudes between 0.5 Hz and $\Omega/2$, divided by the sum of amplitudes between 0.5 Hz and the minimum of $(20\,\Omega\,, 100$ Hz). A_2 is the sum of amplitudes between $0.7\,\Omega$ and $1.4\,\Omega$ divided by the sum of amplitudes between 0.5 Hz and the minimum of $(20\,\Omega\,, 100$ Hz). A_3 is the sum of amplitudes in 0.6 Hz bands around the second to eighth harmonics $(2\,\Omega - 8\,\Omega)$, divided by the sum of amplitudes in the range of 0.5 Hz to the minimum of $(20\,\Omega\,, 100$ Hz).

VF is detected if $M \leq M_0 = 1.55,\ A_1 < A_{1,0} = 0.19,\ A_2 \geq A_{2,0} = 0.45$, and $A_3 \leq A_{3,0} = 0.09$.

The critical threshold parameter to obtain the ROC is $A_{2,0}$, where the other threshold parameters ($A_{1,0}$, $A_{3,0}$, M_0) being kept constant.

5.2 Signal comparison algorithm

This algorithm (SCA) compares the ECG with four predefined reference signals (three sinus rhythms and one ventricular fibrillation signal) and makes its decision by calculation of the residuals in the L^1 norm.

The algorithm works in the time domain. After preprocessing, all relative maxima of a modified ECG signal are searched. The relative positions in time t_j and amplitude a_j of these points are considered.

We call this set M_0, with $M_0 = \{(t_j, a_j) | a_j \text{ is a local maximum}\}$. With this information a probability test for being the peak of a possible QRS complex is executed. For a detailed description of this test see steps 1 and 2 below. In a normal ECG, most of the relative maxima M_0 of the ECG signal, which are not the peaks of an QRS complex, are extinguished by this procedure. On the other side, in an ECG signal with fibrillation only such peaks are preserved, which are peaks of a fibrillation period.

In other words: Most of the relative maxima, which exist due to noise in the ECG signal are deleted. Furthermore, nearly all relative maxima, which are peaks of insignificant elevations (in this algorithm also P waves and T waves) are deleted as well. This selection procedure is carried out by setting adaptive thresholds. The value of the thresholds is calculated with the help of different parameters, that were selected by experiments with ECG signals. The result is a set of points X, which is a subset of M_0. In fact, the temporal appearance of the points in X is related to the frequency of the heart beat. The average frequency found by this points is related to a certain probability factor. This factor, together with other results, is finally used to make a decision whether the signal is VF or not.

Now, the central idea of the algorithm is applied. The points in X are used to generate four artificial signals. The first signal looks like a normal sinus rhythm, that has its QRS peaks exactly at the points of X. The reference signal is scaled linearly to fit the different maxima. It has all features that a normal ECG signal should have (narrow QRS complex, P wave, T wave). The second artificial signal is the average of about 700 normal sinus rhythm signals found in 16 files of the MIT data bank and 16 files of the CU data bank. The

third artificial signal has QRS complexes and an elevated T wave. The fourth signal, which we use as a reference for a fibrillation signal, has the shape of a cosine like function, which has its peaks at the points of X and therefore simulates ventricular fibrillation.

The next step is the calculation of the residuals with respect to the reference signals. We call the ECG signal $E(t)$, the reference signals that simulate a healthy heart $S_j(t)$, $j = 1, 2, 3$, and the fibrillation signal $F(t)$. The following calculations are carried out:

$$RF = \int_I |E(t) - F(t)|dt \ , \qquad RS_j = \int_I |E(t) - S_j(t)|dt \ , \quad j = 1, 2, 3.$$
$$FF = \int_I |F(t)|dt \ , \quad FE = \int_I |E(t)|dt \ , \quad FS_j = \int_I |S_j(t)|dt \ , \tag{5.2}$$

where $I = [t_0, t_1]$ with $t_0 = \min\{t_j | t_j \in X\}$ and $t_1 = \max\{t_j | t_j \in X\}$. Thus, I is the temporal interval from the smallest t_j in X to the largest t_j in X.

Now, four further values are calculated:

$$VRF = c_1 \frac{RF}{\min(FF, FE)} \ , \qquad VRS_j = c_2 \frac{RS_j}{\min(FS_j, FE)}, \quad j = 1, 2, 3 \tag{5.3}$$

c_1 and c_2 are two constants that were chosen by experiments with the data. Finally, VRF and VRS are compared. If VRF is smaller than VRS_j for all $j = 1, 2, 3$, the signal is classified as VF, otherwise it is considered as SR.

Now we describe the search for relative maxima, mentioned above, in more detail.

An offset is added to the ECG signal to make its mean value to zero. We construct a set Z containing the values a_j and temporal positions t_j of this new signal, i.e., $Z = \{(t_j, a_j) | a_j$ is the value of the ECG signal at time $t_j\}$. All further steps are executed both with the set Z and the set $-Z$, where $-Z = \{(t_j, b_j) | b_j = -a_j$ is the value of the negative ECG signal at time $t_j\}$ with the help of the reference signals $rECG_\ell$, ℓ being VF, SR_1, SR_2 or SR_3, or, equivalently, $\ell = 0, 1, 2, 3$. Note, that the maxima of Z correspond to the minima of $-Z$. So we get $2 * 4 = 8$ tests to find out whether a signal is VF or SR. If any of the 8 tests yields SR, the signal is considered to be SR.

Step 1: All relative maxima a_j of Z and their corresponding times t_j are searched. The resulting set is called M_0, i.e. $M_0 = \{(t_j, a_j) | a_j$ is a local maximum$\}$, so $M_0 \subset Z$. All a_j in M_0, that are smaller than A, $A = \Delta \cdot \max(a_j)$, where Δ is a threshold, are deleted. The threshold Δ is set to 0.1 for the VF reference signal and to 0.2 for the SR reference signals. We call the reduced set M_1. An example plot is shown in Figure 5.1.

In the following Figure 5.1 we see an ECG episode from the CU data bank (cu21, from $t = 148\,s$ until $t = 156\,s$) together with its selected relative maxima according to the status after processing step 1.

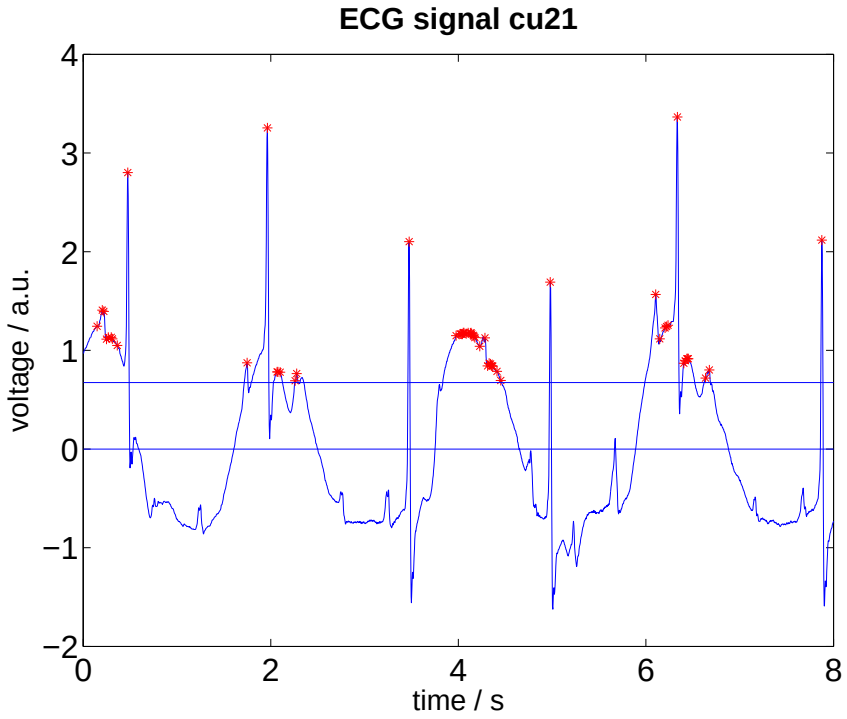

Figure 5.1: *ECG signal cu21 from the CU database with relative maxima after step 1 of SCA algorithm:*

Now, we introduce an index l and set it to $l = 1$.

Step 2: M_l is reduced further: The maximum a_j in M_l is searched. Here, we call it a_{max}. a_{max} has a corresponding temporal position t_{max}. Then, the largest possible temporal interval I_l in Z around t_{max} is searched, so that all values a_j in this interval are equal or smaller than a_{max} and larger than $0.2\,a_{max}$. All pairs (a_j, t_j) except (a_{max}, t_{max}) in M_l, that are referred to the found interval I_l, are deleted. We get a set that we call M_{l+1}. This procedure is repeated with all undealt a_j in M_l, until every a_j has been considered and afterwards either been deleted or kept. After each step, l is increased by 1. This means, first we consider M_1, then $M_2 = M_1 \backslash I_1$, then $M_3 = M_1 \backslash \{I_1 \cup I_2\}$ and so on, until we reach a highest l, called l_{max}. In the end, we get a set that we call M, with $M = M_1 \backslash \{\cup_{j=1}^{l_{max}-1} I_j\}$.

In the end, the a_j in M are the relative maxima in Z, that are higher than A and are the only ones in certain subintervals of Z. Two different a_j in M can only be neighbors in Z, if they are separated by a valley that is deeper than 20 % of the higher peak of the two. An example plot is shown in Figure 5.2.

In Figure 5.2 we again see the ECG episode as in Figure 5.1 together with its newly selected relative maxima according to the status after processing step 2.

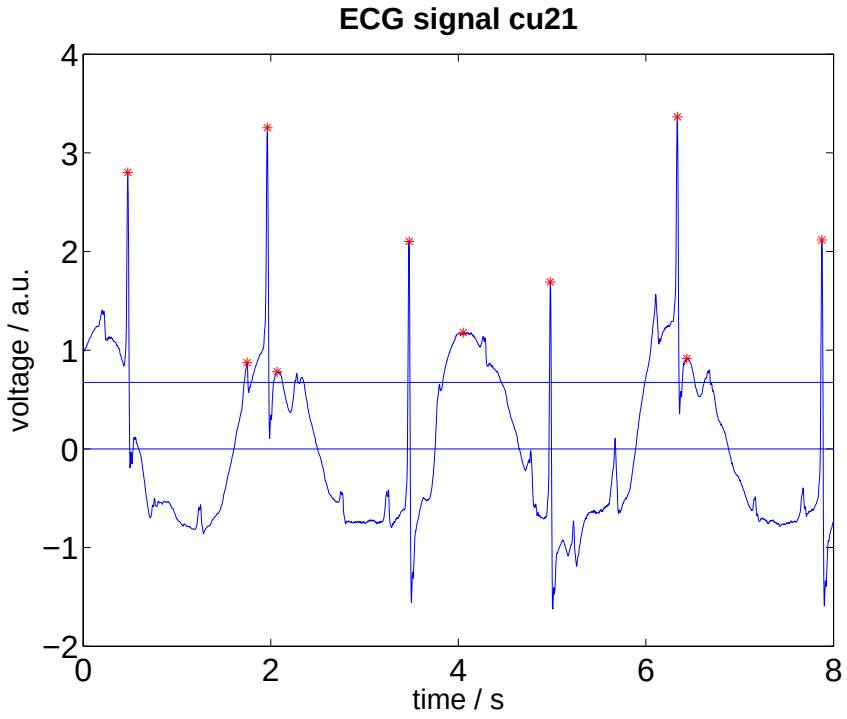

Figure 5.2: *ECG signal cu21 from the CU database with relative maxima after step 2 of SCA algorithm:*

Step 3: Now, a value Ω is calculated from M

$$\Omega = \frac{60 N_M}{t_{max} - t_{min}}, \tag{5.4}$$

where N_M is the number of points in M and $t_{max} - t_{min}$ is the maximum temporal range of the elements in M.

Step 4: If two different elements (a_i, t_i) and (a_j, t_j) of M are separated by a temporal distance $|t_i - t_j|$ smaller than $\frac{24}{\Omega}$, the element with the smaller a is deleted from M. This final set is called X. An example plot is shown in Figure 5.3.

Step 5: Ω is recalculated by Equation (5.4) with the help of the recalculated set X. If $\Omega > 280$, r is set to 2, if $\Omega < 180$, r is set to 0.9, else r is set to 1.

Step 6: The decision is calculated by Equation (5.3). VRF is calculated for the ventricular fibrillation reference signal, VRS for the sinus rhythm reference signal. Example plots are shown in Figures 5.4 and 5.5. c_1 is set to $2/r$, c_2 is set to 1.

In Figure 5.3 we again see the ECG episode as in Figures 5.1 and 5.2 and together with its newly selected relative maxima according to the status after processing step 4.

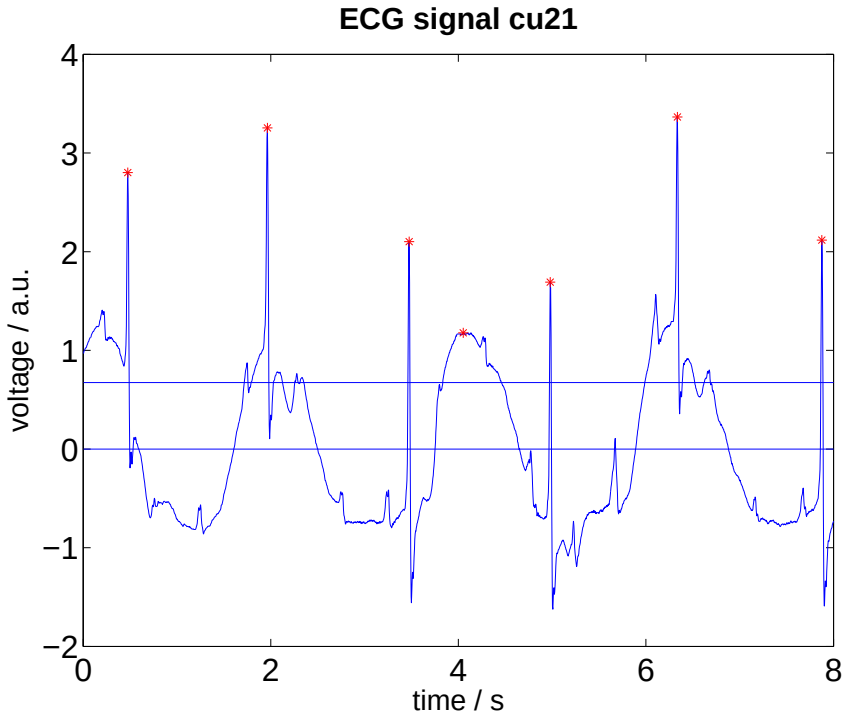

Figure 5.3: *ECG signal cu21 from the CU database with relative maxima after step 4 of SCA algorithm:*

Remark: L^2 Signal comparison algorithm An algorithm similar to SCA that uses the L^2 norm instead of the L^1 norm (SC2), is implemented. The idea is that this norm which describes the situation in terms of signal energies rather than in terms of signal voltages is more appropriate. It is supposed that energies of ECG signals have a higher significance in the cardiac processes.

The first part of the algorithm is identical to SCA. The only difference is the calculation of RF, RS_j, FF, FE and FS_j. Those values are calculated as follows:

$$RF = \int_I |E(t) - F(t)|^2 dt \,, \qquad RS_j = \int_I |E(t) - S_j(t)|^2 dt \,, \quad j = 1, 2, 3,$$
$$FF = \int_I |F(t)|^2 dt \,, \quad FE = \int_I |E(t)|^2 dt \,, \quad FS_j = \int_I |S_j(t)|^2 dt \,, \qquad (5.5)$$

where $I = [t_0, t_1]$ with $t_0 = \min\{t_j | t_j \in X\}$ and $t_1 = \max\{t_j | t_j \in X\}$. Thus, I is the temporal interval from the smallest t_j in X to the largest t_j in X. And

In Figure 5.4 we see the ECG episode together with the corresponding VF reference signal.

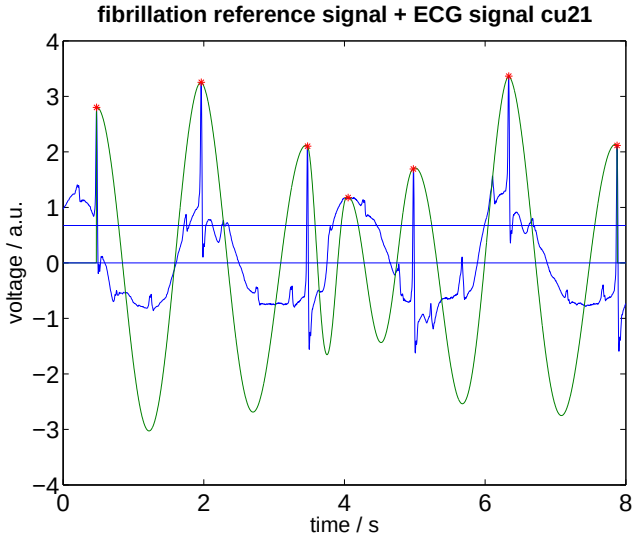

Figure 5.4: *ECG signal cu21 from the CU database with relative maxima and VF reference signal after step 6 of SCA algorithm:*

In Figure 5.5 we see the ECG episode together with the first corresponding SR reference signal.

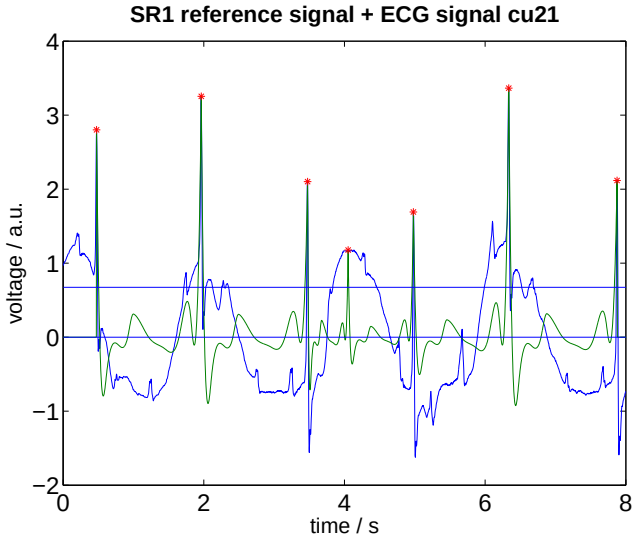

Figure 5.5: *ECG signal cu21 from the CU database with relative maxima and SR reference signal after step 6 of SCA algorithm:*

again, VRF and VRS are calculated:

$$VRF = c_1 \frac{RF}{\min(FF, FE)} \qquad VRS_j = c_2 \frac{RS_j}{\min(FS_j, FE)}, \quad j = 1, 2, 3. \tag{5.6}$$

c_1 and c_2 are the same constants as used in SCA. The decision is done like in SCA. If VRF is smaller than VRS_j for all $j = 1, 2, 3$, the signal is classified as VF, otherwise it is considered as not to be VR, i.e if $VRF/VRS_j < t_j = trs = 1$ for all $j = 1, 2, 3$, the signal is classified as VF, otherwise it is considered as not to be VR. Since the integrals contain differences of function values in a quadratic dependence, here the calculation is called L^2 norm.

The results show that the quality is not improved by using the L^2 norm. The reason could be, that the voltages in the heart have triggering functions rather then an energy transport function, and therefore their electrical energy could possibly be of only little importance.

The critical threshold parameter to obtain the ROC is trs.

5.3 Phase space reconstruction algorithm

This algorithm (PSR) uses a tool which is used in analyzing signals in order to identify chaotic behavior. The signal $x(t)$ is plotted in a diagram in the following way: On the x-axis we plot $x(t)$, on the y-axis $x(t+\Delta)$, Δ being a proper time constant. Such a plot is called a two dimensional phase space reconstruction (PSR) diagram. A chaotic signal produces a curve in the diagram, that fills the area in an irregular way. The curve is uniformly distributed over the entire diagram. However, if the signal is non-chaotic, the curve in the PSR diagram shows a regular form, only little parts of the area are filled, and the curve is concentrated to a restricted region of the plot. In the special case of a periodic signal, where $\Delta = k\times$period, k being an integer, all points lie on a line of 45 degrees.

With this information we try to differentiate SR from VF. We assume VF signals to be chaotic, whereas SR signals to be more regular. We plot the PSR diagram and investigate, how much of the area in the PSR plot is filled by the curve. To achieve this, we produce a 40×40 grid and count the visited boxes. From the result we calculate the box dimension d:

$$d = \frac{\text{visited boxes}}{\text{number of all boxes}} \tag{5.7}$$

If d is higher than a certain threshold d_0, we classify the corresponding ECG episode as VF. In a number of experiments we found that good values are $\Delta = 0.5\,s$, $d_0 = 0.15$, and the number of boxes $= 1600$.

In our algorithm, we first downsample the ECG data to a fictive frequency of 50 Hz, since we do not expect much information in the frequency region above this value. Also, a reduced data set speeds up the calculation. Furthermore, in the PSR plot, we only consider the positions of the discrete ECG data points to calculate the box dimension and do not connect the data points in any kind (straight lines or other curves). The reason is, that connected data in the PSR plot (as shown in Figures 5.12 and 5.13) do not improve the quality of the algorithm, but rather decrease it.

In our first study we did not introduce a fictive sample frequency but let the original sample frequency unchanged, and we used a threshold of 0.32. The values achieved with this parameters are named "PSR$_{old}$" in the tables of Chapter 6.

We tried to improve the quality of the PSR algorithm by investigating three further approaches:

First, the algorithm works as described above. Then, the first $500ms$ of the signal are considered again. The corresponding boxes in the PSR plot and their first neighbors are deleted from the "visiting list". Now the dimension is calculated. So, the calculated dimension is reduced compared to the dimension in the original algorithm version. The idea for carrying out this step is the following: Periodic signals draw special closed loops in the PSR plot. Sinus rhythm is expected to be periodic and does not cover much of the plot area. So its

dimension is rather low. In eliminating boxes that had been visited in the first $0.5s$, which can be seen as a good part of a SR period, the dimension is reduced a lot. However, in VF signals the reduction of the PSR plot concerning to the first $0.5s$ does not have a great effect, although, of course, it is also reduced by a certain amount. All in all we wanted to see whether this approach improves the quality of the algorithm. The optimal value of $0.5s$ for the reconsidered signal part and the optimal value of 1 for the considered neighborhood were found by experiments. So, this algorithm carries out a zero/one weighting of selected adaptive parts in the PSR plot. In this version, the thresholdr d_0 is set to 0.1. The results in the tables are called "PSR_2".

A further modification of "PSR_2" is investigated: Additionally to the described adaptive (depending on the first $500ms$ of the ECG signal) zero/one weighting an additional weighting is carried out. We have chosen a function, that does not change areas in the upper right corner of the PSR plot. This corner fills the area of the PSR plot, that lies right of $0.4l$ and higher than $0.4h$, l and h being the length and the height of the PSR plot, respectively. Areas outside this corner are deleted. The idea is, that SR signals generally visit areas outside the upper right corner more often than VF signals. Here, the threshold d_0 is set to 0.03. By this approach improved results should be achieved. Still, in our experiments the results were not improved, as seen in the tables in the lines called "$\text{PSR}_{2,2}$".

The third approach to improve the quality is the following: Not only the visited boxes are counted, but also the number, how often the boxes were visited, is considered. Each box gets a number, which is the inverse of the number of the corresponding "visits", except if the number of visits is zero. In the latter case the box gets the number zero. The dimension is calculated by summing up all numbers stored in the boxes. Here, the idea of the construction was the following: In SR, the signal is expected to be periodic and so in the PSR plot there exists a trend that only a small number of boxes are visited, but this boxes are visited more often. Since a low box dimension is classified as SR, a high number of visits per box should result in an only low increase of the box dimension. Therefore, the number of visits in each box was inverted to calculate the box dimension. In SR signals, the average number of visits per box is higher than in VF signals, so this approach should improve the algorithm. The threshold d_0 is set to 0.1. The results in the tables are called "PSR_3".

As one can see in the results, the approaches from "PSR_2", "$\text{PSR}_{2,2}$" and "PSR_3" did not improve the quality of the "PSR" algorithm significantly.

The critical threshold parameter to obtain the ROC in all variations of the PSR algorithm is d_0.

Figure 5.6 shows a SR signal from the CU database.

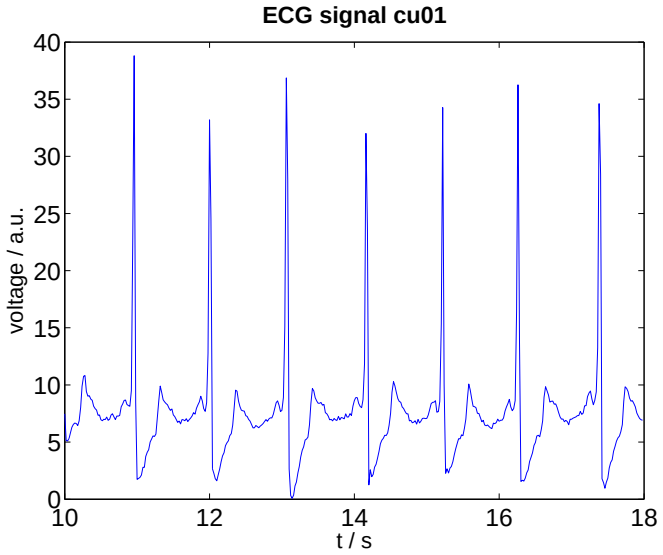

Figure 5.6: *SR episode in the ECG signal cu01 from the CU database.*

Figure 5.7 shows a phase space reconstruction plot corresponding to the SR signal from the previous figure. In order to illustrate the plot better, the dots are connected with red lines.

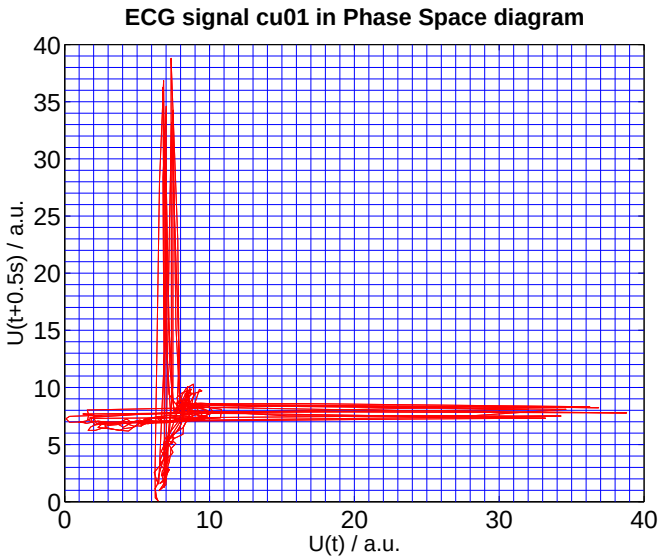

Figure 5.7: *SR episode in the ECG signal cu01 from the CU database, plotted in a phase space reconstruction diagram with a* 40×40 *grid. The data points are connected with red lines.*

Figure 5.8 shows the visited boxes in the phase space reconstruction plot corresponding to the SR signal from Figure 5.6. The individual dots are not connected.

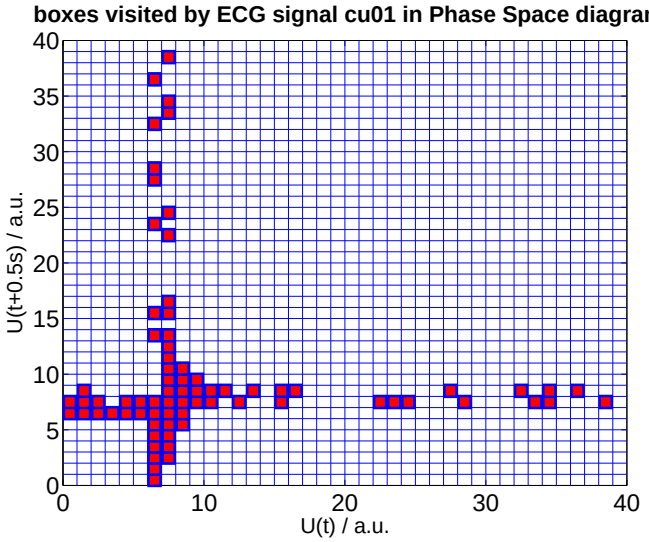

Figure 5.8: *Data points of a SR episode in the ECG signal cu01 from the CU database, visited boxes visualized in a phase space reconstruction diagram,* $d = 74/1600 = 0.05$.

Figure 5.9 shows a VF signal from the CU database.

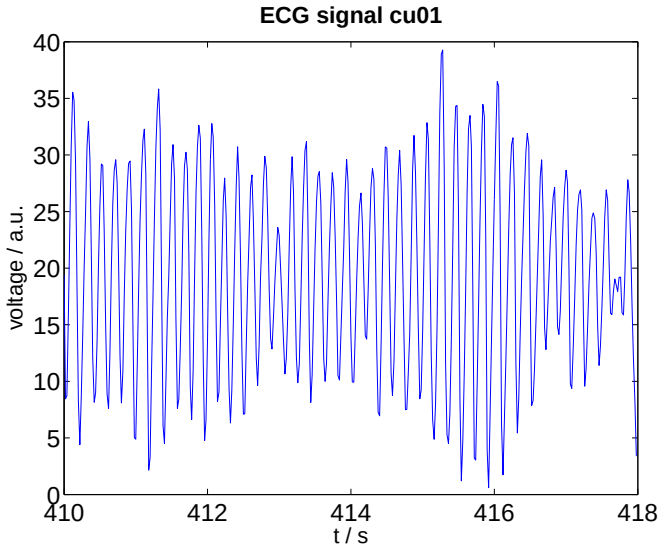

Figure 5.9: *VF episode in the ECG signal cu01 from the CU database.*

Figure 5.10 shows a phase space reconstruction plot corresponding to the VF signal from the previous figure. Again, the discrete data points are connected with red lines.

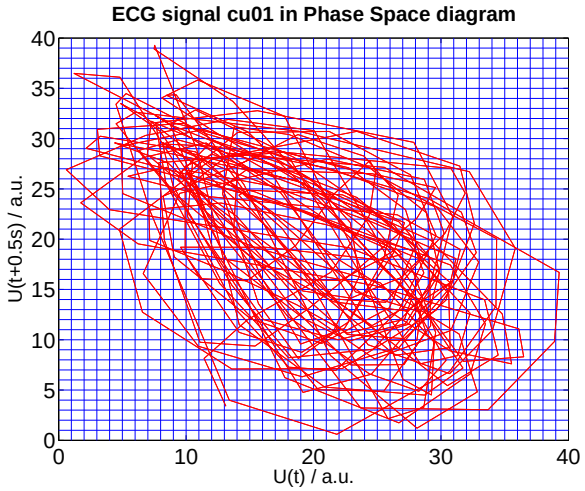

Figure 5.10: *VF episode in the ECG signal cu01 from the CU database, plotted in a phase space reconstruction diagram with a* 40×40 *grid. The data points are connected with red lines.*

Figure 5.11 shows the visited boxes in the phase space reconstruction plot corresponding to the VF signal from Figure 5.9. The individual dots are not connected.

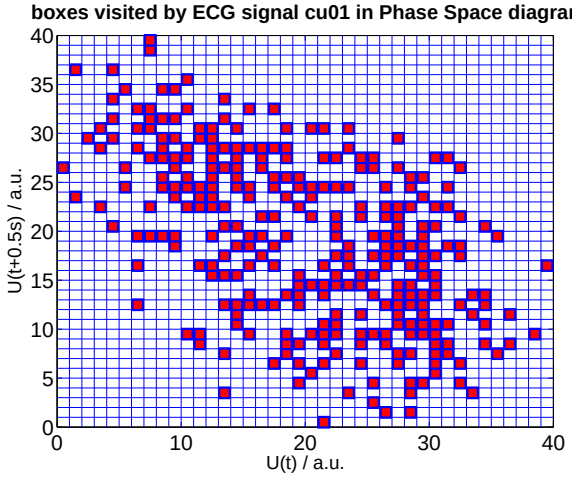

Figure 5.11: *Data points of a VF episode in the ECG signal cu01 from the CU database, visited boxes visualized in a phase space reconstruction diagram,* $d = 295/1600 = 0.18$.

Figure 5.12 shows the connected visited boxes in the phase space reconstruction plot corresponding to the SR signal from Figure 5.6.

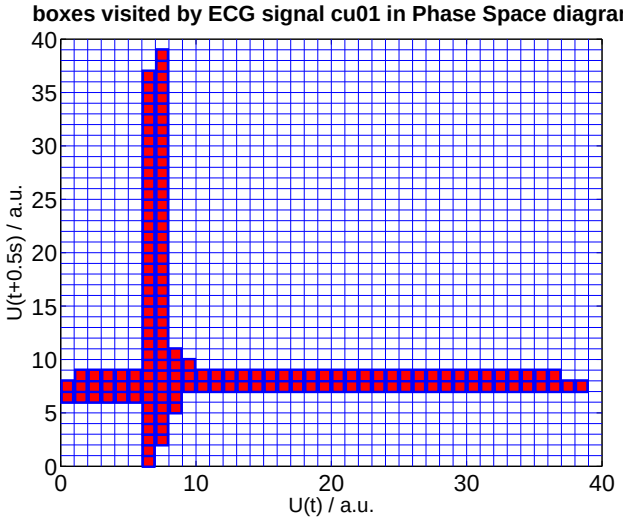

Figure 5.12: *Connected data points of a SR episode in the ECG signal cu01 from the CU database, visited boxes visualized in a phase space reconstruction diagram,* $d = 156/1600 = 0.1$.

Figure 5.13 shows the connected visited boxes in the phase space reconstruction plot corresponding to the VF signal from Figure 5.9.

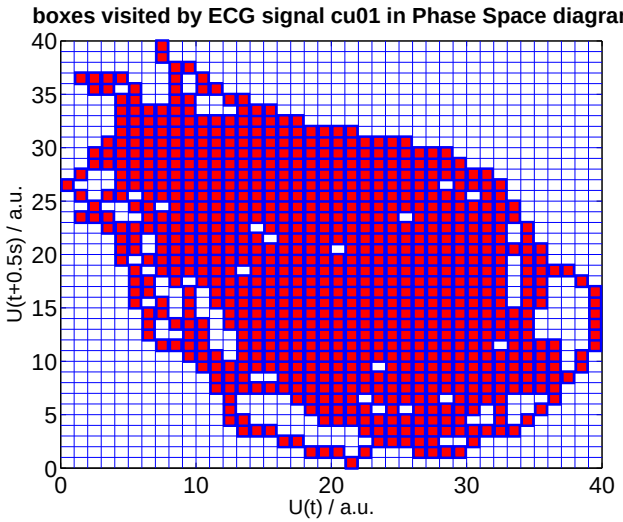

Figure 5.13: *Connected data points of a VF episode in the ECG signal cu01 from the CU database, visited boxes visualized in a phase space reconstruction diagram,* $d = 812/1600 = 0.51$.

5.4 Hilbert Transform algorithm

This algorithm (HILB) again uses a tool which is used in analyzing signals in order to identify chaotic behavior. The signal $x(t)$ is plotted in a diagram in the following way: On the x-axis we plot $x(t)$, on the y-axis we plot the Hilbert transform of the signal $x(t)$.

From [19], chapter 11, we see that the Hilbert transform $x_H(t)$ of a signal $x(t)$ is defined by:

$$x_H(t) = \frac{1}{\pi}\text{P.V.}\int_{-\infty}^{\infty} \frac{x(\tau)}{t-\tau}\, d\tau, \tag{5.8}$$

where P.V. means that the integral is taken in the sense of the Cauchy principal value. As one can see from Equation (5.8), the Hilbert transform can be considered as the convolution of the functions $x(t)$ and $\frac{1}{\pi t}$. Due to the properties of convolution, the Fourier transform $\widehat{X_H}(\omega)$ of $x_H(t)$ is the product of the Fourier transforms of $x(t)$ and $\frac{1}{\pi t}$. For physically relevant Fourier frequencies $\omega > 0$, $\widehat{X_H}(\omega) = -i\widehat{X}(\omega)$. This means that the Hilbert transform can be realized by an ideal filter whose amplitude response is unity and phase response is a constant $\frac{\pi}{2}$ lag at all Fourier frequencies.

This approach is very similar to the phase space reconstruction. Phase space reconstruction plots of irregular signals are chaotic and fill the phase space in a more or less uniform way. The same is true for the illustration of the Hilbert transform algorithm. Regular plots like ECG signals are regular in both the phase space reconstruction plot and the Hilbert transform plot. The difference is, that the phase space reconstruction algorithm uses a further parameter (Δ), that influences the plot and therefore the result of the analysis. ECG signals in PSR plots can result in circle like curves, but also in curves with a lot of straight lines with sharp edges (see plots in Section 5.3), depending on the choice of Δ. On the other side, plots of ECG signals calculated by the Hilbert Transform algorithm always show circle like curves, see Figures 5.14 and 5.16.

Again, we try to differentiate SR from VF. We assume VF signals to be chaotic, whereas SR signals to be regular. We plot the results of the Hilbert transform algorithm in a diagram and investigate, how much of the area in the plot is filled by the curve. To achieve this, we produce a 40×40 grid and count the visited boxes. From the result we again calculate the box dimension d. To calculate the box dimension we use the same strategy as in the PSR algorithm. We use the same thresholds d_0 and also sample down the signal in the same way.

The crtitical threshold parameter to obtain the ROC is d_0.

Figure 5.14 shows a Hilbert transform plot corresponding to the SR signal from Figure 5.6. In order to illustrate the plot better, the dots are connected with red lines.

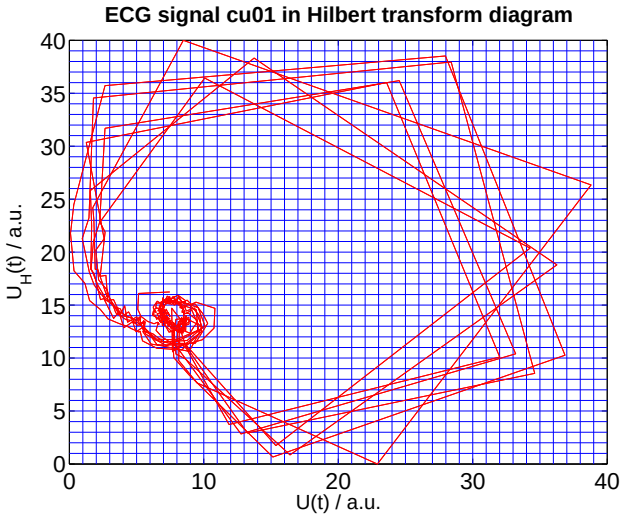

Figure 5.14: *SR episode in the ECG signal cu01 from the CU database, plotted in a Hilbert transform diagram with a* 40×40 *grid. The data points are connected with red lines.*

Figure 5.15 shows the visited boxes in the Hilbert transform plot corresponding to the SR signal from Figure 5.6. The individual dots are not connected.

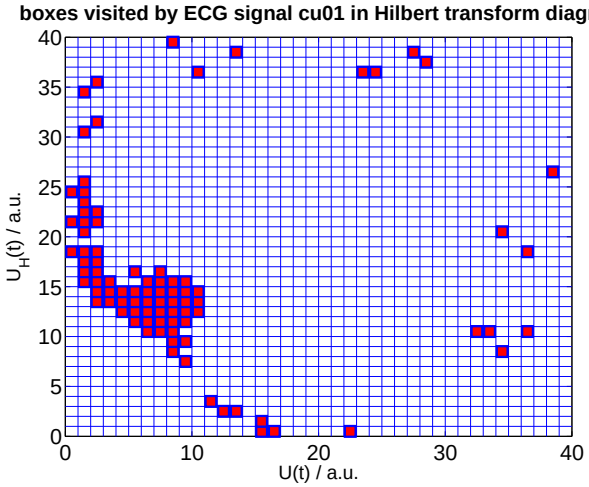

Figure 5.15: *Data points of a SR episode in the ECG signal cu01 from the CU database, visited boxes visualized in a Hilbert transform diagram,* $d = 88/1600 = 0.06$.

Figure 5.16 shows a Hilbert transform plot corresponding to the VF signal from Figure 5.9. Again, the discrete data points are connected with red lines.

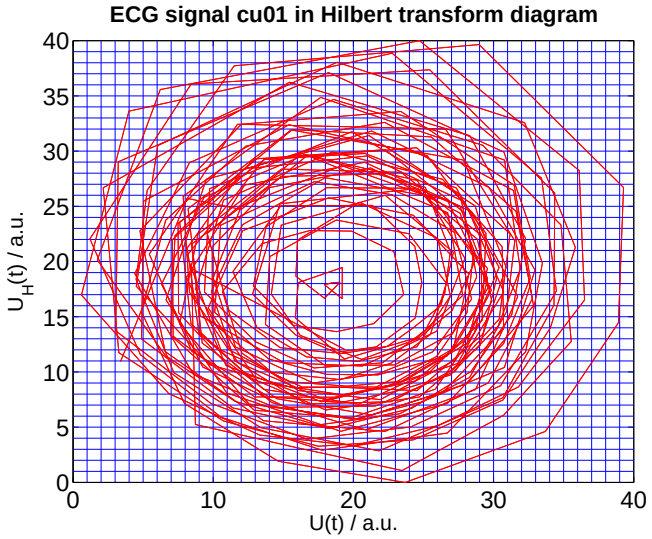

Figure 5.16: *VF episode in the ECG signal cu01 from the CU database, plotted in a Hilbert transform diagram with a* 40×40 *grid. The data points are connected with red lines.*

Figure 5.17 shows the visited boxes in the Hilbert transform plot corresponding to the VF signal from Figure 5.9. The individual dots are not connected.

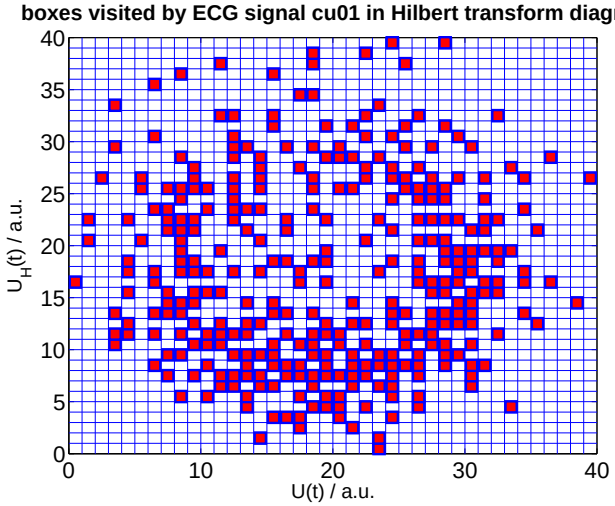

Figure 5.17: *Data points of a VF episode in the ECG signal cu01 from the CU database, visited boxes visualized in a Hilbert transform diagram,* $d = 333/1600 = 0.21$.

Similarly to the modifications in the PSR algorithm, we tried to improve also

the quality of the HILB algorithm by introducing three further approaches:

First, the algorithm works as described above. Then, as in "PSR_2", the first $500ms$ of the signal are considered again. The corresponding boxes in the Hilbert transform plot and their first neighbors are deleted from the "visiting list". Now the dimension is calculated. So, the calculated dimension is reduced compared to the dimension in the original algorithm version. The idea for carrying out this step is again the following: Periodic signals draw closed loops in the Hilbert transform plot. Sinus rhythm is expected to be periodic and does not cover much of the plot area. So its dimension is rather low. In eliminating boxes that had been visited in the first $0.5s$, which can be seen as a good part of a SR period, the dimension is reduced a lot. However, in VF signals the reduction of the Hilbert transform plot concerning to the first $0.5s$ does not have a great effect, although, of course, it is also reduced by a certain amount. Again, we wanted to see whether this approach improves the quality of the algorithm. Also this algorithm carries out a zero/one weighting of selected adaptive parts in the Hilbert transform plot. In this version, the threshold d_0 is set to 0.1. The results in the tables are called "HILB_2".

A further modification of "HILB_2" is investigated, which differs slightly from the "$\text{PSR}_{2,2}$" approach in the weighting function. Additionally to the described adaptive (depending on the first $500ms$ of the ECG signal) zero/one weighting an additional weighting is carried out. We have chosen a function, that multiplies areas near the center of the Hilbert transform plot with a high value as well as areas very far away from this center. Areas in a certain distance from the center are multiplied with a low value. So the weighting function decreases the values of the Hilbert transform plot, that lie on a ring around the center. The idea is, that SR signals generally visit this ring more often than VF signals. Here, the threshold d_0 is set to 0.017. By this approach, improved results should be achieved. Still, in our experiments the results were not improved, as seen in the tables in the lines called "$\text{HILB}_{2,2}$".

The third approach to improve the quality works exactly like the "PSR_3" algorithm: Not only the visited boxes are counted, but also the number, how often the boxes were visited, is considered. Each box gets a number, which is the inverse of the number of the corresponding "visits", except if the number of visits is zero. In the latter case the box gets the number zero. The dimension is calculated by summing up all numbers stored in the boxes. The idea of the construction was the same as in "PSR_3": In SR, the signal is expected to be periodic and so in the Hilbert transform plot there exists a trend that only a small number of boxes are visited, but this boxes are visited more often. Since a low box dimension is classified as SR, a high number of visits per box should result in an only low increase of the box dimension. Therefore, the number of visits in each box was inverted to calculate the box dimension. In SR signals, the average number of visits per box is higher than in VF signals, so this approach should improve the algorithm. The threshold d_0 is set to 0.12. The results in the tables are called "HILB_3".

As one can see in the results, the approaches from "HILB_2", "$\text{HILB}_{2,2}$" and

"HILB_3" did not improve the quality of the "HILB" algorithm significantly.

5.5 Wavelet based algorithms

In [15], (definition 1.1.1), one can see that a function $\psi \in L^2(\mathbb{R})$, for that holds

$$0 \ < \ c_\psi := 2\pi \int\limits_{\mathbb{R}} \frac{|\hat{\psi}(\omega)|^2}{|\omega|} \, d\omega \ < \ \infty, \tag{5.9}$$

is called *wavelet*. Here, $\hat{\psi}$ denotes the Fourier transform of ψ. The continuous wavelet transform $L_\psi f(a,b)$ of a function $f \in L^2(\mathbb{R})$ is defined by

$$L_\psi f(a,b) = \frac{1}{\sqrt{c_\psi \, |a|}} \int\limits_{\mathbb{R}} f(t) \ \psi \left(\frac{t-b}{a} \right) \, dt, \tag{5.10}$$

with $a \in \mathbb{R} \setminus \{0\}, \ b \in \mathbb{R}$.

The wavelet transform $L_\psi f$ contains information about the frequency distribution as well as information on the time distribution of a signal.

Moreover, from 1.1.9 in [15] it can be seen that the inversion of the continuous wavelet transform can be carried out in the following way:

$$f(t) = \frac{1}{\sqrt{c_\psi}} \int\limits_{\mathbb{R}} \int\limits_{\mathbb{R}} \frac{1}{\sqrt{|a|}} \ \psi \left(\frac{t-b}{a} \right) \ (L_\psi f(a,b)) \ \frac{da \ db}{a^2}. \tag{5.11}$$

According to lemma 1.1.7 from [15], the Fourier transform of $L_\psi f$ is given by

$$(\widehat{L_\psi f})(a,\omega) = \sqrt{\frac{2\pi \, |a|}{c_\psi}} \ \hat{\psi}(-a\,\omega) \ \hat{f}(\omega) = \sqrt{\frac{2\pi \, |a|)}{c_\psi}} \ \overline{\hat{\psi}(a\,\omega)} \ \hat{f}(\omega) \tag{5.12}$$

5.5.1 WVL_1, WVL_2 and WVL_3

Three simple wavelet based algorithms (WVL_1, WVL_2 and WVL_3) operate like SPEC in the frequency domain.

The idea of this first two algorithms is the following: First, a continuous wavelet transform (WT) of the ECG signal is carried out using a Mexican hat wavelet as mother wavelet ψ_m,

$$\psi_m(t) = (1 - t^2)\exp(-t^2/2). \tag{5.13}$$

Then a Fourier transform is performed. Now, the maximum absolute values with respect to a are investigated in order to make the decisions for the defibrillation process.

However, one can show that this maximum values are located on a hyperbola in the (a, ω) plane of the Fourier transform of the WT of the ECG signal, i.e. on a curve that has the representation $a\,\omega = C$, C being a constant. The values on this curve in the (a, ω) plane are the FT of the ECG signal multiplied by a weight function $y(\omega)$. Therefore, if one searches for the maximum values of $\widehat{L_\psi f}$ in the (a, ω) plane of the WT, it is sufficient to search for the maxima in the weighted FT of the ECG signal $\hat{f}(\omega)$.

Proof: First we introduce some symbols:

$f \ldots$ observed function,
$\psi \ldots$ wavelet,
$WT \ldots$ continuous wavelet transform,
$FT \ldots$ Fourier transform,
$L = WT(f) \ldots$ wavelet transform of f,
$a \ldots$ wavelet dilatation parameter,
$\omega \ldots$ angular frequency,
$c, c_i, \ldots$ constants, $i \in \mathbb{N}$,
$p, p_i \ldots$ parameters of the wavelets,
$g(p_1, p_2), h(p_1, p_2), k(p), l(p) \ldots$ functions of parameters p_i.

From [15], lemma 1.1.7, we can see

$$FT(L) = c_1\sqrt{|a|}\; FT(\psi)\; FT(f). \tag{5.14}$$

Since we know that the signal f is band limited in the frequency domain, $FT(L)$ has a maximum value for every a.

$FT(\psi)$ is a function of $a\omega$ and a parameter p, with p not depending on a or ω

$$FT(\psi) = g(a\,\omega, p). \tag{5.15}$$

Now, we substitute $a\,\omega$ by z and obtain $g(a\,\omega, p) = g(z, p)$. For the derivative of $g(a\omega, p)$ with respect to a we obtain

$$\begin{aligned}\frac{d}{da}\left(f(a\,\omega, p)\right) &= \frac{d}{d(a\,\omega)}\left(f(a\,\omega, p)\right) \cdot \frac{d(a\,\omega)}{da} \\ &= \omega\,\frac{d}{dz}\left(f(z, p)\right) = \omega\; h(z, p) = \omega\; h(a\,\omega, p). \end{aligned} \tag{5.16}$$

We want to find the maxima in $FT(L)$. If we first search for the maxima in $FT(L)$ with respect to the a-axis, we have to find the derivative of Equation (5.14) with respect to a and have to set it to zero. From now on we consider a to be positive.

$$\begin{aligned} & FT(f)\; c_1\; \frac{d}{da}\left(\sqrt{a}\; g(a\,\omega, p)\right) \doteq 0 \\ & \rightarrow \left(\frac{1}{2\sqrt{a}}\; g(a\,\omega, p) + \sqrt{a}\,\omega\; h(a\,\omega, p)\right) \doteq 0 \\ & \rightarrow \left(g(a\,\omega, p) + 2a\,\omega\; h(a\,\omega, p)\right) \doteq 0. \end{aligned} \tag{5.17}$$

We see that this is a function of $a\,\omega = z$ and p. We know, that the spectrum of the function f is bandlimited. Therefore, Equation (5.14) has a maximum value. Hence, we can find a value for z, that solves Equation (5.17). Since Equation (5.17) is a function of z and p, z is a function of the parameter p. For a constant p, z is a constant, that only depends on p

$$z = l(p) = c_p. \tag{5.18}$$

$l(p)$ is not always solvable analytically, but there always exists a solution, that can be found numerically. With $z = a\,\omega$ we get

$$a = \frac{c_p}{\omega}, \tag{5.19}$$

and furthermore the maxima of $FT(L)$ referred to a

$$\begin{aligned} FT(L)_{\text{maxima referred to a}} &= \sqrt{a}\; c_1\; FT(\psi)\; FT(f) \\ &= c_1\; \frac{\sqrt{c_p}}{\sqrt{\omega}}\; FT(f)\; g(a\omega, p) \\ &= c_1 \sqrt{c_p} \frac{1}{\sqrt{\omega}} FT(f)\; g(c_p, p) \\ &= c_2 \frac{1}{\sqrt{\omega}} FT(f)\; g(c_p, p) \\ &= c_2 \frac{1}{\sqrt{\omega}} FT(f)\; c_3 \\ &= c_4 \frac{1}{\sqrt{\omega}} FT(f). \end{aligned}$$

So, the maxima of $FT(L)$ lie on a curve with $a\,\omega = c_p$. The values of $FT(L)$ on this curve can be calculated by a weighting of $FT(f)$

$$FT(L)_{\text{maxima referred to a}} = c_4 \frac{1}{\sqrt{\omega}} FT(f). \tag{5.20}$$

So, the weight function y is

$$\text{weight} = y \sim \frac{1}{\sqrt{\omega}}. \tag{5.21}$$

We are not interested in the exact values of the maxima of $FT(L)$, because in the ventricular fibrillation detection we work with arbitrary units of the amplitude and rescale the ECG signals many times. Therefore, we do not need to calculate the value of c_4 and set it to 1.

In detail, the algorithms work in the following way:

In WVL_1 this function is handled similar to the spectrum in the algorithm SPEC. First, each data segment is multiplied by a Hamming window and transformed into the frequency domain by fast Fourier transform (FFT). The result is multiplied by $\frac{1}{\sqrt{\omega}}$ for reasons described above. But only two parameters are calculated and thresholds for the decision are set. First, a threshold of 15% of the maximum value of the FFT signal is chosen. All signal parts below this threshold are set to zero. Afterwards A_1 and A_2 are calculated. A_1 is the maximum amplitude of the FFT between 0.5 Hz and 3.5 Hz. A_2 is the maximum amplitude of the FFT between 3.5 Hz and 20 Hz. If the ratio A_1/A_3 is smaller than 1.5, VF is detected.

WVL_2 is a slight modification of WVL_1. Each data segment is multiplied by a Hamming window and transformed into the frequency domain by fast Fourier transform (FFT). The result is squared (so the energy distribution is observed). Also here, the result is multiplied by $\frac{1}{\sqrt{\omega}}$. Three parameters A_1, A_2 and A_3 are calculated. A_1 is the energy content of the ECG signal between 0.5 Hz and 3.5 Hz, A_2 is the energy content of the ECG signal between 3.5 Hz and 9 Hz, and A_3 is the energy content of the ECG signal between 9 Hz and 50 Hz.

If $(A_1 + A_3)/A_2$ is smaller than 0.5, VF is detected.

In WVL_3 the function $\frac{1}{\sqrt{\omega}}\,\hat{f}(\omega)$ is handled exactly like the spectrum in the algorithm SPEC. The same spectrum parameters are calculated and also the thresholds for the decision, $A_{1,0}, A_{2,0}, A_{3,0}, M_0$, have the same values like the algorithm in SPEC.

In WVL_1, the critical threshold parameter to obtain the IROC is $A_{1,0}/A_{3,0}$, in WVL_2 it is $(A_{1,0} + A_{3,0})/A_{2,0}$, and in WVL_3 it is M_0.

5.5.2 WVL_4

This method of detecting ventricular fibrillation uses a discrete wavelet transform.

The continuous wavelet transform is performed by Equation (5.10). The inverse continuous wavelet transform is carried out by Equation (5.11). For certain criteria it can be shown that it is not necessary to know $L_\psi f(a,b)$ for every a and b to perform a perfect reconstruction. It can be shown that the inverse wavelet transform, Equation (5.11), can be reduced to a double summation over certain discrete values of a and b to get the original signal without loss of information.

In [1], section 3.2.2 it is shown that the discrete wavelet transform with dyadic grid the wavelet $\psi_{m,n}(t)$ can be written as

$$\psi_{m,n}(t) = \frac{1}{\sqrt{2^m}}\,\psi(\frac{t-n2^m}{2^m}), \tag{5.22}$$

with $n, m \in \mathbb{Z}$ and $\psi(\frac{t-b}{a})$ being the continuous wavelet. So, the wavelet is brought from the continuous form into a discrete form. Using the dyadic grid wavelet, the discrete wavelet transform (DWT) can be written as:

$$T_{m,n} = \int_{-\infty}^{\infty} f(t)\,\psi_{m,n}(t)\,dt. \tag{5.23}$$

Dyadic grid wavelets are called orthonormal, if

$$\int_{-\infty}^{\infty} \psi_{m,n}(t)\,\psi_{m',n'}(t)\,dt = \begin{cases} 1 & \text{if } m = m' \text{ and } n = n' \\ 0 & \text{otherwise} \end{cases}$$

By choosing an orthonormal wavelet basis, $\psi_{m,n}(t)$, it is possible to reconstruct the original signal in terms of the wavelet coefficients,

$$f(t) = \sum_{m=-\infty}^{\infty} \sum_{n=-\infty}^{\infty} T_{m,n}\,\psi_{m,n}(t). \tag{5.24}$$

Now, we can summarize different terms together. We define the *continuous approximation* of the signal at scale m_0

$$f_{m_0}(t) := \sum_{m=m_0+1}^{\infty} \sum_{n=-\infty}^{\infty} T_{m,n}\psi_{m,n}(t), \tag{5.25}$$

and the *signal detail* at scale m

$$d_m(t) := \sum_{n=-\infty}^{\infty} T_{m,n}\psi_{m,n}(t). \tag{5.26}$$

Hence, we can write Equation (5.24) as

$$f(t) = f_{m_0}(t) + \sum_{m=-\infty}^{m_0} d_m(t). \tag{5.27}$$

It is easy to show that

$$f_{m-1}(t) = f_m(t) + d_m(t), \tag{5.28}$$

which tells us that if we add the signal detail at an arbitrary scale (index m) to the approximation at that scale we get the signal approximation at an increased resolution (i.e. at a smaller scale, index $m-1$). This is called a ***multiresolution representation***.

Now we want to consider the technique used in the fibrillation detection algorithm WVL_4. It is split into two parts:

(i) Finding VF:

The first part uses the algorithm SPEC (Section 2.4) to search the for typical VF properties in the ECG. If the algorithm decides that the ECG part contains VF, then the result is accepted as true and no further investigation is carried out. This procedure can be justified by the high specificity of the SPEC algorithm. If the algorithm yields that the ECG part is "no VF", a further investigation is carried out to confirm this result or to disprove it:

(ii) Discrete Wavelet Transform (DWT):

This part is only carried out, if the first part of the algorithm considers the ECG episode yields "no VF". In this case a discrete wavelet transform is applied, that searches for QRS complexes. If more than two but less than 40 QRS complexes are found within an 8 second episode, "no VF" is diagnosed. Otherwise the two spectral parameters $FSMN$ and A_2 from the first part are investigated again. If $FSMN < 2.5$ and $A_2 > 0.2$, the considered ECG part is diagnosed as VF. Figures 5.18 and 5.19 show two ECG parts that are treated with this algorithm.

The mentioned range for the number of found QRS complexes has a reason: Sometimes, especially in ECGs with a high amount of noise, the DWT part makes wrong interpretations and "finds" QRS complexes also in QRS free episodes. Therefore, a minimal number of three QRS complexes is demanded to confirm the existence of QRS complexes. On the other side, if the DWT part "finds" more than 40 QRS complexes (equal to a pulse of 300 beats per minute), the signal is likely to be VF, since such high sinus rhythms do not appear. The limits of the range were chosen from experiments with data.

The DWT algorithm works in the following way:

The third scale of a discrete wavelet transform with 12 scales and a Daubechies8 wavelet family is used. Experiments have shown that this scale makes it easiest

to distinguish VF from "no VF". If the signal in the third scale has a value higher than a certain threshold, the according ECG part is considered as a QRS complex. The threshold used in this investigation is set to $0.14\,\max(\text{ECG signal})$. Multiple peaks belonging to the same QRS complex are removed.

In WVL_4, no IROC is calculated due to the special structure of the algorithm. Since it exists of two parts and the second part is not executed always, we do not have a parameter that includes the calculations of both algorithm parts in every ECG segment. Since we cannot calculate an IROC. It would be possible to use the parameters of the SPEC algorithm as an IROC parameter, but this would not cover the whole complexity of the WVL_4 algorithm.

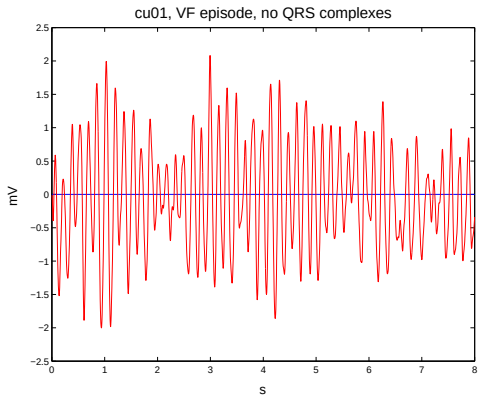

Figure 5.18: *DWT: no QRS-complexes (blue line is zero) detected in an 8s VF episode (red) of cu01 from [17]*

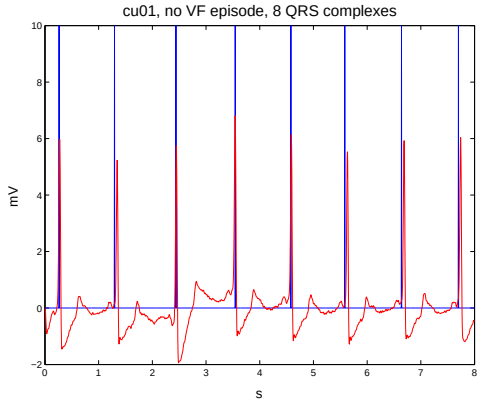

Figure 5.19: *DWT: 8 QRS-complexes (blue line has spikes) detected in an 8s SR episode (red) of cu01 from [17]*

Chapter 6

Evaluation and Results, Numerical Values

All algorithms are implemented in MATLAB using a graphical user interface. For the analysis, we selected the data in steps of one second and investigated intervals from 3 to 10 seconds window length. These sequences were tested with all algorithms. Finally we recorded the results together with the annotation in an output file.

The perfect algorithm would have values for the sensitivity, specificity, positive predictivity, accuracy, and IROC of 1. In this investigation the analyzed signals were not changed by, for example, adding noise or CPR artifacts.

The algorithms under investigation are expected to be used in AEDs. Hence, no preselection of ECG signals was carried out since this equals the situation of a bystander more appropriately.

The data sets were taken from the BIH-MIT data bank (48 files, 2 channels per file, each channel 1805 seconds long), the CU data bank (35 files, 1 channel per file, each channel 508 seconds long), and the AHA data bank (files 7001 - 8210, 40 files, 2 channels per file, each channel 1800 seconds long). From the BIH-MIT and AHA data bank we used both channels. Thus, the total number of tests per algorithm and window length is $2 \cdot 48 \cdot (1805 - \text{window length} + 1) + 35 \cdot (508 - \text{window length} + 1) + 2 \cdot 40 \cdot (1800 - \text{window length} + 1)$. Hence, for a window length of $8s$ the number of decisions is 333 583.

6.1 Numerical results

The quality parameters found in the experiments using window lengths of 3 to 10 seconds are presented in the following tables. The sensitivity (Sns.) and specificity (Spc.) were calculated by Equations (1.1) and (1.2). These equations are the appropriate ones to quantify the quality of VF detection algorithms. Furthermore, the accuracy (Ac.) and the positive predictivity (PP.), the integrated receiver operator characteristic (IROC) and the calculation time (ct.)

were determined. In order to describe the QRS detection algorithms as well, the quality parameters for this kind of algorithms were calculated by slightly altered equations:

Sensitivity is then the probability to detect QRS complexes. It is given by the quotient

$$\frac{\text{detected cases of SR}}{\text{all cases of SR}} = \frac{TP}{TP+FN}, \tag{6.1}$$

with TP being the number of true positive decisions, FN the number of false negative decisions.

Specificity is the probability to identify "no SR" correctly.

It is given by the quotient

$$\frac{\text{detected cases of "no SR"}}{\text{all cases of "no SR"}} = \frac{TN}{TN+FP}, \tag{6.2}$$

where TN is the number of true negative decisions, and FP is the number of false positive decisions.

The positive predictivity reads as

$$\frac{\text{detected cases of "SR"}}{\text{all cases classified by the algorithm as "SR"}} = \frac{TP}{TP+FP}. \tag{6.3}$$

Finally, the accuracy is given by

$$\frac{\text{all true decisions of "SR" and "no SR"}}{\text{all decisions}} = \frac{TP+TN}{TP+FP+TN+FN}. \tag{6.4}$$

The calculation time was computed only for the algorithms working as VF detectors, since it is the same in the QRS detection mode. The reason is that the time consuming operations are the calculation of parameters, and this operations are identical in both (VF and QRS) cases. The calculation time was quantified by investigating the CU data base on a PowerMac G5 computer with a Dual 2 GHz processor and 1.5 GB DDR SDRAM running parallel two processes of MATLAB. In the following tables, the results of the QRS detection analysis are indexed with "QRS". Beside the two algorithms LI and TOMP all other algorithms were tested for their qualification as QRS detectors too. Where no value could be calculated (either due to division by zero or other reasons), a bar (-) was put into the table.

The results of the Tables 6.1 to 6.32 are plotted in Section 7.2. The first 16 tables show the quality parameters sensitivity, specificity and integrated receiver operator characteristic.

The first table shows the results for a window length of 8 seconds. This window length can easily be used in AEDs and also gives good results. The algorithms are usually adjusted for this window length, hence this table is the most important one.

Data Source	*MIT DB*		*CU DB*		*AHA DB*		*overall results*		
Parameter	Sns.	Spc.	Sns.	Spc.	Sns.	Spc.	Sns.	Spc.	IROC
AAR_{50}	80.4	89.1	72.2	73.7	84.6	63.6	82.9	78.4	86.9
AAR_{100}	100	2.7	69.7	64.3	83.0	72.5	81.4	32.7	44.6
AAR_{250}	100	2.7	60.2	60.1	84.6	61.1	81.5	28.0	53.5
ACF_{95}	33.2	45.9	38.1	58.9	51.5	52.2	49.6	49.0	49.6
ACF_{99}	59.4	30.1	54.7	49.3	71.5	40.3	69.2	35.0	49.6
CPLX	6.3	92.4	56.4	86.6	60.2	91.9	59.2	92.0	86.7
HILB	86.0	97.9	74.7	85.4	84.4	95.1	83.1	96.2	94.5
$HILB_2$	92.3	96.4	77.2	81.9	84.3	91.7	83.4	93.9	93.3
$HILB_{2,2}$	82.2	92.6	66.8	82.9	78.4	90.8	76.9	91.5	89.3
$HILB_3$	87.4	97.8	75.2	84.9	84.1	95.2	82.9	96.2	94.2
LI	3.1	95.1	7.5	94.8	9.3	92.0	9.0	93.9	58.1
LI_m	100	64.7	91.6	25.7	92.7	46.7	92.6	55.9	74.1
MEA	62.9	80.8	60.1	87.5	49.8	88.6	51.2	84.1	80.2
PSR_{old}	79.7	97.6	65.9	87.9	67.6	97.5	67.5	97.1	87.8
PSR	74.8	99.2	70.2	89.3	80.4	96.8	79.0	97.8	94.1
PSR_2	83.9	98.9	71.1	87.4	79.7	94.2	78.6	96.5	93.3
$PSR_{2,2}$	88.5	72.4	85.3	55.0	83.9	64.8	84.1	68.7	85.2
PSR_3	89.9	96.2	79.9	76.0	86.7	88.7	85.8	92.4	94.2
SC2	63.6	98.2	60.4	96.2	62.7	99.8	62.4	98.7	89.4
SCA	72.4	98.0	67.7	94.9	71.7	99.7	71.2	98.5	91.5
SPEC	23.1	100	29.0	99.3	29.2	99.8	29.1	99.9	88.0
$SPEC_m$	55.6	97.6	55.0	93.3	52.3	94.4	52.7	96.2	88.8
STE	54.5	83.4	52.9	66.6	49.6	81.0	50.1	81.7	67.0
TCI	74.5	83.9	71.0	70.5	75.7	86.9	75.1	84.4	80.9
TOMP	68.5	40.6	71.3	48.4	95.9	39.7	92.5	40.6	67.2
VF	29.4	100	30.8	99.5	16.9	100	18.8	100	86.5
WVL_1	37.1	82.0	48.8	83.9	32.4	79.0	34.5	80.9	50.9
WVL_2	11.2	99.5	35.4	98.1	14.6	99.5	17.2	99.4	46.2
WVL_3	28.7	99.9	26.2	99.4	26.8	99.5	26.7	99.7	79.5
WVL_4	81.1	89.0	61.0	72.1	73.5	89.6	72.0	88.4	-

Table 6.1: *Quality of fibrillation detection algorithms used as VF detectors (sensitivity, specificity, receiver operator characteristic) for a window length of 8 seconds in per cent, rounded on 3 digits.*

Data Source	*MIT DB*		*CU DB*		*AHA DB*		*overall results*		
Parameter	Sns.	Spc.	Sns.	Spc.	Sns.	Spc.	Sns.	Spc.	IROC
$AAR_{50,QRS}$	88.9	10.6	73.3	69.6	63.4	87.7	78.1	76.3	82.3
$AAR_{100,QRS}$	2.8	100	65.2	71.8	72.7	88.4	33.4	87.5	52.5
$AAR_{250,QRS}$	2.8	100	61.0	62.8	61.0	87.7	28.5	85.9	60.5
$ACF_{95,QRS}$	45.5	31.6	59.3	39.9	52.7	54.4	49.0	49.9	51.0
$ACF_{99,QRS}$	29.8	52.4	49.7	56.1	40.9	75.3	35.1	70.2	51.0
$CPLX_{QRS}$	92.3	0.6	86.3	53.7	91.3	61.2	91.6	53.1	79.5
$HILB_{QRS}$	97.9	9.4	85.1	71.8	95.1	90.6	96.2	78.7	91.7
$HILB_{2,QRS}$	96.5	13.7	81.7	74.5	91.6	90.2	93.9	79.2	91.5
$HILB_{2,2,QRS}$	92.6	13.6	83.1	65.6	90.7	83.2	91.4	72.8	85.8
$HILB_{3,QRS}$	97.8	9.6	84.6	72.3	95.1	90.3	96.2	78.5	91.3
LI_{QRS}	95.3	15.0	95.1	8.5	92.0	9.5	94.0	10.0	60.6
$LI_{m,QRS}$	65.7	87.4	25.8	91.1	47.1	97.9	56.5	95.8	77.1
MEA_{QRS}	80.9	25.2	87.3	57.8	88.4	51.8	84.1	49.4	77.7
$PSR_{old,QRS}$	97.6	10.3	87.7	63.3	97.4	72.7	97.1	64.2	86.2
PSR_{QRS}	99.2	7.4	89.1	67.8	96.7	86.4	97.8	74.8	91.5
$PSR_{2,QRS}$	98.9	10.3	87.4	69.2	94.2	85.5	96.5	74.6	91.8
$PSR_{2,2,QRS}$	73.2	70.8	54.8	83.5	65.0	88.6	69.1	85.8	85.3
$PSR_{3,QRS}$	96.2	12.8	75.8	77.6	88.7	92.7	92.3	81.4	91.5
$SC2_{QRS}$	98.2	5.5	96.0	58.0	99.6	66.9	98.7	58.6	86.4
SCA_{QRS}	97.9	6.4	94.8	65.2	99.5	76.6	98.4	66.9	88.4
$SPEC_{QRS}$	100	2.1	99.2	27.6	99.8	31.6	99.9	27.6	85.7
$SPEC_{m,QRS}$	97.6	6.6	93.2	52.7	94.5	56.4	96.2	50.1	88.4
STE_{QRS}	83.2	9.5	66.2	50.7	80.1	47.4	81.2	43.4	63.1
TCI_{QRS}	77.3	14.3	61.1	76.9	76.8	87.4	76.4	77.5	76.7
$TOMP_{QRS}$	40.6	61.4	48.0	69.1	39.1	95.6	40.3	88.3	65.4
VF_{QRS}	100	2.6	99.4	29.3	100	18.2	100	17.8	84.4
$WVL_{1,QRS}$	81.6	3.2	83.6	46.6	79.3	34.8	80.8	32.6	47.5
$WVL_{2,QRS}$	99.5	0.9	98.0	34.0	99.5	15.7	99.4	16.3	45.9
$WVL_{3,QRS}$	99.9	2.8	99.2	24.6	99.5	28.9	99.7	25.3	79.7
$WVL_{4,QRS}$	88.9	14.2	71.8	58.9	89.7	79.4	88.4	69.2	-

Table 6.2: *Quality of fibrillation detection algorithms used as QRS detectors (sensitivity, specificity, receiver operator characteristic) for a window length of 8 seconds in per cent, rounded on 3 digits.*

Data Source	*MIT DB*		*CU DB*		*AHA DB*		*overall results*		
Parameter	Sns.	Spc.	Sns.	Spc.	Sns.	Spc.	Sns.	Spc.	IROC
AAR_{50}	84.3	87.9	77.1	72.4	75.5	86.7	75.8	86.7	84.7
AAR_{100}	97.6	38.0	71.0	65.4	82.7	72.6	81.3	52.7	73.2
AAR_{250}	100	7.5	64.0	61.6	85.7	60.0	82.9	30.4	58.7
ACF_{95}	33.2	36.0	44.6	47.7	56.4	35.7	54.6	36.4	41.4
ACF_{99}	51.4	31.1	58.0	42.8	70.1	29.5	68.4	31.0	41.4
CPLX	21.0	80.7	72.9	66.7	78.6	72.9	77.3	77.0	83.7
HILB	0.0	100	0.0	100	0.0	100	0.0	100	94.0
$HILB_2$	96.5	13.7	81.7	74.5	91.6	90.2	93.9	79.2	93.7
$HILB_{2,2}$	0.3	99.7	1.8	99.6	1.6	99.4	1.6	99.6	83.4
$HILB_3$	0.0	100	0.0	100	0.0	100	0.0	100	93.9
LI	10.8	91.6	13.9	89.3	16.1	88.2	15.8	90.2	53.6
LI_m	100	60.0	96.4	22.3	93.9	40.7	94.2	50.8	72.1
MEA	53.1	77.8	57.7	86.3	45.0	87.6	46.7	82.0	71.9
PSR_{old}	19.9	100	0.0	100	0.0	100	0.2	100	88.2
PSR	0.0	100	0.0	100	0.0	100	0.0	100	90.1
PSR_2	0.0	100	0.0	100	0.0	100	0.0	100	93.2
$PSR_{2,2}$	6.6	98.7	8.7	96.9	8.2	97.2	8.3	98.0	79.5
PSR_3	0.0	100	0.0	100	0.0	100	0.0	100	94.7
SC2	74.5	96.8	69.3	92.8	64.0	99.1	64.8	97.5	89.5
SCA	81.8	96.3	75.3	90.6	72.8	98.7	73.2	97.0	91.6
SPEC	13.3	100	19.6	99.4	16.6	99.8	16.9	99.9	89.4
$SPEC_m$	55.6	97.7	52.9	93.4	45.3	93.7	46.3	95.9	90.4
STE	14.7	93.7	20.9	80.0	13.2	96.2	14.2	94.1	43.7
TCI	82.5	78.1	73.5	62.6	75.2	78.3	75.0	77.5	80.9
TOMP	68.5	40.0	74.4	47.1	96.7	38.5	93.6	39.7	67.0
VF	38.1	100	32.6	99.5	17.4	99.9	19.6	99.9	84.9
WVL_1	10.5	80.1	45.6	85.3	27.6	77.9	29.7	79.5	45.7
WVL_2	0.3	99.5	33.5	99.5	11.5	99.5	14.2	99.5	44.7
WVL_3	24.1	100	21.2	99.6	17.0	99.7	17.6	99.9	81.9
WVL_4	81.1	80.7	66.4	65.5	71.8	78.6	71.2	79.2	-

Table 6.3: *Quality of fibrillation detection algorithms used as VF detectors (sensitivity, specificity, receiver operator characteristic) for a window length of 3 seconds in per cent, rounded on 3 digits.*

Data Source	*MIT DB*		*CU DB*		*AHA DB*		*overall results*		
Parameter	Sns.	Spc.	Sns.	Spc.	Sns.	Spc.	Sns.	Spc.	IROC
$AAR_{50,QRS}$	87.8	11.4	72.1	74.6	86.8	81.5	86.7	72.5	83.6
$AAR_{100,QRS}$	38.0	66.1	66.2	72.7	72.8	88.1	53.1	83.5	75.6
$AAR_{250,QRS}$	7.7	100	62.5	66.3	60.0	89.2	31.0	87.4	65.4
$ACF_{95,QRS}$	35.8	50.2	48.3	47.0	36.4	59.3	36.6	56.7	45.0
$ACF_{99,QRS}$	30.9	57.2	43.3	60.0	30.2	73.8	31.2	70.1	45.0
$CPLX_{QRS}$	80.3	2.2	66.1	69.5	72.1	78.6	76.4	68.5	76.4
$HILB_{QRS}$	100	0.0	100	0.0	100	0.0	100	0.0	91.5
$HILB_{2,QRS}$	100	0.0	100	0.0	100	0.0	100	0.0	92.5
$HILB_{2,2,QRS}$	99.7	0.1	99.6	1.6	99.4	1.6	99.6	1.5	80.4
$HILB_{3,QRS}$	100	0.0	100	0.0	100	0.0	100	0.0	91.4
LI_{QRS}	91.8	17.2	89.8	15.4	88.2	16.2	90.3	16.2	55.5
$LI_{m,QRS}$	60.9	87.6	22.3	96.0	41.1	99.0	51.3	97.3	74.7
MEA_{QRS}	77.8	24.2	86.1	55.5	87.4	46.4	82.0	45.0	69.5
$PSR_{old,QRS}$	100	1.6	100	0.0	100	0.0	100	0.2	86.4
PSR_{QRS}	100	0.0	100	0.0	100	0.0	100	0.0	87.7
$PSR_{2,QRS}$	100	0.0	100	0.0	100	0.0	100	0.0	92.1
$PSR_{2,2,QRS}$	98.7	2.7	96.9	8.5	97.3	8.8	98.0	8.1	80.6
$PSR_{3,QRS}$	100	0.0	100	0.0	100	0.0	100	0.0	91.6
$SC2_{QRS}$	96.8	6.5	92.8	66.9	98.8	67.8	97.4	60.5	85.9
SCA_{QRS}	96.3	7.4	90.6	72.8	98.4	77.0	96.9	68.3	87.9
$SPEC_{QRS}$	100	1.2	99.3	18.7	99.8	17.9	99.9	16.0	87.0
$SPEC_{m,QRS}$	97.7	5.6	93.2	50.7	93.8	48.7	95.9	43.9	89.5
STE_{QRS}	93.7	3.2	79.7	20.0	95.2	8.8	93.6	9.6	41.9
TCI_{QRS}	77.7	16.3	62.2	72.2	77.9	77.8	77.1	69.9	76.7
$TOMP_{QRS}$	40.1	63.4	46.8	72.7	37.9	96.4	39.5	89.6	65.1
VF_{QRS}	100	3.2	99.4	31.1	99.9	18.8	99.9	18.6	82.8
$WVL_{1,QRS}$	79.8	0.9	85.1	43.9	78.2	29.6	79.4	28.0	42.9
$WVL_{2,QRS}$	99.5	0.0	99.5	32.3	99.5	12.4	99.5	13.4	44.9
$WVL_{3,QRS}$	100	2.0	99.4	20.1	99.7	18.4	99.9	16.7	82.5
$WVL_{4,QRS}$	80.5	14.3	65.1	63.9	78.8	77.3	79.2	68.2	-

Table 6.4: *Quality of fibrillation detection algorithms used as QRS detectors (sensitivity, specificity, receiver operator characteristic) for a window length of 3 seconds in per cent, rounded on 3 digits.*

Data Source	*MIT DB*		*CU DB*		*AHA DB*		*overall results*		
Parameter	Sns.	Spc.	Sns.	Spc.	Sns.	Spc.	Sns.	Spc.	IROC
AAR_{50}	82.2	88.3	75.8	74.8	74.9	88.7	75.1	87.8	85.2
AAR_{100}	99.3	36.4	69.4	64.9	82.5	74.4	80.9	52.5	72.5
AAR_{250}	100	4.7	62.4	61.4	85.2	60.6	82.3	29.0	56.1
ACF_{95}	42.3	46.2	45.2	54.1	57.9	48.4	56.1	47.4	50.7
ACF_{99}	55.9	38.7	56.0	48.3	72.4	42.7	70.2	40.7	50.7
CPLX	15.0	84.7	72.6	69.7	80.0	75.6	78.4	80.5	84.4
HILB	0.0	100	0.0	100	0.0	100	0.0	100	94.1
$HILB_2$	0.0	100	0.0	100	0.0	100	0.0	100	93.6
$HILB_{2,2}$	10.8	98.9	10.7	97.6	13.9	97.7	13.4	98.4	85.4
$HILB_3$	0.0	100	0.0	100	0.0	100	0.0	100	94.5
LI	7.0	92.9	11.3	91.4	13.2	89.6	12.9	91.5	54.8
LI_m	100	61.5	95.4	23.4	93.6	42.7	93.9	52.5	72.8
MEA	58.0	79.1	59.0	86.9	46.3	88.3	48.1	83.1	75.6
PSR_{old}	59.4	99.9	24.0	99.7	15.4	100	16.9	99.9	88.5
PSR	0.0	100	0.0	100	0.0	100	0.0	100	93.7
PSR_2	0.0	100	0.0	100	0.0	100	0.0	100	93.4
$PSR_{2,2}$	36.4	92.7	47.0	85.5	44.5	89.1	44.8	91.0	81.7
PSR_3	4.5	100	1.4	100	2.3	100	2.2	100	95.1
SC2	73.4	97.5	67.0	94.4	63.3	99.5	63.9	98.1	89.5
SCA	82.2	97.1	72.7	92.2	72.4	99.2	72.5	97.7	91.6
SPEC	18.9	100	25.3	99.3	23.5	99.8	23.7	99.9	88.3
$SPEC_m$	54.9	97.2	54.6	92.6	48.6	93.7	49.5	95.6	89.4
STE	19.6	96.3	25.3	81.7	15.5	97.2	16.8	96.0	49.2
TCI	71.3	86.5	65.6	74.3	63.3	89.5	63.7	87.1	80.9
TOMP	68.5	40.5	71.5	49.1	96.3	39.4	92.8	40.5	67.1
VF	36.7	100	32.2	99.5	17.6	99.9	19.6	99.9	85.4
WVL_1	34.3	79.8	48.7	81.9	30.9	76.9	33.2	78.7	48.4
WVL_2	5.9	99.5	35.8	98.3	13.9	99.4	16.6	99.4	46.5
WVL_3	26.2	100	21.7	99.5	20.7	99.7	20.9	99.8	79.4
WVL_4	80.1	83.5	65.0	68.7	73.2	82.6	72.2	82.5	-

Table 6.5: *Quality of fibrillation detection algorithms used as VF detectors (sensitivity, specificity, receiver operator characteristic) for a window length of 4 seconds in per cent, rounded on 3 digits.*

Data Source	*MIT DB*		*CU DB*		*AHA DB*		*overall results*		
Parameter	Sns.	Spc.	Sns.	Spc.	Sns.	Spc.	Sns.	Spc.	IROC
$AAR_{50,QRS}$	88.2	10.9	74.5	73.2	88.8	80.9	87.8	71.7	84.2
$AAR_{100,QRS}$	36.4	69.0	65.8	71.3	74.6	88.0	52.9	83.6	75.2
$AAR_{250,QRS}$	4.7	100	62.3	64.8	60.5	88.4	29.5	86.6	62.9
$ACF_{95,QRS}$	45.7	30.7	54.7	47.5	48.8	60.9	47.4	55.7	52.0
$ACF_{99,QRS}$	38.3	38.2	49.0	58.1	43.2	76.3	40.7	69.5	52.0
$CPLX_{QRS}$	84.4	1.5	69.2	69.1	74.8	80.3	79.9	69.7	77.2
$HILB_{QRS}$	100	0.0	100	0.0	100	0.0	100	0.0	91.6
$HILB_{2,QRS}$	100	0.0	100	0.0	100	0.0	100	0.0	92.3
$HILB_{2,2,QRS}$	98.9	2.2	97.5	10.3	97.7	14.8	98.4	12.7	82.0
$HILB_{3,QRS}$	100	0.0	100	0.0	100	0.0	100	0.0	91.8
LI_{QRS}	93.1	17.2	91.8	12.7	89.6	13.3	91.6	13.7	56.7
$LI_{m,QRS}$	62.4	87.2	23.5	95.0	43.2	98.8	53.0	96.9	75.5
MEA_{QRS}	79.1	24.5	86.7	56.7	88.1	48.0	83.0	46.3	73.1
$PSR_{old,QRS}$	99.9	4.9	99.6	22.9	100	16.6	99.9	16.0	86.9
PSR_{QRS}	100	0.0	100	0.0	100	0.0	100	0.0	90.9
$PSR_{2,QRS}$	100	0.0	100	0.0	100	0.0	100	0.0	92.0
$PSR_{2,2,QRS}$	92.9	17.3	85.3	45.3	89.2	47.5	91.1	43.7	82.5
$PSR_{3,QRS}$	100	0.4	100	1.3	100	2.4	100	2.1	91.9
$SC2_{QRS}$	97.4	6.2	94.3	64.6	99.3	67.3	98.0	59.8	86.3
SCA_{QRS}	97.0	7.1	92.1	70.2	99.0	77.0	97.6	67.9	88.2
$SPEC_{QRS}$	100	1.6	99.2	24.0	99.8	25.4	99.9	22.5	85.9
$SPEC_{m,QRS}$	97.2	5.7	92.4	52.2	93.8	52.4	95.6	46.9	88.7
STE_{QRS}	96.3	3.4	81.5	24.3	96.3	11.4	95.6	12.1	46.8
TCI_{QRS}	69.2	24.3	50.4	81.0	66.6	89.8	67.3	81.0	76.7
$TOMP_{QRS}$	40.5	62.4	48.7	69.5	38.8	96.0	40.2	88.7	65.2
VF_{QRS}	100	3.1	99.3	30.6	99.9	19.0	99.9	18.6	83.4
$WVL_{1,QRS}$	79.4	2.8	81.7	46.7	77.2	33.3	78.6	31.4	45.3
$WVL_{2,QRS}$	99.5	0.5	98.3	34.4	99.4	15.0	99.4	15.7	46.3
$WVL_{3,QRS}$	100	2.2	99.3	20.4	99.7	22.4	99.8	19.8	79.7
$WVL_{4,QRS}$	83.3	13.9	68.4	63.0	82.8	78.9	82.5	69.3	-

Table 6.6: *Quality of fibrillation detection algorithms used as QRS detectors (sensitivity, specificity, receiver operator characteristic) for a window length of 4 seconds in per cent, rounded on 3 digits.*

Data Source	*MIT DB*		*CU DB*		*AHA DB*		*overall results*		
Parameter	Sns.	Spc.	Sns.	Spc.	Sns.	Spc.	Sns.	Spc.	IROC
AAR_{50}	81.5	90.9	73.6	74.8	71.2	88.7	71.7	89.3	84.3
AAR_{100}	99.0	28.5	69.8	63.6	83.3	70.7	81.7	46.5	70.1
AAR_{250}	100	2.3	61.2	59.5	85.2	59.1	82.2	27.0	52.4
ACF_{95}	27.6	34.7	38.3	44.0	49.5	34.8	47.8	35.2	38.7
ACF_{99}	44.8	22.1	55.1	34.8	68.0	25.0	66.1	23.8	38.7
CPLX	21.0	83.8	71.4	72.1	79.9	78.3	78.2	81.1	85.2
HILB	0.0	100	0.0	100	0.0	100	0.0	100	94.6
$HILB_2$	37.1	99.9	23.5	98.8	25.3	99.8	25.2	99.8	93.6
$HILB_{2,2}$	29.0	97.7	27.8	94.2	36.0	95.8	34.8	96.8	87.1
$HILB_3$	58.0	99.9	45.2	98.5	50.7	99.8	50.0	99.8	94.5
LI	5.2	93.8	10.1	92.6	11.8	90.4	11.5	92.4	55.3
LI_m	100	62.6	94.6	24.1	93.3	44.2	93.6	53.7	73.3
MEA	59.4	79.8	59.0	87.3	47.6	88.6	49.2	83.6	77.4
PSR_{old}	72.4	99.6	48.8	97.4	42.1	99.7	43.3	99.5	88.5
PSR	0.0	100	0.0	100	0.0	100	0.0	100	94.2
PSR_2	1.7	100	0.9	99.9	1.3	100	1.2	100	93.4
$PSR_{2,2}$	66.8	85.9	69.2	75.3	65.8	81.3	66.3	83.7	83.1
PSR_3	73.8	99.7	65.8	93.3	72.6	98.8	71.7	99.0	94.8
SC2	71.7	97.8	64.8	95.2	63.5	99.6	63.8	98.4	89.6
SCA	79.0	97.5	71.3	93.2	72.6	99.4	72.5	98.0	91.7
SPEC	15.0	100	20.3	99.5	18.2	99.9	18.4	99.9	88.9
$SPEC_m$	52.8	97.8	52.4	94.3	46.2	94.9	47.0	96.5	90.0
STE	30.8	91.7	36.6	74.5	25.7	93.4	27.1	91.6	54.9
TCI	83.2	80.0	74.8	65.0	78.8	81.1	78.3	79.7	80.9
TOMP	68.5	39.6	76.7	44.6	97.0	38.1	94.1	39.3	67.2
VF	37.1	100	31.8	99.5	17.3	99.9	19.4	99.9	85.9
WVL_1	25.2	81.4	47.7	83.4	29.6	78.5	31.9	80.4	48.4
WVL_2	2.4	99.5	35.3	98.5	13.2	99.5	15.9	99.4	45.1
WVL_3	26.6	100	21.6	99.6	19.7	99.8	20.0	99.9	81.1
WVL_4	81.8	85.5	64.7	70.0	73.5	85.3	72.5	84.7	-

Table 6.7: *Quality of fibrillation detection algorithms used as VF detectors (sensitivity, specificity, receiver operator characteristic) for a window length of 5 seconds in per cent, rounded on 3 digits.*

Data Source	*MIT DB*		*CU DB*		*AHA DB*		*overall results*		
Parameter	Sns.	Spc.	Sns.	Spc.	Sns.	Spc.	Sns.	Spc.	IROC
$AAR_{50,QRS}$	90.8	10.7	74.5	71.0	88.9	76.9	89.3	68.5	82.6
$AAR_{100,QRS}$	28.5	72.3	64.5	71.8	70.8	88.3	46.9	84.2	72.8
$AAR_{250,QRS}$	2.3	100	60.4	63.6	59.0	88.3	27.5	86.4	59.4
$ACF_{95,QRS}$	34.4	47.6	44.3	40.0	35.5	52.0	35.3	50.0	41.1
$ACF_{99,QRS}$	21.8	59.8	35.1	56.5	25.8	71.6	24.0	68.3	41.1
$CPLX_{QRS}$	83.5	2.2	71.6	67.8	77.5	80.4	80.6	69.6	78.0
$HILB_{QRS}$	100	0.0	100	0.0	100	0.0	100	0.0	91.9
$HILB_{2,QRS}$	99.9	3.1	98.8	22.6	99.8	27.3	99.8	23.9	92.1
$HILB_{2,2,QRS}$	97.7	4.9	94.1	26.8	95.8	38.3	96.8	32.9	83.3
$HILB_{3,QRS}$	99.9	4.8	98.3	43.4	99.8	54.8	99.8	47.5	91.8
LI_{QRS}	94.0	16.6	93.0	11.5	90.4	11.9	92.5	12.4	57.8
$LI_{m,QRS}$	63.5	87.9	24.2	94.2	44.7	98.6	54.2	96.8	76.1
MEA_{QRS}	79.8	24.8	87.1	56.6	88.4	49.3	83.5	47.4	74.7
$PSR_{old,QRS}$	99.6	6.1	97.2	46.7	99.7	45.5	99.5	41.1	86.8
PSR_{QRS}	100	0.0	100	0.0	100	0.0	100	0.0	91.5
$PSR_{2,QRS}$	100	0.1	99.9	0.9	100	1.4	100	1.2	92.2
$PSR_{2,2,QRS}$	86.3	35.2	75.1	67.2	81.4	70.1	83.8	65.6	83.6
$PSR_{3,QRS}$	99.7	6.2	93.1	63.3	98.7	78.3	99.0	67.9	91.8
$SC2_{QRS}$	97.7	6.1	95.0	62.3	99.4	67.5	98.3	59.6	86.4
SCA_{QRS}	97.4	6.8	93.1	68.7	99.2	77.2	97.9	67.9	88.4
$SPEC_{QRS}$	100	1.3	99.5	19.4	99.9	19.7	99.9	17.5	86.4
$SPEC_{m,QRS}$	97.8	5.4	94.1	50.0	95.0	49.7	96.5	44.6	89.4
STE_{QRS}	91.6	4.9	74.2	35.2	92.4	21.9	91.1	21.6	51.6
TCI_{QRS}	79.7	13.0	64.8	73.0	80.7	81.7	79.4	72.6	76.7
$TOMP_{QRS}$	39.7	63.5	44.3	74.7	37.5	96.8	39.0	90.1	65.2
VF_{QRS}	100	3.2	99.4	30.2	99.9	18.7	99.9	18.3	83.8
$WVL_{1,QRS}$	81.0	2.2	83.1	45.8	78.8	31.9	80.2	30.1	45.4
$WVL_{2,QRS}$	99.5	0.2	98.5	33.9	99.5	14.2	99.4	15.1	45.1
$WVL_{3,QRS}$	100	2.2	99.5	20.4	99.8	21.2	99.9	18.9	81.6
$WVL_{4,QRS}$	85.4	14.2	69.8	62.5	85.5	79.3	84.7	69.6	-

Table 6.8: *Quality of fibrillation detection algorithms used as QRS detectors (sensitivity, specificity, receiver operator characteristic) for a window length of 5 seconds in per cent, rounded on 3 digits.*

Data Source	*MIT DB*		*CU DB*		*AHA DB*		*overall results*		
Parameter	Sns.	Spc.	Sns.	Spc.	Sns.	Spc.	Sns.	Spc.	IROC
AAR_{50}	80.8	90.8	72.5	75.7	71.5	89.1	71.7	89.4	84.6
AAR_{100}	99.7	32.1	70.1	63.6	83.1	73.1	81.5	49.5	71.6
AAR_{250}	100	2.5	61.4	59.0	85.4	59.9	82.3	27.4	52.9
ACF_{95}	29.4	42.9	37.7	53.1	49.7	43.9	47.9	43.8	45.6
ACF_{99}	50.7	29.0	55.0	43.7	68.8	33.6	66.8	31.5	45.6
CPLX	16.1	86.4	71.0	74.2	79.7	80.2	77.9	83.4	86.3
HILB	60.1	99.9	46.7	98.4	53.9	99.9	53.0	99.8	94.6
$HILB_2$	78.3	99.4	61.1	94.2	67.5	98.2	66.7	98.7	93.5
$HILB_{2,2}$	55.9	96.1	44.2	90.2	56.5	94.0	54.8	95.0	87.9
$HILB_3$	79.4	99.4	68.7	93.7	77.2	98.6	76.0	98.9	94.6
LI	5.2	94.4	9.0	93.2	10.8	91.1	10.5	93.0	56.1
LI_m	100	63.4	93.4	24.7	93.2	45.2	93.3	54.5	73.6
MEA	62.6	80.2	59.8	87.2	48.9	88.5	50.5	83.8	78.6
PSR_{old}	76.2	99.1	57.9	94.5	56.4	99.2	56.8	98.9	88.3
PSR	12.9	100	5.9	99.9	7.3	100	7.2	100	94.2
PSR_2	55.6	99.9	35.8	97.7	41.5	99.5	40.9	99.7	93.4
$PSR_{2,2}$	79.4	80.4	78.1	66.8	76.1	74.6	76.4	77.6	84.1
PSR_3	82.2	98.7	76.4	85.6	83.1	95.9	82.2	97.0	94.6
SC2	69.2	98.0	63.3	95.5	63.0	99.7	63.1	98.5	89.5
SCA	77.6	97.7	69.9	94.0	72.3	99.5	72.1	98.2	91.7
SPEC	18.5	100	22.8	99.5	22.3	99.9	22.3	99.9	88.2
$SPEC_m$	52.8	97.7	52.9	93.5	48.3	94.5	48.9	96.3	89.0
STE	35.7	92.5	41.4	73.8	32.0	92.2	33.2	91.5	59.8
TCI	75.9	84.6	70.0	71.6	72.2	87.9	72.0	85.3	80.9
TOMP	68.5	40.0	74.7	46.0	96.6	38.8	93.5	39.8	67.2
VF	36.0	100	31.2	99.5	17.1	99.9	19.1	100	86.1
WVL_1	36.0	80.7	49.2	83.6	32.0	78.5	34.2	80.0	50.4
WVL_2	10.8	99.5	35.6	98.2	14.4	99.4	17.1	99.4	46.1
WVL_3	26.9	100	22.6	99.6	21.7	99.8	21.8	99.9	79.5
WVL_4	80.4	87.0	61.6	71.4	73.2	86.9	71.8	86.2	-

Table 6.9: *Quality of fibrillation detection algorithms used as VF detectors (sensitivity, specificity, receiver operator characteristic) for a window length of 6 seconds in per cent, rounded on 3 digits.*

Data Source	*MIT DB*		*CU DB*		*AHA DB*		*overall results*		
Parameter	Sns.	Spc.	Sns.	Spc.	Sns.	Spc.	Sns.	Spc.	IROC
$AAR_{50,QRS}$	90.7	10.5	75.3	69.8	89.2	77.2	89.4	68.5	82.9
$AAR_{100,QRS}$	32.2	72.0	64.5	72.1	73.3	88.5	50.0	84.4	74.5
$AAR_{250,QRS}$	2.6	100	60.0	63.8	59.8	88.5	27.9	86.6	59.9
$ACF_{95,QRS}$	42.6	36.5	53.4	39.0	44.5	52.3	43.8	48.8	46.9
$ACF_{99,QRS}$	28.7	52.2	44.1	56.4	34.3	72.4	31.6	68.0	46.9
$CPLX_{QRS}$	86.1	1.6	73.6	67.4	79.4	80.3	82.9	69.5	78.9
$HILB_{QRS}$	99.9	4.9	98.3	44.9	99.8	58.2	99.8	50.2	91.9
$HILB_{2,QRS}$	99.4	7.3	94.1	58.8	98.2	72.8	98.7	63.3	92.0
$HILB_{2,2,QRS}$	96.1	9.0	90.2	43.0	93.9	60.1	95.0	51.9	84.4
$HILB_{3,QRS}$	99.4	6.8	93.5	66.0	98.6	83.2	98.8	72.1	91.7
LI_{QRS}	94.6	15.9	93.6	10.2	91.1	11.0	93.2	11.5	58.9
$LI_{m,QRS}$	64.4	87.4	24.8	93.0	45.6	98.4	55.1	96.4	76.5
MEA_{QRS}	80.3	25.0	87.0	57.5	88.3	50.8	83.8	48.6	76.1
$PSR_{old,QRS}$	99.1	6.8	94.3	55.4	99.2	60.9	98.9	53.9	86.6
PSR_{QRS}	100	1.1	99.9	5.7	100	7.9	100	6.8	91.5
$PSR_{2,QRS}$	99.9	4.8	97.7	34.6	99.5	44.8	99.7	38.8	92.1
$PSR_{2,2,QRS}$	81.0	50.4	66.6	76.0	74.8	80.8	77.9	76.7	84.4
$PSR_{3,QRS}$	98.7	8.3	85.4	73.8	95.9	89.2	97.0	77.8	91.8
$SC2_{QRS}$	97.9	5.9	95.4	60.8	99.5	67.0	98.4	59.1	86.4
SCA_{QRS}	97.6	6.8	93.9	67.4	99.3	77.1	98.2	67.6	88.4
$SPEC_{QRS}$	100	1.6	99.4	21.7	99.9	24.1	99.9	21.1	85.7
$SPEC_{m,QRS}$	97.7	5.8	93.3	50.6	94.6	52.0	96.3	46.4	88.5
STE_{QRS}	92.4	5.3	73.5	39.8	91.2	28.7	91.1	27.4	56.1
TCI_{QRS}	75.1	16.9	58.0	78.1	73.9	88.2	73.9	78.6	76.7
$TOMP_{QRS}$	40.1	62.7	45.6	72.7	38.2	96.4	39.6	89.4	65.2
VF_{QRS}	100	3.1	99.4	29.7	99.9	18.5	99.9	18.1	84.1
$WVL_{1,QRS}$	80.4	3.1	83.3	47.0	78.8	34.4	79.9	32.3	46.8
$WVL_{2,QRS}$	99.5	0.9	98.1	34.2	99.4	15.6	99.4	16.2	45.9
$WVL_{3,QRS}$	100	2.4	99.4	21.3	99.8	23.4	99.9	20.7	79.6
$WVL_{4,QRS}$	86.9	14.0	71.1	59.5	87.1	79.0	86.3	69.0	-

Table 6.10: *Quality of fibrillation detection algorithms used as QRS detectors (sensitivity, specificity, receiver operator characteristic) for a window length of 6 seconds in per cent, rounded on 3 digits.*

Data Source	*MIT DB*		*CU DB*		*AHA DB*		*overall results*		
Parameter	Sns.	Spc.	Sns.	Spc.	Sns.	Spc.	Sns.	Spc.	IROC
AAR_{50}	83.9	91.4	74.1	72.6	85.2	60.8	83.7	78.6	87.1
AAR_{100}	100	3.0	70.2	61.1	84.4	71.4	82.6	32.3	45.0
AAR_{250}	100	3.0	61.3	59.8	85.2	60.8	82.2	28.1	54.0
ACF_{95}	33.6	45.5	36.2	57.1	50.7	50.0	48.7	47.8	48.5
ACF_{99}	54.9	30.6	54.1	47.6	70.7	38.6	68.4	34.5	48.5
CPLX	12.2	88.2	66.7	78.7	74.8	85.1	73.2	86.5	86.3
HILB	78.7	99.3	69.5	92.4	80.3	97.8	78.8	98.4	94.5
$HILB_2$	88.8	98.1	72.9	88.0	80.2	95.2	79.3	96.5	93.5
$HILB_{2,2}$	68.5	94.4	57.7	86.4	70.4	92.4	68.6	93.3	88.8
$HILB_3$	83.9	98.6	73.2	89.1	82.3	96.8	81.1	97.5	94.5
LI	3.8	94.8	8.2	94.1	10.0	91.6	9.7	93.5	57.2
LI_m	100	64.1	92.6	25.3	93.0	46.0	93.0	55.3	73.9
MEA	62.2	80.5	59.9	87.4	49.5	88.6	50.9	84.0	79.7
PSR_{old}	77.6	98.4	62.8	91.4	63.5	98.5	63.6	98.1	88.0
PSR	69.2	99.8	57.6	95.6	67.5	99.1	66.2	99.4	94.2
PSR_2	79.4	99.6	62.7	92.8	70.7	97.3	69.7	98.4	93.4
$PSR_{2,2}$	86.0	76.0	82.5	60.3	81.0	69.2	81.3	72.7	84.7
PSR_3	87.1	97.4	78.8	80.3	85.4	92.4	84.5	94.7	94.4
SC2	66.1	98.1	61.6	95.9	62.9	99.7	62.7	98.6	89.4
SCA	74.1	97.8	68.7	94.4	72.0	99.6	71.6	98.4	91.5
SPEC	21.7	100	26.7	99.3	27.3	99.8	27.2	99.9	88.9
$SPEC_m$	57.3	97.6	54.7	93.4	51.2	94.3	51.7	96.1	89.9
STE	47.9	85.4	48.9	68.2	43.3	84.5	44.1	84.3	63.8
TCI	80.4	80.8	74.8	65.9	79.9	82.1	79.3	80.6	80.9
TOMP	68.5	40.3	73.0	47.3	96.2	39.3	93.0	40.2	67.2
VF	32.2	100	31.0	99.5	17.1	100	19.0	100	86.3
WVL_1	34.3	82.3	48.0	83.2	30.5	79.4	32.8	81.2	50.1
WVL_2	5.2	99.5	35.4	98.4	13.7	99.5	16.4	99.4	45.3
WVL_3	29.7	99.9	26.0	99.3	26.0	99.6	26.0	99.8	80.2
WVL_4	79.0	88.3	60.7	72.0	73.6	88.5	72.0	87.6	-

Table 6.11: *Quality of fibrillation detection algorithms used as VF detectors (sensitivity, specificity, receiver operator characteristic) for a window length of 7 seconds in per cent, rounded on 3 digits.*

Data Source	*MIT DB*		*CU DB*		*AHA DB*		*overall results*		
Parameter	Sns.	Spc.	Sns.	Spc.	Sns.	Spc.	Sns.	Spc.	IROC
$AAR_{50,QRS}$	91.4	12.8	72.2	71.3	60.7	88.4	78.3	77.3	82.8
$AAR_{100,QRS}$	3.1	100	62.0	72.3	71.5	89.5	32.9	88.5	52.7
$AAR_{250,QRS}$	3.1	100	60.7	63.8	60.7	88.4	28.6	86.5	60.9
$ACF_{95,QRS}$	45.0	32.1	57.4	37.5	50.6	53.4	47.8	48.9	50.0
$ACF_{99,QRS}$	30.2	50.4	48.0	55.4	39.1	74.4	34.6	69.2	50.0
$CPLX_{QRS}$	88.0	1.3	78.2	63.4	84.3	75.7	86.1	65.4	79.1
$HILB_{QRS}$	99.3	6.9	92.1	66.8	97.8	86.5	98.3	74.7	91.8
$HILB_{2,QRS}$	98.2	10.3	87.8	70.3	95.2	86.1	96.5	75.2	91.8
$HILB_{2,2,QRS}$	94.4	11.2	86.5	56.7	92.3	74.8	93.2	65.0	85.2
$HILB_{3,QRS}$	98.6	8.1	88.8	70.3	96.8	88.6	97.5	76.8	91.4
LI_{QRS}	95.0	16.2	94.4	9.3	91.6	10.2	93.6	10.8	59.6
$LI_{m,QRS}$	65.1	87.2	25.3	92.2	46.4	98.2	55.8	96.1	76.8
MEA_{QRS}	80.6	25.3	87.2	57.5	88.4	51.4	84.0	49.1	77.3
$PSR_{old,QRS}$	98.4	8.4	91.2	60.2	98.5	68.4	98.1	60.3	86.4
PSR_{QRS}	99.8	5.9	95.5	55.3	99.1	72.8	99.3	62.7	91.6
$PSR_{2,QRS}$	99.6	7.9	92.8	60.8	97.3	75.9	98.4	66.0	92.0
$PSR_{2,2,QRS}$	76.7	61.6	60.1	80.6	69.3	85.8	73.0	82.3	85.0
$PSR_{3,QRS}$	97.5	10.5	80.2	76.3	92.3	91.4	94.6	80.0	91.7
$SC2_{QRS}$	98.1	5.8	95.8	59.2	99.5	66.9	98.6	58.8	86.3
SCA_{QRS}	97.8	6.6	94.4	66.3	99.4	76.9	98.3	67.3	88.4
$SPEC_{QRS}$	100	1.9	99.2	25.6	99.8	29.5	99.9	25.8	86.5
$SPEC_{m,QRS}$	97.6	6.3	93.2	52.4	94.3	55.2	96.1	49.1	89.4
STE_{QRS}	85.2	8.0	67.8	46.9	83.6	40.6	83.8	37.6	59.9
TCI_{QRS}	80.5	11.8	65.8	73.4	81.7	82.9	80.3	73.4	76.7
$TOMP_{QRS}$	40.4	61.9	46.9	70.8	38.7	95.9	40.0	88.8	65.3
VF_{QRS}	100	2.8	99.4	29.5	100	18.4	100	18.0	84.3
$WVL_{1,QRS}$	82.0	2.9	82.9	46.0	79.7	32.8	81.1	31.0	46.8
$WVL_{2,QRS}$	99.5	0.4	98.4	34.0	99.5	14.9	99.4	15.6	45.2
$WVL_{3,QRS}$	99.9	2.9	99.2	24.6	99.6	28.1	99.8	24.7	80.6
$WVL_{4,QRS}$	88.2	13.8	71.7	58.8	88.6	79.4	87.6	69.1	-

Table 6.12: *Quality of fibrillation detection algorithms used as QRS detectors (sensitivity, specificity, receiver operator characteristic) for a window length of 7 seconds in per cent, rounded on 3 digits.*

Data Source	*MIT DB*		*CU DB*		*AHA DB*		*overall results*		
Parameter	Sns.	Spc.	Sns.	Spc.	Sns.	Spc.	Sns.	Spc.	IROC
AAR_{50}	82.2	88.6	73.3	71.7	75.6	84.4	75.3	86.2	84.5
AAR_{100}	100	4.4	69.1	62.6	84.3	71.5	82.4	33.2	47.4
AAR_{250}	100	4.4	59.3	61.2	75.6	84.4	73.6	38.1	39.9
ACF_{95}	36.7	45.2	38.6	60.1	52.1	53.7	50.2	49.2	50.0
ACF_{99}	61.2	28.6	55.3	50.2	71.1	41.3	69.0	34.5	50.0
CPLX	5.9	92.9	56.6	86.7	61.7	92.0	60.5	92.3	86.8
HILB	90.9	96.2	77.7	78.5	86.4	91.9	85.3	93.8	94.4
$HILB_2$	94.8	94.1	79.4	75.8	86.2	87.9	85.3	90.8	93.1
$HILB_{2,2}$	90.6	90.9	72.2	79.5	82.8	89.4	81.5	89.8	89.8
$HILB_3$	91.6	97.0	76.2	81.2	84.8	93.5	83.7	94.9	94.1
LI	2.8	95.4	7.4	95.2	9.0	92.3	8.7	94.2	59.1
LI_m	100	65.2	91.0	26.3	92.5	47.3	92.4	56.5	74.3
MEA	62.2	81.0	60.3	87.4	50.7	88.5	52.1	84.2	80.7
PSR_{old}	80.1	96.4	68.0	85.2	69.8	95.9	69.7	95.7	87.6
PSR	84.3	98.1	74.7	83.2	83.4	93.6	82.3	95.6	94.0
PSR_2	89.9	97.7	75.1	82.0	83.1	90.4	82.1	94.1	93.2
$PSR_{2,2}$	90.2	69.5	86.5	50.8	85.8	61.3	86.0	65.5	85.5
PSR_3	92.0	94.9	80.4	72.7	87.5	85.0	86.6	90.1	94.0
SC2	59.8	98.3	58.4	96.5	62.4	99.8	61.9	98.8	89.3
SCA	70.6	98.1	66.4	95.3	71.2	99.7	70.6	98.6	91.4
SPEC	18.5	100	26.0	99.4	26.6	99.8	26.4	99.9	88.4
$SPEC_m$	53.1	97.9	53.7	94.2	50.7	94.9	51.1	96.6	89.5
STE	65.0	73.4	58.6	60.9	60.1	72.7	59.9	72.6	68.8
TCI	76.9	81.1	74.6	66.3	80.6	82.7	79.8	81.0	80.9
TOMP	68.5	39.9	74.2	45.5	96.9	38.6	93.7	39.7	67.4
VF	28.0	100	30.2	99.6	17.0	100	18.8	100	86.6
WVL_1	39.2	83.3	48.7	84.1	31.1	80.4	33.5	82.2	51.3
WVL_2	7.0	99.5	34.9	98.2	14.1	99.5	16.7	99.4	45.6
WVL_3	28.0	99.9	25.3	99.5	25.6	99.7	25.6	99.8	80.1
WVL_4	78.0	89.5	59.9	73.1	73.2	90.1	71.5	88.9	-

Table 6.13: *Quality of fibrillation detection algorithms used as VF detectors (sensitivity, specificity, receiver operator characteristic) for a window length of 9 seconds in per cent, rounded on 3 digits.*

Data Source	*MIT DB*		*CU DB*		*AHA DB*		*overall results*		
Parameter	Sns.	Spc.	Sns.	Spc.	Sns.	Spc.	Sns.	Spc.	IROC
$AAR_{50,QRS}$	88.5	11.2	71.3	70.7	84.6	81.6	86.2	72.0	82.9
$AAR_{100,QRS}$	4.5	100	63.6	71.2	71.6	89.4	33.8	88.2	55.0
$AAR_{250,QRS}$	4.5	100	62.2	61.9	84.6	81.6	38.9	81.1	48.5
$ACF_{95,QRS}$	44.8	35.0	60.6	40.3	54.2	54.9	49.3	50.8	51.3
$ACF_{99,QRS}$	28.3	56.0	50.6	56.7	41.8	74.9	34.7	70.3	51.3
$CPLX_{QRS}$	92.8	0.5	86.3	53.8	91.4	62.8	91.9	54.3	79.7
$HILB_{QRS}$	96.3	12.5	78.1	74.7	91.9	92.5	93.7	80.8	91.6
$HILB_{2,QRS}$	94.2	18.0	75.6	76.9	87.8	92.0	90.8	81.4	91.3
$HILB_{2,2,QRS}$	90.9	15.6	79.6	70.8	89.2	87.7	89.7	77.1	86.1
$HILB_{3,QRS}$	97.0	11.5	80.9	73.3	93.4	90.9	94.9	79.4	91.1
LI_{QRS}	95.6	14.2	95.5	8.4	92.3	9.2	94.3	9.7	61.2
$LI_{m,QRS}$	66.2	86.8	26.3	90.6	47.6	97.8	57.0	95.6	77.3
MEA_{QRS}	81.0	25.6	87.3	58.2	88.3	52.8	84.2	50.3	78.3
$PSR_{old,QRS}$	96.4	12.1	85.0	65.4	95.9	74.9	95.7	66.4	85.8
PSR_{QRS}	98.1	10.3	83.0	72.2	93.5	89.5	95.6	78.0	91.5
$PSR_{2,QRS}$	97.7	13.1	82.0	73.2	90.3	89.0	94.1	78.1	91.6
$PSR_{2,2,QRS}$	70.4	77.7	50.7	84.9	61.5	90.3	66.0	88.1	85.5
$PSR_{3,QRS}$	95.0	14.5	72.5	78.1	85.0	93.3	90.0	82.2	91.4
$SC2_{QRS}$	98.3	5.2	96.4	56.1	99.6	66.5	98.7	58.0	86.3
SCA_{QRS}	98.0	6.2	95.2	64.0	99.6	76.1	98.5	66.4	88.3
$SPEC_{QRS}$	100	1.6	99.4	24.9	99.8	28.7	99.9	25.1	86.2
$SPEC_{m,QRS}$	97.9	5.9	94.1	51.6	94.9	54.6	96.5	48.5	89.1
STE_{QRS}	73.0	12.3	60.4	56.1	71.9	58.3	72.0	52.6	64.5
TCI_{QRS}	80.8	11.0	66.2	73.2	82.2	83.7	80.7	73.9	76.7
$TOMP_{QRS}$	39.9	62.1	45.2	72.2	38.0	96.6	39.4	89.5	65.7
VF_{QRS}	100	2.5	99.4	28.8	100	18.4	100	17.8	84.5
$WVL_{1,QRS}$	83.0	3.2	83.8	46.6	80.7	33.5	82.1	31.6	47.9
$WVL_{2,QRS}$	99.5	0.6	98.1	33.6	99.5	15.2	99.4	15.8	45.5
$WVL_{3,QRS}$	99.9	2.8	99.3	23.8	99.7	27.6	99.8	24.3	80.4
$WVL_{4,QRS}$	89.4	14.0	72.8	57.7	90.2	79.0	89.0	68.7	-

Table 6.14: *Quality of fibrillation detection algorithms used as QRS detectors (sensitivity, specificity, receiver operator characteristic) for a window length of 9 seconds in per cent, rounded on 3 digits.*

Data Source	*MIT DB*		*CU DB*		*AHA DB*		*overall results*		
Parameter	Sns.	Spc.	Sns.	Spc.	Sns.	Spc.	Sns.	Spc.	IROC
AAR_{50}	76.6	90.7	69.9	76.0	68.4	88.7	68.7	89.2	82.3
AAR_{100}	100	4.1	69.1	60.1	85.0	73.1	83.0	33.5	47.4
AAR_{250}	100	4.1	57.6	61.3	68.4	88.7	67.3	39.6	38.8
ACF_{95}	38.5	44.0	37.9	60.5	52.6	53.9	50.5	48.6	49.7
ACF_{99}	62.9	27.3	56.1	50.6	71.8	40.9	69.7	33.7	49.7
CPLX	6.3	93.0	54.1	88.8	57.8	93.1	56.8	92.8	87.0
HILB	92.3	94.2	79.7	72.5	87.8	88.2	86.7	90.9	94.3
$HILB_2$	95.8	91.1	80.6	70.1	87.6	83.4	86.7	87.2	92.9
$HILB_{2,2}$	95.5	89.1	76.8	76.4	85.0	87.6	84.0	88.0	90.1
$HILB_3$	92.0	96.0	76.5	77.6	85.4	91.7	84.3	93.5	93.9
LI	2.4	95.6	7.1	95.7	8.7	92.5	8.4	94.4	59.4
LI_m	100	65.7	90.3	26.7	92.4	47.7	92.2	56.9	74.4
MEA	60.8	81.1	60.6	87.7	51.0	88.4	52.3	84.2	81.0
PSR_{old}	80.8	95.0	69.5	83.6	71.0	94.0	70.9	94.1	87.4
PSR	87.8	96.6	76.8	78.4	85.6	89.1	84.5	92.9	94.0
PSR_2	91.6	96.2	77.3	77.4	85.3	86.0	84.3	91.3	93.0
$PSR_{2,2}$	93.4	66.9	87.4	46.9	87.5	58.5	87.6	62.7	85.7
PSR_3	92.3	93.6	80.5	70.0	87.8	81.9	86.9	88.0	93.7
SC2	58.4	98.3	57.2	96.9	62.0	99.8	61.3	98.9	89.2
SCA	68.2	98.1	65.4	95.7	71.0	99.8	70.3	98.7	91.2
SPEC	20.3	100	27.4	99.4	28.4	99.8	28.2	99.9	87.9
$SPEC_m$	50.7	97.9	53.2	94.1	51.3	94.8	51.5	96.5	88.4
STE	68.2	68.3	62.1	58.8	65.9	68.5	65.5	68.0	69.8
TCI	72.4	83.6	71.6	69.7	77.2	86.5	76.4	84.1	80.9
TOMP	68.5	40.1	72.8	46.4	96.6	39.0	93.3	40.0	67.2
VF	27.3	100	29.8	99.6	17.1	100	18.8	100	86.7
WVL_1	37.8	83.1	48.6	83.5	32.7	80.0	34.8	81.9	52.1
WVL_2	10.8	99.5	35.0	98.1	14.6	99.5	17.2	99.4	46.1
WVL_3	25.9	99.9	25.7	99.5	25.9	99.6	25.9	99.8	79.4
WVL_4	78.3	90.2	59.0	73.6	73.1	90.6	71.3	89.6	-

Table 6.15: *Quality of fibrillation detection algorithms used as VF detectors (sensitivity, specificity, receiver operator characteristic) for a window length of 10 seconds in per cent, rounded on 3 digits.*

Data Source	*MIT DB*		*CU DB*		*AHA DB*		*overall results*		
Parameter	Sns.	Spc.	Sns.	Spc.	Sns.	Spc.	Sns.	Spc.	IROC
$AAR_{50,QRS}$	90.6	10.7	75.7	67.2	88.8	73.7	89.2	65.5	80.1
$AAR_{100,QRS}$	4.1	100	61.1	71.3	73.2	90.2	34.1	88.9	54.9
$AAR_{250,QRS}$	4.1	100	62.3	60.2	88.8	73.7	40.4	74.9	47.4
$ACF_{95,QRS}$	43.7	38.5	61.0	39.6	54.3	55.5	48.7	51.5	51.2
$ACF_{99,QRS}$	27.1	61.5	51.0	57.3	41.4	75.5	33.9	71.6	51.2
$CPLX_{QRS}$	92.8	0.5	88.4	51.5	92.5	58.9	92.5	51.1	79.9
$HILB_{QRS}$	94.2	15.6	72.1	76.6	88.1	93.7	90.8	82.3	91.4
$HILB_{2,QRS}$	91.2	21.5	69.9	78.3	83.4	93.2	87.2	82.9	91.2
$HILB_{2,2,QRS}$	89.1	17.1	76.4	75.4	87.4	89.9	87.9	79.5	86.3
$HILB_{3,QRS}$	96.1	13.1	77.3	73.8	91.7	91.4	93.5	80.0	90.9
LI_{QRS}	95.8	13.4	96.0	8.0	92.6	8.9	94.5	9.3	61.7
$LI_{m,QRS}$	66.7	86.8	26.8	89.8	48.1	97.6	57.5	95.4	77.5
MEA_{QRS}	81.1	25.4	87.5	58.3	88.2	53.1	84.2	50.5	78.5
$PSR_{old,QRS}$	95.1	13.4	83.3	66.7	94.0	76.2	94.1	67.6	85.6
PSR_{QRS}	96.7	12.8	78.1	74.2	89.1	91.6	92.8	80.1	91.3
$PSR_{2,QRS}$	96.3	15.8	77.4	75.6	86.0	91.1	91.3	80.3	91.5
$PSR_{2,2,QRS}$	67.9	82.6	46.8	85.7	58.5	91.5	63.2	89.7	85.8
$PSR_{3,QRS}$	93.6	16.2	69.8	78.3	82.0	93.6	87.9	82.6	91.1
$SC2_{QRS}$	98.3	5.0	96.8	54.9	99.7	66.1	98.8	57.6	86.3
SCA_{QRS}	98.1	5.9	95.6	63.1	99.6	75.9	98.6	66.1	88.2
$SPEC_{QRS}$	100	2.0	99.3	26.2	99.8	30.7	99.9	26.8	85.6
$SPEC_{m,QRS}$	97.9	6.3	94.0	51.2	94.9	55.3	96.5	49.1	88.2
STE_{QRS}	67.8	12.6	58.2	59.5	67.7	64.5	67.4	57.8	65.0
TCI_{QRS}	78.4	12.7	62.6	75.9	78.3	87.1	77.6	77.0	76.7
$TOMP_{QRS}$	40.2	61.5	46.1	70.9	38.4	96.3	39.7	89.1	65.0
VF_{QRS}	100	2.4	99.5	28.3	100	18.4	100	17.8	84.7
$WVL_{1,QRS}$	82.8	3.1	83.2	46.4	80.3	35.2	81.8	32.9	48.4
$WVL_{2,QRS}$	99.5	0.9	98.1	33.7	99.5	15.8	99.4	16.3	45.9
$WVL_{3,QRS}$	100	2.7	99.3	24.1	99.6	28.0	99.8	24.6	79.7
$WVL_{4,QRS}$	90.2	14.1	73.3	56.7	90.7	78.9	89.6	68.5	-

Table 6.16: *Quality of fibrillation detection algorithms used as QRS detectors (sensitivity, specificity, receiver operator characteristic) for a window length of 10 seconds in per cent, rounded on 3 digits.*

The next tables show the quality parameters positive predictivity, accuracy and calculation time. Again, the results for a window length of 8 seconds are displayed first.

Data Source	*MIT DB*		*CU DB*		*AHA DB*		*overall results*		
Parameter	PP.	Ac.	PP.	Ac.	PP.	Ac.	PP.	Ac.	ct.
AAR_{50}	1.2	89.0	43.6	73.3	32.5	67.2	26.6	78.8	3.4
AAR_{100}	0.2	2.9	35.5	65.5	38.5	74.3	10.2	36.9	3.8
AAR_{250}	0.2	2.9	29.9	60.1	31.0	65.1	9.6	32.6	5.5
ACF_{95}	0.1	45.9	19.7	54.5	18.2	52.1	8.3	49.0	3.6
ACF_{99}	0.1	30.2	22.2	50.4	19.9	45.7	9.1	37.9	3.8
CPLX	0.1	92.3	52.7	80.3	60.7	86.5	40.8	89.2	2.4
HILB	6.3	97.8	59.1	83.0	78.3	93.3	67.6	95.1	1.9
$HILB_2$	4.1	96.4	54.6	80.8	67.7	90.4	56.4	93.0	1.9
$HILB_{2,2}$	1.8	92.6	52.5	79.4	63.9	88.7	46.0	90.2	1.9
$HILB_3$	6.2	97.8	58.5	82.8	78.3	93.3	67.3	95.1	1.8
LI	0.1	94.9	27.5	76.5	19.4	77.8	12.1	86.6	14
LI_m	0.5	64.8	24.6	39.5	26.5	54.6	16.4	59.0	14
MEA	0.5	80.8	56.0	81.8	47.5	81.9	23.2	81.3	2.6
PSR_{old}	5.1	97.5	59.0	83.3	84.8	92.4	68.5	94.6	2.0
PSR	13.4	99.2	65.0	85.1	83.8	94.0	77.3	96.2	1.8
PSR_2	11.0	98.8	61.4	83.8	74.0	91.7	68.2	95.0	1.8
$PSR_{2,2}$	0.5	72.5	34.9	61.6	33.1	68.1	20.2	70.0	1.8
PSR_3	3.8	96.2	48.5	76.8	61.3	88.4	51.5	91.8	1.8
SC2	5.6	98.2	80.7	88.7	98.3	93.4	82.2	95.6	5.7
SCA	5.6	97.9	77.8	89.2	98.0	94.9	81.6	96.2	5.8
SPEC	60.6	99.8	92.0	84.6	97.3	87.7	96.1	93.8	1.9
$SPEC_m$	3.8	97.6	68.6	85.3	65.9	87.2	56.3	92.5	1.9
STE	0.5	83.4	29.5	63.8	35.1	75.6	20.4	79.0	1.9
TCI	0.8	83.9	38.9	70.6	54.4	84.9	31.1	83.6	2.2
TOMP	0.2	40.6	26.7	53.2	24.8	49.4	12.7	45.0	0.82
VF	82.4	99.9	94.5	85.2	98.9	85.7	97.7	93.0	1.9
WVL_1	0.3	81.9	44.5	76.6	24.2	71.0	14.5	76.9	1.9
WVL_2	3.6	99.4	83.1	85.0	84.9	84.9	73.6	92.4	1.9
WVL_3	38.9	99.8	92.1	84.1	91.8	87.0	90.5	93.5	1.9
WVL_4	1.2	88.9	36.6	69.8	59.3	86.8	36.8	87.0	41

Table 6.17: *Quality of fibrillation detection algorithms used as VF detectors (positive predictivity, accuracy, calculation time) for a window length of 8 seconds. Positive predictivity and accuracy in per cent, rounded on 3 digits; calculation time in per cent of the real time of the data, rounded on 2 digits.*

Data Source	*MIT DB*		*CU DB*		*AHA DB*		*overall res.*	
Parameter	PP.	Ac.	PP.	Ac.	PP.	Ac.	PP.	Ac.
$AAR_{50,QRS}$	98.0	87.3	89.1	72.5	96.5	67.3	97.1	77.9
$AAR_{100,QRS}$	100	4.8	88.7	66.7	97.1	75.2	96.4	38.3
$AAR_{250,QRS}$	100	4.8	84.8	61.4	96.3	65.2	95.3	33.7
$ACF_{95,QRS}$	97.0	45.2	78.1	55.1	86.0	52.9	90.8	49.1
$ACF_{99,QRS}$	96.8	30.2	80.4	51.1	89.8	46.3	92.2	38.2
$CPLX_{QRS}$	97.8	90.4	87.1	79.2	92.6	86.5	95.2	88.2
$HILB_{QRS}$	98.1	96.1	91.1	82.0	98.2	94.4	97.8	94.6
$HILB_{2,QRS}$	98.2	94.8	91.6	80.0	98.0	91.4	97.8	92.6
$HILB_{2,2,QRS}$	98.1	91.0	89.1	79.1	96.6	89.5	97.1	89.7
$HILB_{3,QRS}$	98.1	96.0	91.2	81.8	98.1	94.4	97.8	94.6
LI_{QRS}	98.2	93.7	79.0	76.3	84.3	78.9	91.3	86.4
$LI_{m,QRS}$	99.6	66.1	91.3	39.9	99.2	55.1	99.3	60.0
MEA_{QRS}	98.1	79.7	88.2	81.0	90.7	82.6	94.4	81.0
$PSR_{old,QRS}$	98.1	95.8	89.6	82.4	95.0	93.5	96.5	94.1
PSR_{QRS}	98.1	97.3	90.4	84.3	97.4	95.1	97.5	95.7
$PSR_{2,QRS}$	98.1	97.1	90.6	83.2	97.2	92.8	97.4	94.5
$PSR_{2,2,QRS}$	99.2	73.2	91.8	61.4	96.8	68.7	98.0	70.6
$PSR_{3,QRS}$	98.1	94.5	92.0	76.2	98.5	89.3	98.0	91.3
$SC2_{QRS}$	98.0	96.3	89.2	87.8	94.1	94.4	96.0	95.0
SCA_{QRS}	98.1	96.1	90.8	88.4	95.8	95.9	96.8	95.6
$SPEC_{QRS}$	98.0	98.0	83.2	83.7	88.6	89.0	93.3	93.4
$SPEC_{m,QRS}$	98.0	95.8	87.7	84.4	92.0	88.4	95.1	92.0
STE_{QRS}	97.8	81.7	82.9	62.8	89.0	74.9	93.5	77.8
TCI_{QRS}	97.7	76.0	90.5	64.5	97.0	78.5	97.2	76.5
$TOMP_{QRS}$	98.1	41.0	84.9	52.5	97.9	48.1	97.2	44.7
VF_{QRS}	98.0	98.0	83.6	84.2	86.6	87.0	92.5	92.5
$WVL_{1,QRS}$	97.6	80.0	85.0	75.6	86.6	72.3	92.4	76.5
$WVL_{2,QRS}$	98.0	97.5	84.3	84.2	86.2	86.2	92.3	91.9
$WVL_{3,QRS}$	98.0	98.0	82.7	83.1	88.1	88.3	93.1	93.0
$WVL_{4,QRS}$	98.0	87.4	86.4	69.0	95.8	88.1	96.7	86.7

Table 6.18: *Quality of fibrillation detection algorithms used as QRS detectors (positive predictivity, accuracy) for a window length of 8 seconds in per cent, rounded on 3 digits.*

Data Source	*MIT DB*		*CU DB*		*AHA DB*		*overall results*		
Parameter	PP.	Ac.	PP.	Ac.	PP.	Ac.	PP.	Ac.	ct.
AAR_{50}	1.1	87.9	43.9	73.4	53.9	84.7	34.9	85.8	2.8
AAR_{100}	0.3	38.1	36.4	66.6	38.4	74.3	13.9	55.2	2.9
AAR_{250}	0.2	7.7	31.8	62.1	30.7	64.4	10.1	34.9	3.3
ACF_{95}	0.1	36.0	18.2	47.1	15.3	39.2	7.4	38.0	2.9
ACF_{99}	0.1	31.1	21.0	46.0	17.0	36.4	8.5	34.2	3.0
CPLX	0.2	80.6	36.4	68.0	37.4	73.8	23.9	77.0	-
HILB	-	99.8	-	78.1	-	82.9	-	91.4	1.3
$HILB_2$	-	99.8	-	78.1	-	82.9	-	91.4	1.3
$HILB_{2,2}$	0.2	99.6	55.7	78.2	34.8	82.7	26.4	91.2	1.3
$HILB_3$	-	99.8	-	78.1	-	82.9	-	91.4	1.4
LI	0.2	91.5	25.4	73.7	22.1	75.9	13.1	83.8	4.7
LI_m	0.4	60.1	24.5	37.6	24.6	49.8	15.1	54.5	4.6
MEA	0.4	77.8	52.3	80.4	42.8	80.3	19.5	79.0	1.4
PSR_{old}	79.2	99.9	100	79.3	-	82.9	79.5	91.5	1.4
PSR	-	99.8	-	78.1	-	82.9	-	91.4	1.3
PSR_2	-	99.8	-	78.1	-	82.9	-	91.4	1.3
$PSR_{2,2}$	0.8	98.5	44.1	77.6	38.0	82.0	28.2	90.3	1.3
PSR_3	-	99.8	-	78.1	-	82.9	-	91.4	1.3
SC2	3.7	96.8	71.6	88.0	93.7	93.1	71.0	94.7	3.6
SCA	3.6	96.3	67.7	87.5	92.1	94.3	69.5	95.0	3.8
SPEC	36.9	99.8	88.8	82.8	95.3	85.6	93.1	92.8	1.4
$SPEC_m$	3.8	97.6	67.7	85.0	59.7	85.4	51.6	91.7	1.4
STE	0.4	93.6	21.4	67.7	41.6	82.0	18.3	87.2	1.3
TCI	0.6	78.1	33.9	64.8	41.7	77.8	23.7	77.2	1.5
TOMP	0.2	40.1	26.9	52.7	24.5	48.5	12.7	44.3	0.79
VF	94.0	99.9	94.3	85.6	97.9	85.8	97.0	93.1	1.4
WVL_1	0.1	80.0	44.8	77.1	20.5	69.3	11.9	75.3	1.4
WVL_2	0.1	99.4	95.0	85.8	83.4	84.5	73.6	92.2	1.4
WVL_3	60.0	99.8	92.6	83.3	93.0	85.6	92.2	92.8	1.4
WVL_4	0.7	80.7	33.5	65.7	40.9	77.4	24.2	78.5	40

Table 6.19: *Quality of fibrillation detection algorithms used as VF detectors (positive predictivity, accuracy, calculation time) for a window length of 3 seconds. Positive predictivity and accuracy in per cent, rounded on 3 digits; calculation time in per cent of the real time of the data, rounded on 2 digits.*

Data Source	*MIT DB*		*CU DB*		*AHA DB*		*overall res.*	
Parameter	PP.	Ac.	PP.	Ac.	PP.	Ac.	PP.	Ac.
$AAR_{50,QRS}$	97.9	86.2	90.7	72.7	96.2	86.0	96.9	85.4
$AAR_{100,QRS}$	98.2	38.6	89.3	67.7	97.0	75.2	97.0	55.9
$AAR_{250,QRS}$	100	9.5	86.4	63.3	96.7	64.6	96.1	36.1
$ACF_{95,QRS}$	97.2	36.1	76.9	48.0	82.6	40.0	89.5	38.4
$ACF_{99,QRS}$	97.2	31.4	79.9	46.9	86.0	37.1	91.4	34.7
$CPLX_{QRS}$	97.5	78.7	88.8	66.8	94.7	73.1	96.1	75.7
$HILB_{QRS}$	98.0	98.0	77.4	77.4	84.2	84.2	91.0	91.0
$HILB_{2,QRS}$	98.0	98.0	77.4	77.4	84.2	84.2	91.0	91.0
$HILB_{2,2,QRS}$	98.0	97.7	77.6	77.5	84.3	83.9	91.0	90.7
$HILB_{3,QRS}$	98.0	98.0	77.4	77.4	84.2	84.2	91.0	91.0
LI_{QRS}	98.2	90.3	79.5	73.8	84.8	76.8	91.6	83.6
$LI_{m,QRS}$	99.6	61.4	95.4	38.1	99.5	50.3	99.5	55.4
MEA_{QRS}	98.0	76.7	87.6	79.5	89.7	80.9	93.8	78.7
$PSR_{old,QRS}$	98.0	98.0	78.6	78.6	84.2	84.2	91.0	91.0
PSR_{QRS}	98.0	98.0	77.4	77.4	84.2	84.2	91.0	91.0
$PSR_{2,QRS}$	98.0	98.0	77.4	77.4	84.2	84.2	91.0	91.0
$PSR_{2,2,QRS}$	98.0	96.7	78.4	77.0	85.0	83.3	91.5	89.9
$PSR_{3,QRS}$	98.0	98.0	77.4	77.4	84.2	84.2	91.0	91.0
$SC2_{QRS}$	98.0	94.9	91.1	87.2	94.2	93.9	96.1	94.1
SCA_{QRS}	98.0	94.5	92.4	86.8	95.8	95.0	96.9	94.3
$SPEC_{QRS}$	98.0	98.0	81.7	82.0	86.6	86.9	92.3	92.3
$SPEC_{m,QRS}$	98.0	95.8	87.4	84.1	90.7	86.6	94.5	91.2
STE_{QRS}	97.9	91.8	78.5	66.9	84.7	81.5	91.3	86.1
TCI_{QRS}	97.8	76.5	89.1	64.3	94.9	77.9	96.3	76.4
$TOMP_{QRS}$	98.1	40.5	86.3	52.4	98.3	47.2	97.5	44.0
VF_{QRS}	98.0	98.0	84.1	84.7	86.8	87.1	92.6	92.6
$WVL_{1,QRS}$	97.5	78.2	84.7	76.3	85.5	70.5	91.8	74.8
$WVL_{2,QRS}$	98.0	97.5	84.3	85.1	85.8	85.7	92.1	91.8
$WVL_{3,QRS}$	98.0	98.0	82.0	82.4	86.7	86.9	92.4	92.4
$WVL_{4,QRS}$	97.8	79.2	86.9	64.9	94.9	78.6	96.2	78.2

Table 6.20: *Quality of fibrillation detection algorithms used as QRS detectors (positive predictivity, accuracy) for a window length of 3 seconds in per cent, rounded on 3 digits.*

Data Source	*MIT DB*		*CU DB*		*AHA DB*		*overall results*		
Parameter	PP.	Ac.	PP.	Ac.	PP.	Ac.	PP.	Ac.	ct.
AAR_{50}	1.1	88.3	45.8	75.0	57.7	86.3	36.7	86.7	2.9
AAR_{100}	0.3	36.5	35.7	65.9	40.0	75.8	13.8	54.9	3.0
AAR_{250}	0.2	4.8	31.2	61.6	30.9	64.8	9.8	33.6	3.6
ACF_{95}	0.1	46.2	20.5	52.2	18.8	50.0	9.1	48.1	3.0
ACF_{99}	0.2	38.8	22.1	49.9	20.7	47.8	10.0	43.3	3.1
CPLX	0.2	84.6	38.6	70.3	40.4	76.4	27.3	80.3	1.6
HILB	-	99.8	-	78.1	-	82.9	-	91.4	1.4
$HILB_2$	-	99.8	0.0	78.1	-	82.9	0.0	91.4	1.4
$HILB_{2,2}$	1.6	98.8	55.4	78.6	55.8	83.4	43.8	91.1	1.4
$HILB_3$	-	99.8	100	78.1	-	82.9	100	91.4	1.4
LI	0.2	92.8	25.6	74.8	20.7	76.5	12.4	84.8	5.8
LI_m	0.4	61.6	24.6	38.4	25.2	51.4	15.6	56.0	5.8
MEA	0.5	79.1	54.0	81.1	45.1	81.1	20.9	80.1	1.5
PSR_{old}	40.0	99.8	95.0	84.0	98.5	85.5	93.1	92.8	1.4
PSR	-	99.8	-	78.1	-	82.9	-	91.4	1.4
PSR_2	-	99.8	-	78.1	-	82.9	-	91.4	1.4
$PSR_{2,2}$	0.8	92.6	47.6	77.1	45.8	81.5	31.8	87.0	1.4
PSR_3	100	99.8	93.0	78.4	99.6	83.3	99.0	91.6	1.4
SC2	4.6	97.4	75.8	88.7	96.1	93.3	75.9	95.2	3.8
SCA	4.5	97.1	70.9	88.1	94.9	94.6	74.6	95.5	3.9
SPEC	62.1	99.8	90.4	83.9	97.0	86.8	95.6	93.4	1.4
$SPEC_m$	3.2	97.1	66.1	84.8	61.4	86.0	51.4	91.7	1.4
STE	0.9	96.2	26.6	70.0	53.7	83.3	28.2	89.2	1.4
TCI	0.9	86.4	40.1	72.5	55.5	85.0	31.5	85.1	1.6
TOMP	0.2	40.5	26.9	53.7	24.7	49.1	12.7	44.9	0.80
VF	91.3	99.9	94.0	85.5	98.0	85.8	97.0	93.1	1.5
WVL_1	0.3	79.7	41.4	75.0	21.6	69.0	12.7	74.8	1.4
WVL_2	2.1	99.4	85.0	85.4	81.8	84.7	72.5	92.3	1.4
WVL_3	46.9	99.8	91.9	83.4	93.9	86.2	92.4	93.1	1.4
WVL_4	0.8	83.5	35.2	67.9	46.5	81.0	27.8	81.6	39

Table 6.21: *Quality of fibrillation detection algorithms used as VF detectors (positive predictivity, accuracy, calculation time) for a window length of 4 seconds. Positive predictivity and accuracy in per cent, rounded on 3 digits; calculation time in per cent of the real time of the data, rounded on 2 digits.*

Data Source	*MIT DB*		*CU DB*		*AHA DB*		*overall res.*	
Parameter	PP.	Ac.	PP.	Ac.	PP.	Ac.	PP.	Ac.
$AAR_{50,QRS}$	97.9	86.6	90.5	74.2	96.1	87.6	96.9	86.4
$AAR_{100,QRS}$	98.3	37.1	88.7	67.0	97.1	76.7	97.0	55.7
$AAR_{250,QRS}$	100	6.7	85.8	62.8	96.5	64.9	95.7	34.7
$ACF_{95,QRS}$	96.9	45.4	79.2	53.1	86.9	50.7	91.5	48.1
$ACF_{99,QRS}$	96.8	38.3	81.0	50.9	90.6	48.5	93.1	43.3
$CPLX_{QRS}$	97.6	82.7	89.1	69.2	95.3	75.7	96.4	79.0
$HILB_{QRS}$	98.0	98.0	77.4	77.4	84.2	84.2	90.9	90.9
$HILB_{2,QRS}$	98.0	98.0	77.4	77.4	84.2	84.2	90.9	90.9
$HILB_{2,2,QRS}$	98.0	96.9	78.8	77.8	85.9	84.6	91.9	90.6
$HILB_{3,QRS}$	98.0	98.0	77.4	77.4	84.2	84.2	90.9	90.9
LI_{QRS}	98.2	91.6	79.4	74.8	84.6	77.5	91.5	84.6
$LI_{m,QRS}$	99.6	62.9	94.5	38.8	99.5	52.0	99.4	56.9
MEA_{QRS}	98.1	78.0	88.0	80.2	90.0	81.8	94.0	79.7
$PSR_{old,QRS}$	98.1	97.9	82.5	83.1	86.4	86.8	92.3	92.3
PSR_{QRS}	98.0	98.0	77.4	77.4	84.2	84.2	90.9	90.9
$PSR_{2,QRS}$	98.0	98.0	77.4	77.4	84.2	84.2	90.9	90.9
$PSR_{2,2,QRS}$	98.2	91.3	84.2	76.3	90.0	82.6	94.2	86.8
$PSR_{3,QRS}$	98.0	98.0	77.6	77.6	84.5	84.6	91.1	91.1
$SC2_{QRS}$	98.0	95.6	90.7	87.9	94.2	94.2	96.1	94.6
SCA_{QRS}	98.1	95.2	91.9	87.4	95.8	95.5	96.9	94.9
$SPEC_{QRS}$	98.0	98.0	82.7	83.0	87.7	88.1	92.9	92.9
$SPEC_{m,QRS}$	98.0	95.3	87.6	83.8	91.3	87.2	94.8	91.2
STE_{QRS}	98.0	94.4	79.7	69.2	85.2	82.8	91.7	88.1
TCI_{QRS}	97.8	68.3	90.6	57.0	97.2	70.2	97.3	68.5
$TOMP_{QRS}$	98.1	41.0	85.4	53.2	98.1	47.9	97.3	44.6
VF_{QRS}	98.0	98.0	83.9	84.6	86.8	87.1	92.5	92.6
$WVL_{1,QRS}$	97.5	77.8	84.8	74.1	86.0	70.2	92.1	74.4
$WVL_{2,QRS}$	98.0	97.5	84.5	84.5	86.1	86.0	92.3	91.9
$WVL_{3,QRS}$	98.0	98.0	82.0	82.4	87.2	87.5	92.6	92.6
$WVL_{4,QRS}$	97.9	81.9	87.1	67.3	95.4	82.2	96.4	81.3

Table 6.22: *Quality of fibrillation detection algorithms used as QRS detectors (positive predictivity, accuracy) for a window length of 4 seconds in per cent, rounded on 3 digits.*

Data Source	*MIT DB*		*CU DB*		*AHA DB*		*overall results*		
Parameter	PP.	Ac.	PP.	Ac.	PP.	Ac.	PP.	Ac.	ct.
AAR_{50}	1.5	90.9	45.0	74.5	56.6	85.7	38.7	87.8	3.0
AAR_{100}	0.2	28.6	35.0	65.0	37.0	72.8	12.6	49.5	3.2
AAR_{250}	0.2	2.5	29.8	59.9	30.1	63.5	9.6	31.7	3.8
ACF_{95}	0.1	34.7	15.2	42.8	13.6	37.3	6.4	36.3	3.4
ACF_{99}	0.1	22.2	18.2	39.0	15.8	32.4	7.5	27.5	3.4
CPLX	0.2	83.7	40.2	72.0	43.2	78.6	27.9	80.9	1.7
HILB	-	99.8	-	78.1	-	82.9	-	91.4	1.4
$HILB_2$	49.8	99.8	85.0	82.3	96.6	87.1	93.7	93.4	1.4
$HILB_{2,2}$	2.0	97.6	57.4	79.6	63.9	85.6	50.5	91.5	1.4
$HILB_3$	53.5	99.8	89.2	86.8	98.4	91.4	96.3	95.5	1.5
LI	0.1	93.7	26.3	75.4	20.3	77.0	12.4	85.5	7.7
LI_m	0.4	62.6	24.7	38.8	25.7	52.7	15.9	57.1	7.5
MEA	0.5	79.8	54.9	81.4	46.3	81.6	21.8	80.6	1.6
PSR_{old}	22.7	99.5	83.0	87.3	96.2	89.8	89.3	94.7	1.5
PSR	-	99.8	-	78.1	-	82.9	-	91.4	1.4
PSR_2	71.4	99.8	78.3	78.2	99.4	83.1	96.2	91.5	1.4
$PSR_{2,2}$	0.8	85.9	44.0	73.9	42.1	78.7	27.6	82.2	1.4
PSR_3	26.3	99.6	73.3	87.2	92.4	94.3	87.3	96.7	1.4
SC2	5.1	97.7	77.9	88.9	97.0	93.4	78.4	95.4	4.0
SCA	4.9	97.4	73.4	88.7	96.2	94.8	77.4	95.8	4.2
SPEC	65.2	99.8	92.2	83.1	96.2	85.9	95.3	93.0	1.5
$SPEC_m$	3.9	97.8	70.7	85.6	65.3	86.6	56.0	92.3	1.5
STE	0.6	91.6	27.4	66.6	44.6	81.8	23.1	86.1	1.5
TCI	0.7	80.0	35.9	67.0	46.3	80.7	26.5	79.6	1.7
TOMP	0.2	39.7	26.7	51.3	24.5	48.2	12.6	43.9	0.81
VF	88.3	99.9	94.3	85.4	98.2	85.8	97.2	93.1	1.5
WVL_1	0.2	81.3	43.0	76.0	22.2	70.2	13.2	76.2	1.5
WVL_2	0.8	99.4	86.3	85.4	83.5	84.7	72.9	92.3	1.5
WVL_3	55.5	99.8	93.8	83.4	94.9	86.1	93.8	93.1	1.5
WVL_4	0.9	85.5	36.2	68.9	50.9	83.3	30.7	83.7	39

Table 6.23: *Quality of fibrillation detection algorithms used as VF detectors (positive predictivity, accuracy, calculation time) for a window length of 5 seconds. Positive predictivity and accuracy in per cent, rounded on 3 digits; calculation time in per cent of the real time of the data, rounded on 2 digits.*

Data Source	*MIT DB*		*CU DB*		*AHA DB*		*overall res.*	
Parameter	PP.	Ac.	PP.	Ac.	PP.	Ac.	PP.	Ac.
$AAR_{50,QRS}$	98.0	89.2	89.8	73.7	95.3	87.0	96.6	87.4
$AAR_{100,QRS}$	98.0	29.4	88.6	66.2	97.0	73.5	96.8	50.3
$AAR_{250,QRS}$	100	4.3	85.0	61.1	96.4	63.6	95.3	32.8
$ACF_{95,QRS}$	96.9	34.7	72.9	43.3	79.7	38.1	87.7	36.6
$ACF_{99,QRS}$	96.3	22.6	74.7	39.7	82.8	33.0	88.4	28.0
$CPLX_{QRS}$	97.6	81.8	89.0	70.7	95.5	77.9	96.4	79.6
$HILB_{QRS}$	98.0	98.0	77.3	77.3	84.2	84.2	90.9	90.9
$HILB_{2,QRS}$	98.0	98.0	81.3	81.5	87.9	88.3	92.9	93.0
$HILB_{2,2,QRS}$	98.0	95.8	81.4	78.8	89.2	86.7	93.5	91.0
$HILB_{3,QRS}$	98.1	98.0	85.6	85.9	92.1	92.7	95.0	95.1
LI_{QRS}	98.2	92.4	79.3	75.4	84.5	78.0	91.4	85.3
$LI_{m,QRS}$	99.6	64.0	93.8	39.3	99.4	53.2	99.4	58.1
MEA_{QRS}	98.1	78.7	88.0	80.5	90.3	82.2	94.1	80.3
$PSR_{old,QRS}$	98.1	97.7	86.9	86.4	90.7	91.1	94.5	94.3
PSR_{QRS}	98.0	98.0	77.3	77.3	84.2	84.2	90.9	90.9
$PSR_{2,QRS}$	98.0	98.0	77.5	77.5	84.3	84.4	91.0	91.0
$PSR_{2,2,QRS}$	98.5	85.3	88.6	73.3	93.5	79.6	96.1	82.2
$PSR_{3,QRS}$	98.1	97.8	89.6	86.3	96.0	95.5	96.9	96.2
$SC2_{QRS}$	98.0	95.9	90.2	88.0	94.2	94.3	96.1	94.8
SCA_{QRS}	98.1	95.6	91.6	87.9	95.8	95.7	96.9	95.2
$SPEC_{QRS}$	98.0	98.0	81.8	82.2	86.8	87.1	92.4	92.5
$SPEC_{m,QRS}$	98.0	95.9	87.3	84.6	90.9	87.8	94.6	91.8
STE_{QRS}	97.9	89.8	80.7	65.8	86.3	81.2	92.2	84.9
TCI_{QRS}	97.8	78.3	89.7	66.5	95.9	80.9	96.7	78.8
$TOMP_{QRS}$	98.1	40.2	86.5	50.8	98.4	46.9	97.6	43.6
VF_{QRS}	98.0	98.0	83.9	84.5	86.7	87.1	92.5	92.6
$WVL_{1,QRS}$	97.6	79.4	84.8	75.1	86.0	71.4	92.1	75.7
$WVL_{2,QRS}$	98.0	97.5	84.5	84.6	86.0	86.0	92.2	91.9
$WVL_{3,QRS}$	98.0	98.0	82.0	82.5	87.1	87.3	92.6	92.6
$WVL_{4,QRS}$	98.0	83.9	87.2	68.2	95.6	84.6	96.6	83.4

Table 6.24: *Quality of fibrillation detection algorithms used as QRS detectors (positive predictivity, accuracy) for a window length of 5 seconds in per cent, rounded on 3 digits.*

Data Source	*MIT DB*		*CU DB*		*AHA DB*		*overall results*		
Parameter	PP.	Ac.	PP.	Ac.	PP.	Ac.	PP.	Ac.	ct.
AAR_{50}	1.4	90.8	45.6	75.0	57.5	86.1	39.0	87.9	3.1
AAR_{100}	0.2	32.3	35.1	65.0	39.0	74.9	13.2	52.3	3.4
AAR_{250}	0.2	2.7	29.7	59.6	30.6	64.2	9.6	32.1	4.1
ACF_{95}	0.1	42.9	17.5	49.9	15.5	44.9	7.4	44.1	3.4
ACF_{99}	0.1	29.1	20.4	46.0	17.6	39.6	8.4	34.5	3.5
CPLX	0.2	86.3	42.0	73.5	45.4	80.1	30.5	82.9	1.9
HILB	57.0	99.9	89.1	87.0	98.7	92.0	96.7	95.8	1.5
$HILB_2$	17.0	99.3	74.9	86.9	88.5	92.9	82.6	95.9	1.5
$HILB_{2,2}$	2.3	96.0	55.9	80.1	66.0	87.6	50.8	91.5	1.5
$HILB_3$	19.0	99.4	75.4	88.2	91.9	94.9	86.2	96.9	1.6
LI	0.2	94.2	25.8	75.7	20.1	77.3	12.4	86.0	8.9
LI_m	0.5	63.5	24.6	39.0	26.0	53.4	16.1	57.9	8.7
MEA	0.5	80.2	55.2	81.5	46.9	81.8	22.5	80.9	1.8
PSR_{old}	12.7	99.1	73.5	86.9	93.6	91.9	83.5	95.3	1.6
PSR	97.4	99.9	94.2	79.2	99.0	84.1	98.4	92.0	1.4
PSR_2	52.0	99.8	81.6	84.1	94.6	89.6	91.9	94.6	1.4
$PSR_{2,2}$	0.7	80.4	39.8	69.3	38.3	74.9	24.3	77.5	1.4
PSR_3	9.2	98.6	59.9	83.6	80.8	93.7	72.1	95.7	1.4
SC2	5.3	97.9	78.9	88.8	97.6	93.4	79.9	95.5	4.5
SCA	5.3	97.6	75.4	89.0	97.1	94.9	79.3	96.0	4.7
SPEC	62.4	99.8	92.2	83.5	97.2	86.6	96.1	93.3	1.6
$SPEC_m$	3.7	97.7	68.3	85.1	64.4	86.6	55.1	92.2	1.5
STE	0.8	92.4	29.4	67.0	46.0	81.9	26.9	86.6	1.6
TCI	0.8	84.6	39.4	71.3	55.2	85.2	31.3	84.1	1.8
TOMP	0.2	40.1	26.7	52.0	24.6	48.7	12.7	44.4	0.82
VF	86.6	99.9	94.2	85.3	98.5	85.8	97.3	93.0	1.6
WVL_1	0.3	80.6	44.1	76.4	23.5	70.5	13.8	76.1	1.6
WVL_2	3.5	99.4	83.6	85.1	83.8	84.9	73.1	92.4	1.6
WVL_3	52.4	99.8	93.3	83.5	94.8	86.4	93.6	93.2	1.6
WVL_4	1.0	87.0	36.1	69.3	53.6	84.6	32.8	85.0	39

Table 6.25: *Quality of fibrillation detection algorithms used as VF detectors (positive predictivity, accuracy, calculation time) for a window length of 6 seconds. Positive predictivity and accuracy in per cent, rounded on 3 digits; calculation time in per cent of the real time of the data, rounded on 2 digits.*

Data Source	*MIT DB*		*CU DB*		*AHA DB*		*overall res.*	
Parameter	PP.	Ac.	PP.	Ac.	PP.	Ac.	PP.	Ac.
$AAR_{50,QRS}$	98.0	89.0	89.5	74.1	95.4	87.3	96.6	87.5
$AAR_{100,QRS}$	98.2	33.0	88.7	66.2	97.1	75.7	97.0	53.1
$AAR_{250,QRS}$	100	4.6	84.9	60.8	96.5	64.3	95.4	33.2
$ACF_{95,QRS}$	97.0	42.4	76.1	50.3	83.2	45.7	89.6	44.3
$ACF_{99,QRS}$	96.7	29.2	78.6	46.7	86.8	40.3	90.9	34.9
$CPLX_{QRS}$	97.7	84.4	89.1	72.3	95.5	79.5	96.5	81.7
$HILB_{QRS}$	98.1	98.0	85.9	86.2	92.7	93.2	95.3	95.3
$HILB_{2,QRS}$	98.1	97.5	88.6	86.1	95.0	94.1	96.4	95.5
$HILB_{2,2,QRS}$	98.1	94.3	84.4	79.5	92.6	88.5	95.2	91.0
$HILB_{3,QRS}$	98.1	97.6	90.4	87.2	96.9	96.2	97.3	96.4
LI_{QRS}	98.2	93.0	79.1	75.6	84.5	78.4	91.4	85.8
$LI_{m,QRS}$	99.6	64.8	92.8	39.5	99.4	53.9	99.4	58.8
MEA_{QRS}	98.1	79.2	88.2	80.6	90.5	82.4	94.3	80.6
$PSR_{old,QRS}$	98.1	97.2	88.5	85.9	93.1	93.1	95.6	94.9
PSR_{QRS}	98.0	98.0	78.3	78.5	85.2	85.4	91.5	91.5
$PSR_{2,QRS}$	98.1	98.0	83.6	83.4	90.5	90.8	94.2	94.1
$PSR_{2,2,QRS}$	98.7	80.3	90.4	68.8	95.4	75.7	97.1	77.7
$PSR_{3,QRS}$	98.1	96.8	91.7	82.8	97.9	94.8	97.8	95.2
$SC2_{QRS}$	98.0	96.0	89.9	88.0	94.1	94.3	96.1	94.9
SCA_{QRS}	98.1	95.8	91.3	88.2	95.8	95.8	96.8	95.4
$SPEC_{QRS}$	98.0	98.0	82.2	82.7	87.5	87.9	92.8	92.8
$SPEC_{m,QRS}$	98.0	95.8	87.3	84.1	91.3	87.8	94.8	91.8
STE_{QRS}	97.9	90.6	81.6	66.2	87.2	81.3	92.7	85.4
TCI_{QRS}	97.8	73.9	90.6	62.3	97.1	76.2	97.2	74.3
$TOMP_{QRS}$	98.1	40.5	85.9	51.5	98.2	47.4	97.4	44.1
VF_{QRS}	98.0	98.0	83.7	84.4	86.7	87.0	92.5	92.6
$WVL_{1,QRS}$	97.6	78.8	85.1	75.5	86.4	71.7	92.3	75.6
$WVL_{2,QRS}$	98.0	97.5	84.4	84.3	86.2	86.1	92.3	91.9
$WVL_{3,QRS}$	98.0	98.0	82.1	82.6	87.4	87.7	92.7	92.7
$WVL_{4,QRS}$	98.0	85.4	86.5	68.6	95.7	85.8	96.6	84.7

Table 6.26: *Quality of fibrillation detection algorithms used as QRS detectors (positive predictivity, accuracy) for a window length of 6 seconds in per cent, rounded on 3 digits.*

Data Source	*MIT DB*		*CU DB*		*AHA DB*		*overall results*		
Parameter	PP.	Ac.	PP.	Ac.	PP.	Ac.	PP.	Ac.	ct.
AAR_{50}	1.6	91.4	43.2	72.9	31.1	65.0	27.0	79.1	3.1
AAR_{100}	0.2	3.2	33.8	63.1	37.9	73.6	10.3	36.6	3.5
AAR_{250}	0.2	3.2	30.1	60.1	31.1	65.0	9.7	32.8	4.2
ACF_{95}	0.1	45.4	18.2	52.7	17.4	50.2	8.0	47.9	3.5
ACF_{99}	0.1	30.7	21.4	49.0	19.2	44.1	8.9	37.4	3.5
CPLX	0.2	88.1	45.2	76.2	50.9	83.3	33.7	85.4	2.1
HILB	15.0	99.2	71.9	87.3	88.2	94.8	82.0	96.7	1.7
$HILB_2$	7.3	98.1	63.1	84.7	77.6	92.6	68.4	95.1	1.7
$HILB_{2,2}$	2.0	94.3	54.5	80.1	65.8	88.7	49.0	91.1	1.7
$HILB_3$	9.3	98.6	65.3	85.6	84.1	94.3	75.2	96.1	1.6
LI	0.1	94.6	26.7	76.1	19.9	77.6	12.3	86.4	10
LI_m	0.5	64.2	24.6	39.3	26.3	54.0	16.3	58.5	9.7
MEA	0.5	80.5	55.6	81.7	47.4	81.9	22.9	81.2	2.0
PSR_{old}	7.6	98.4	65.9	85.5	89.8	92.5	76.2	95.2	1.6
PSR	41.4	99.8	78.7	87.2	93.8	93.7	90.6	96.5	1.5
PSR_2	22.8	99.5	71.2	86.2	84.5	92.8	80.3	95.9	1.5
$PSR_{2,2}$	0.6	76.1	37.0	65.2	35.2	71.2	21.9	73.4	1.5
PSR_3	5.3	97.4	53.1	80.0	69.8	91.2	60.0	93.8	1.5
SC2	5.5	98.1	79.8	88.7	98.0	93.4	81.2	95.6	4.7
SCA	5.4	97.8	76.5	89.1	97.5	94.9	80.5	96.1	4.9
SPEC	63.9	99.9	90.7	84.1	97.2	87.4	95.9	93.7	1.6
$SPEC_m$	3.8	97.6	68.5	85.3	65.0	86.9	55.5	92.3	1.6
STE	0.5	85.4	28.9	64.2	36.6	77.4	20.8	80.8	1.6
TCI	0.7	80.8	36.7	67.8	48.1	81.8	27.7	80.5	1.9
TOMP	0.2	40.4	26.7	52.6	24.7	49.1	12.7	44.8	0.82
VF	83.6	99.9	94.6	85.2	98.7	85.7	97.5	93.0	1.6
WVL_1	0.3	82.3	43.0	75.9	23.5	71.0	14.1	77.1	1.6
WVL_2	1.7	99.4	85.4	85.3	84.3	84.8	73.5	92.3	1.6
WVL_3	38.8	99.8	91.2	84.0	92.4	86.9	90.8	93.4	1.6
WVL_4	1.1	88.2	36.4	69.6	56.9	85.9	35.2	86.3	40

Table 6.27: *Quality of fibrillation detection algorithms used as VF detectors (positive predictivity, accuracy, calculation time) for a window length of 7 seconds. Positive predictivity and accuracy in per cent, rounded on 3 digits; calculation time in per cent of the real time of the data, rounded on 2 digits.*

Data Source	*MIT DB*		*CU DB*		*AHA DB*		*overall res.*	
Parameter	PP.	Ac.	PP.	Ac.	PP.	Ac.	PP.	Ac.
$AAR_{50,QRS}$	98.1	89.8	89.5	72.0	96.5	65.1	97.2	78.2
$AAR_{100,QRS}$	100	5.1	88.4	64.4	97.3	74.4	96.6	38.0
$AAR_{250,QRS}$	100	5.1	85.1	61.4	96.5	65.1	95.5	33.8
$ACF_{95,QRS}$	97.0	44.8	76.9	53.1	85.2	51.0	90.4	47.9
$ACF_{99,QRS}$	96.7	30.7	79.6	49.6	89.0	44.7	91.9	37.7
$CPLX_{QRS}$	97.7	86.2	88.6	75.0	94.8	83.0	96.2	84.2
$HILB_{QRS}$	98.1	97.4	90.4	86.4	97.5	96.0	97.5	96.2
$HILB_{2,QRS}$	98.1	96.4	91.0	83.9	97.3	93.7	97.5	94.6
$HILB_{2,2,QRS}$	98.1	92.7	87.2	79.8	95.1	89.5	96.4	90.7
$HILB_{3,QRS}$	98.1	96.8	91.0	84.6	97.8	95.5	97.7	95.6
LI_{QRS}	98.2	93.4	79.1	76.0	84.4	78.7	91.4	86.2
$LI_{m,QRS}$	99.6	65.5	92.2	39.8	99.3	54.6	99.3	59.5
MEA_{QRS}	98.1	79.5	88.2	80.8	90.6	82.5	94.3	80.9
$PSR_{old,QRS}$	98.1	96.6	89.3	84.5	94.3	93.7	96.2	94.7
PSR_{QRS}	98.1	97.9	87.9	86.3	95.1	94.9	96.4	96.0
$PSR_{2,QRS}$	98.1	97.7	88.9	85.5	95.5	93.9	96.7	95.4
$PSR_{2,2,QRS}$	99.0	76.4	91.3	64.8	96.3	71.9	97.6	73.9
$PSR_{3,QRS}$	98.1	95.7	92.0	79.3	98.3	92.2	97.9	93.3
$SC2_{QRS}$	98.0	96.2	89.5	87.9	94.1	94.4	96.0	95.0
SCA_{QRS}	98.1	95.9	91.0	88.3	95.8	95.9	96.8	95.5
$SPEC_{QRS}$	98.0	98.0	82.9	83.3	88.3	88.7	93.1	93.2
$SPEC_{m,QRS}$	98.0	95.7	87.7	84.4	91.8	88.1	95.0	91.9
STE_{QRS}	97.8	83.7	82.3	63.3	88.2	76.8	93.1	79.6
TCI_{QRS}	97.8	79.1	90.0	67.5	96.2	81.9	96.8	79.7
$TOMP_{QRS}$	98.1	40.8	85.3	52.0	98.1	47.8	97.3	44.4
VF_{QRS}	98.0	98.0	83.6	84.3	86.7	87.0	92.5	92.6
$WVL_{1,QRS}$	97.6	80.4	84.8	74.9	86.3	72.3	92.2	76.6
$WVL_{2,QRS}$	98.0	97.5	84.4	84.5	86.1	86.1	92.2	91.9
$WVL_{3,QRS}$	98.0	98.0	82.7	83.1	88.0	88.2	93.0	93.0
$WVL_{4,QRS}$	98.0	86.7	86.3	68.9	95.8	87.2	96.6	85.9

Table 6.28: *Quality of fibrillation detection algorithms used as QRS detectors (positive predictivity, accuracy) for a window length of 7 seconds in per cent, rounded on 3 digits.*

Data Source	*MIT DB*		*CU DB*		*AHA DB*		*overall results*		
Parameter	PP.	Ac.	PP.	Ac.	PP.	Ac.	PP.	Ac.	ct.
AAR_{50}	1.2	88.6	42.3	72.0	50.0	82.9	34.0	85.3	3.5
AAR_{100}	0.2	4.5	34.4	64.1	38.0	73.7	10.4	37.4	3.9
AAR_{250}	0.2	4.5	30.2	60.8	50.0	82.9	10.1	41.2	5.9
ACF_{95}	0.1	45.2	20.4	55.6	18.9	53.5	8.5	49.3	4.1
ACF_{99}	0.1	28.7	22.7	51.3	20.1	46.4	9.0	37.5	4.4
CPLX	0.1	92.8	52.9	80.4	61.4	86.8	42.3	89.6	-
HILB	3.9	96.2	50.6	78.3	69.0	91.0	56.4	93.0	1.9
$HILB_2$	2.6	94.1	48.2	76.6	59.5	87.6	46.8	90.4	1.9
$HILB_{2,2}$	1.6	90.9	50.0	77.9	61.8	88.3	43.0	89.1	1.9
$HILB_3$	4.8	97.0	53.5	80.1	72.9	92.0	60.9	94.0	1.9
LI	0.1	95.2	28.9	76.8	19.5	78.0	12.3	86.8	17
LI_m	0.5	65.3	24.6	39.8	26.7	55.0	16.6	59.5	17
MEA	0.5	80.9	55.9	81.7	47.8	82.0	23.6	81.5	4.4
PSR_{old}	3.5	96.3	54.9	81.6	78.1	91.4	60.2	93.5	2.2
PSR	6.7	98.0	55.8	81.3	72.9	91.8	64.1	94.5	1.8
PSR_2	6.0	97.7	54.2	80.5	64.1	89.1	56.9	93.1	1.8
$PSR_{2,2}$	0.5	69.5	33.3	58.7	31.5	65.5	19.0	67.2	1.8
PSR_3	2.9	94.9	45.5	74.4	54.8	85.4	45.1	89.8	1.8
SC2	5.5	98.2	81.5	88.5	98.5	93.4	82.8	95.6	6.0
SCA	5.7	98.0	78.8	89.2	98.2	94.8	82.4	96.2	6.5
SPEC	63.9	99.8	92.0	84.0	96.9	87.3	95.9	93.6	2.0
$SPEC_m$	4.0	97.8	71.2	85.8	67.3	87.3	58.1	92.7	2.0
STE	0.4	73.3	28.4	60.4	31.4	70.6	17.0	71.5	2.0
TCI	0.7	81.1	36.9	68.0	49.1	82.3	28.3	80.9	2.3
TOMP	0.2	40.0	26.5	51.5	24.6	48.6	12.7	44.3	0.82
VF	81.6	99.9	94.7	85.0	99.1	85.7	97.8	93.0	1.9
WVL_1	0.4	83.2	44.7	76.7	24.8	72.0	15.0	78.1	2.0
WVL_2	2.3	99.4	83.7	85.0	85.0	84.8	73.6	92.4	2.1
WVL_3	42.1	99.8	92.8	84.0	93.9	86.9	92.5	93.4	2.0
WVL_4	1.2	89.4	37.1	70.3	60.4	87.2	37.7	87.5	43

Table 6.29: *Quality of fibrillation detection algorithms used as VF detectors (positive predictivity, accuracy, calculation time) for a window length of 9 seconds. Positive predictivity and accuracy in per cent, rounded on 3 digits; calculation time in per cent of the real time of the data, rounded on 2 digits.*

Data Source	*MIT DB*		*CU DB*		*AHA DB*		*overall res.*	
Parameter	PP.	Ac.	PP.	Ac.	PP.	Ac.	PP.	Ac.
$AAR_{50,QRS}$	98.0	86.9	89.2	71.2	96.1	84.1	96.9	84.9
$AAR_{100,QRS}$	100	6.4	88.2	65.3	97.3	74.4	96.6	38.8
$AAR_{250,QRS}$	100	6.4	84.6	62.1	96.1	84.1	95.4	42.7
$ACF_{95,QRS}$	97.1	44.6	78.6	56.2	86.4	54.3	91.0	49.4
$ACF_{99,QRS}$	96.9	28.9	80.8	51.9	89.8	47.1	92.2	37.9
$CPLX_{QRS}$	97.8	90.9	87.1	79.3	92.9	86.8	95.3	88.5
$HILB_{QRS}$	98.1	94.6	91.3	77.3	98.5	92.0	98.0	92.6
$HILB_{2,QRS}$	98.2	92.6	91.7	75.9	98.3	88.5	98.0	90.0
$HILB_{2,2,QRS}$	98.1	89.4	90.2	77.6	97.5	89.0	97.5	88.6
$HILB_{3,QRS}$	98.1	95.3	91.1	79.2	98.2	93.0	97.9	93.5
LI_{QRS}	98.2	93.9	79.0	76.6	84.3	79.1	91.3	86.6
$LI_{m,QRS}$	99.6	66.6	91.0	40.2	99.1	55.6	99.2	60.5
MEA_{QRS}	98.1	79.9	88.3	81.0	90.8	82.7	94.5	81.1
$PSR_{old,QRS}$	98.1	94.7	89.9	80.7	95.3	92.6	96.6	93.0
PSR_{QRS}	98.1	96.3	91.0	80.5	97.9	92.9	97.8	94.0
$PSR_{2,QRS}$	98.2	96.0	91.2	80.0	97.7	90.1	97.7	92.6
$PSR_{2,2,QRS}$	99.3	70.5	91.9	58.5	97.1	66.1	98.2	68.0
$PSR_{3,QRS}$	98.2	93.3	91.8	73.8	98.5	86.3	98.1	89.3
$SC2_{QRS}$	98.0	96.4	88.8	87.7	94.0	94.4	96.0	95.1
SCA_{QRS}	98.0	96.2	90.5	88.4	95.7	95.8	96.7	95.6
$SPEC_{QRS}$	98.0	98.0	82.7	83.2	88.1	88.5	93.1	93.1
$SPEC_{m,QRS}$	98.0	96.0	87.5	84.9	91.7	88.5	95.0	92.2
STE_{QRS}	97.6	71.8	83.3	59.5	90.1	69.7	93.9	70.2
TCI_{QRS}	97.8	79.4	89.9	67.7	96.4	82.5	96.9	80.1
$TOMP_{QRS}$	98.1	40.4	85.5	51.0	98.3	47.3	97.4	43.9
VF_{QRS}	98.0	98.0	83.5	84.1	86.6	87.0	92.5	92.5
$WVL_{1,QRS}$	97.6	81.4	85.0	75.7	86.5	73.2	92.4	77.6
$WVL_{2,QRS}$	98.0	97.5	84.2	84.2	86.1	86.1	92.3	91.9
$WVL_{3,QRS}$	98.0	98.0	82.5	82.9	87.9	88.2	93.0	93.0
$WVL_{4,QRS}$	98.0	87.9	86.1	69.5	95.8	88.4	96.6	87.1

Table 6.30: *Quality of fibrillation detection algorithms used as QRS detectors (positive predictivity, accuracy) for a window length of 9 seconds in per cent, rounded on 3 digits.*

Data Source	*MIT DB*		*CU DB*		*AHA DB*		*overall results*		
Parameter	PP.	Ac.	PP.	Ac.	PP.	Ac.	PP.	Ac.	ct.
AAR_{50}	1.3	90.7	45.3	74.7	55.6	85.2	37.6	87.5	3.7
AAR_{100}	0.2	4.2	33.0	62.1	39.6	75.1	10.5	37.7	4.0
AAR_{250}	0.2	4.2	29.7	60.5	55.6	85.2	9.5	42.0	6.1
ACF_{95}	0.1	44.0	20.3	55.8	19.1	53.6	8.4	48.8	4.2
ACF_{99}	0.1	27.4	23.2	51.8	20.1	46.2	9.0	36.7	4.4
CPLX	0.1	92.8	56.1	81.5	63.4	87.0	42.6	89.7	-
HILB	2.6	94.2	45.2	74.1	60.6	88.1	47.3	90.5	1.9
$HILB_2$	1.8	91.1	43.3	72.4	52.2	84.1	38.9	87.1	1.9
$HILB_{2,2}$	1.4	89.2	48.0	76.5	58.7	87.2	39.7	87.6	1.9
$HILB_3$	3.7	96.0	49.2	77.3	68.2	90.6	55.2	92.7	2.0
LI	0.1	95.4	30.6	77.1	19.4	78.1	12.3	87.0	18
LI_m	0.5	65.8	24.6	40.1	26.8	55.4	16.7	60.0	20
MEA	0.5	81.0	56.6	82.0	47.7	82.0	23.7	81.5	6.2
PSR_{old}	2.6	95.0	52.9	80.6	71.1	90.1	53.0	92.1	2.2
PSR	4.1	96.6	50.2	78.0	62.1	88.5	52.8	92.2	1.9
PSR_2	3.8	96.1	49.3	77.4	55.8	85.9	47.9	90.7	1.9
$PSR_{2,2}$	0.5	67.0	31.9	55.9	30.4	63.5	18.2	64.9	1.9
PSR_3	2.3	93.6	43.2	72.3	50.2	82.9	40.6	87.9	1.9
SC2	5.5	98.3	83.0	88.6	98.7	93.3	83.3	95.6	6.4
SCA	5.7	98.1	80.0	89.3	98.5	94.8	83.1	96.2	6.9
SPEC	61.1	99.8	91.8	84.3	97.0	87.6	95.9	93.7	2.0
$SPEC_m$	3.8	97.8	70.7	85.6	67.2	87.3	58.0	92.7	2.1
STE	0.4	68.3	28.5	59.5	30.3	68.1	16.1	67.7	2.1
TCI	0.7	83.6	38.5	70.1	54.2	84.9	31.0	83.4	2.4
TOMP	0.2	40.2	26.5	52.0	24.7	48.9	12.7	44.6	0.84
VF	78.8	99.9	94.9	84.9	99.3	85.7	98.0	93.0	2.0
WVL_1	0.4	83.0	43.8	76.2	25.3	71.9	15.3	77.9	2.1
WVL_2	3.4	99.3	83.1	84.9	85.4	84.9	73.8	92.4	2.1
WVL_3	42.0	99.8	92.6	84.0	93.3	87.0	92.1	93.5	2.1
WVL_4	1.3	90.2	37.2	70.5	61.7	87.6	39.2	88.1	44

Table 6.31: *Quality of fibrillation detection algorithms used as VF detectors (positive predictivity, accuracy, calculation time) for a window length of 10 seconds. Positive predictivity and accuracy in per cent, rounded on 3 digits; calculation time in per cent of the real time of the data, rounded on 2 digits.*

Data Source	*MIT DB*		*CU DB*		*AHA DB*		*overall res.*	
Parameter	PP.	Ac.	PP.	Ac.	PP.	Ac.	PP.	Ac.
$AAR_{50,QRS}$	98.0	89.0	88.6	73.7	94.7	86.4	96.3	87.1
$AAR_{100,QRS}$	100	6.1	87.8	63.4	97.5	75.9	96.8	39.1
$AAR_{250,QRS}$	100	6.1	84.1	61.8	94.7	86.4	94.2	43.5
$ACF_{95,QRS}$	97.2	43.6	78.5	56.3	86.6	54.5	91.0	48.9
$ACF_{99,QRS}$	97.1	27.8	81.2	52.4	89.9	46.8	92.3	37.3
$CPLX_{QRS}$	97.8	90.9	86.8	80.4	92.3	87.2	95.0	88.8
$HILB_{QRS}$	98.2	92.6	91.2	73.1	98.7	89.0	98.1	90.0
$HILB_{2,QRS}$	98.2	89.8	91.6	71.8	98.5	84.9	98.1	86.8
$HILB_{2,2,QRS}$	98.1	87.7	91.3	76.2	97.9	87.8	97.7	87.1
$HILB_{3,QRS}$	98.2	94.4	90.9	76.5	98.3	91.7	97.9	92.3
LI_{QRS}	98.2	94.1	79.0	76.9	84.3	79.3	91.3	86.8
$LI_{m,QRS}$	99.6	67.1	90.5	40.5	99.1	56.0	99.2	60.9
MEA_{QRS}	98.1	80.0	88.3	81.2	90.9	82.6	94.5	81.2
$PSR_{old,QRS}$	98.1	93.4	90.0	79.7	95.4	91.2	96.7	91.7
PSR_{QRS}	98.2	94.9	91.1	77.3	98.2	89.5	97.9	91.7
$PSR_{2,QRS}$	98.2	94.6	91.5	77.0	98.1	86.8	97.9	90.3
$PSR_{2,2,QRS}$	99.5	68.2	91.7	55.7	97.3	63.8	98.4	65.6
$PSR_{3,QRS}$	98.2	92.1	91.6	71.7	98.5	83.8	98.1	87.4
$SC2_{QRS}$	98.0	96.4	88.5	87.7	94.0	94.3	95.9	95.1
SCA_{QRS}	98.0	96.2	90.3	88.5	95.6	95.8	96.7	95.7
$SPEC_{QRS}$	98.0	98.0	82.9	83.4	88.4	88.8	93.2	93.3
$SPEC_{m,QRS}$	98.0	96.0	87.4	84.7	91.8	88.6	95.0	92.2
STE_{QRS}	97.4	66.7	83.8	58.5	91.0	67.2	94.2	66.5
TCI_{QRS}	97.7	77.0	90.4	65.5	97.0	79.7	97.1	77.6
$TOMP_{QRS}$	98.0	40.6	85.1	51.5	98.2	47.6	97.3	44.2
VF_{QRS}	98.0	98.0	83.3	84.0	86.6	87.0	92.5	92.5
$WVL_{1,QRS}$	97.6	81.2	84.8	75.2	86.8	73.1	92.5	77.4
$WVL_{2,QRS}$	98.0	97.5	84.2	84.1	86.2	86.2	92.3	91.9
$WVL_{3,QRS}$	98.0	98.0	82.5	83.0	88.0	88.2	93.0	93.0
$WVL_{4,QRS}$	98.1	88.6	85.9	69.7	95.8	88.9	96.6	87.7

Table 6.32: *Quality of fibrillation detection algorithms used as QRS detectors (positive predictivity, accuracy) for a window length of 10 seconds in per cent, rounded on 3 digits.*

Chapter 7

Illustrations of Results

This chapter illustrates some results from the Tables 6.1 - 6.32. The dependence of the "Integrated Receiver Operator Characteristic" and the Sensitivity and Specificity on the window length are shown in plots.

7.1 Illustration of decision process

In order to illustrate the results of the analysis of a certain algorithm analyzing a special ECG file, a MATLAB program was written. It shows the desired value, the algorithms decision and some parameters in dependence on the signal time in different colors.

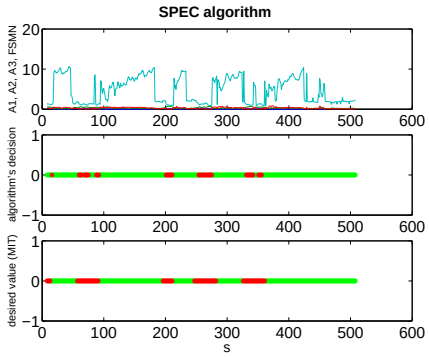

Figure 7.1: *Results of SPEC analysis (file cu21) from [17]*
middle: algorithm's decision:
red: defibrillation recommended
green: defibrillation not recommended
bottom: annotation from file:
red: ventricular fibrillation
green: no ventricular fibrillation
calculated sensitivity: 0.488
calculated specificity: 0.995

7.2 Quality dependence on window length

The experiments were carried out for different window lengths. The reason is to find out, which window length yields the best quality. Here, the quality parameters of some algorithms are shown in a receiver operator characteristic plot. Good algorithms lie in the upper left corner.

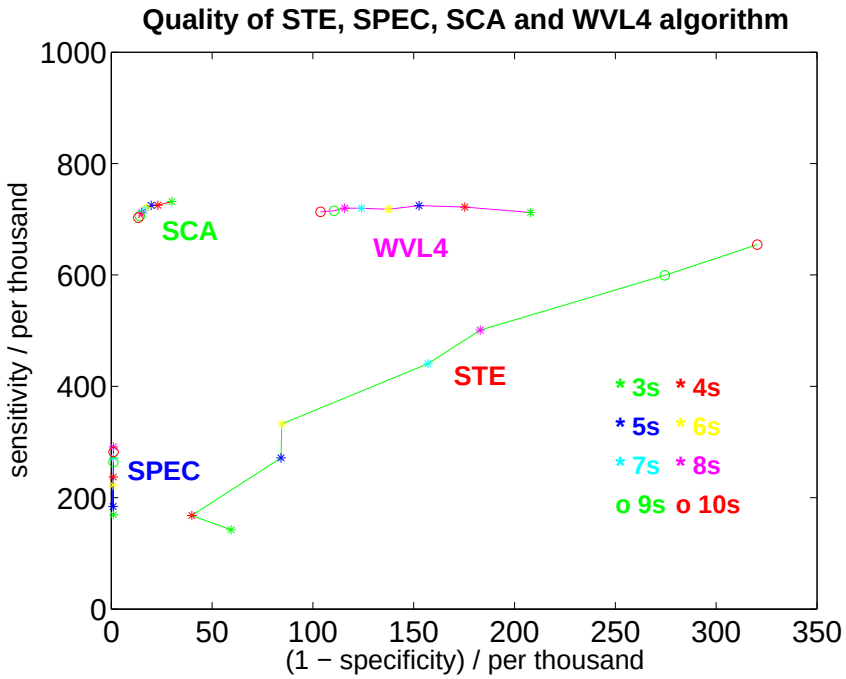

Figure 7.2: *Quality of four different algorithms: Receiver operator characteristic, i.e., sensitivity in dependence on both (1-specificity) and window length.*

The following two figures show the integrated receiver operator characteristic of the algorithms in dependence on the used window length. For clarity two plots are used.

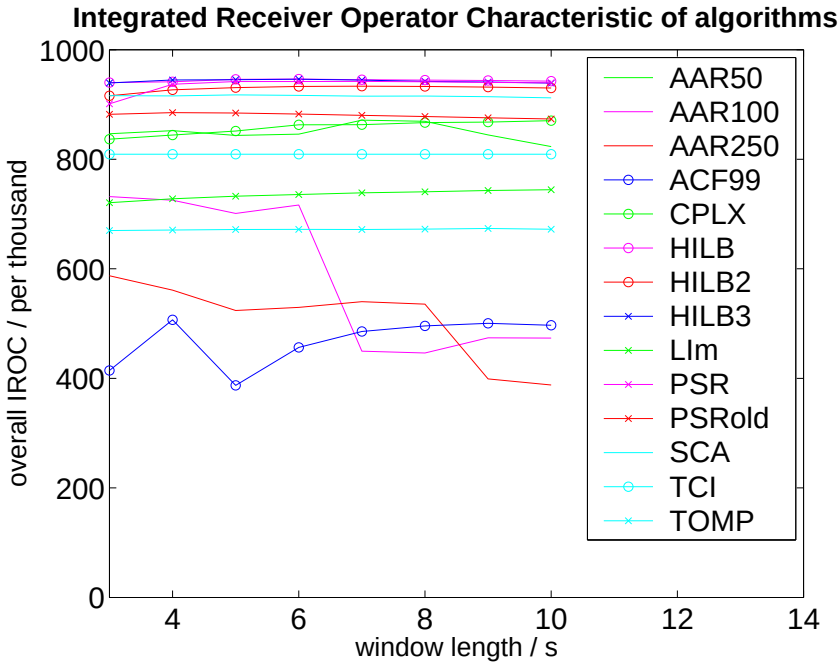

Figure 7.3: *Integrated Receiver Operator Characteristic of different algorithms: IROC in dependence on window length.*

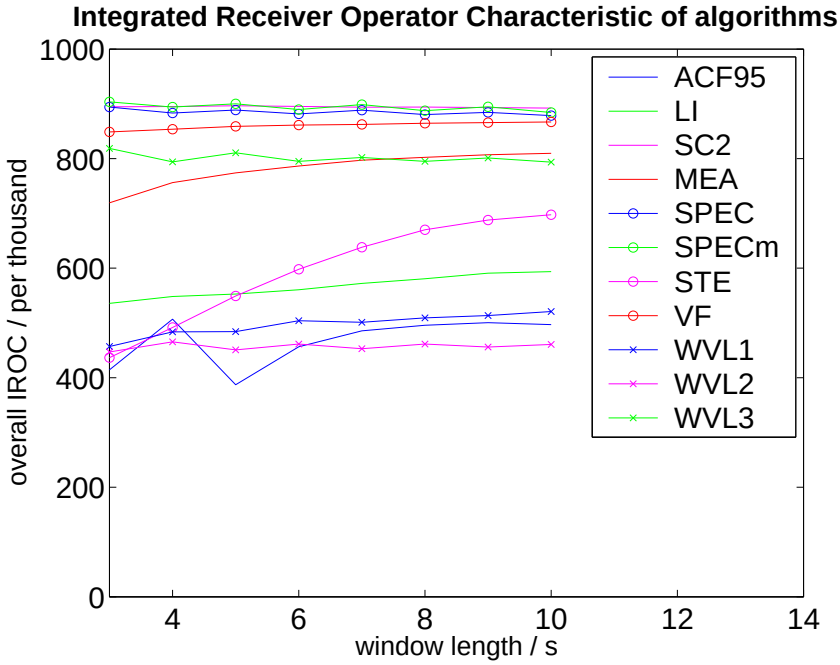

Figure 7.4: *Integrated Receiver Operator Characteristic of different algorithms: IROC in dependence on window length.*

The following figure shows the IROC curves for the algorithms with the best quality results.

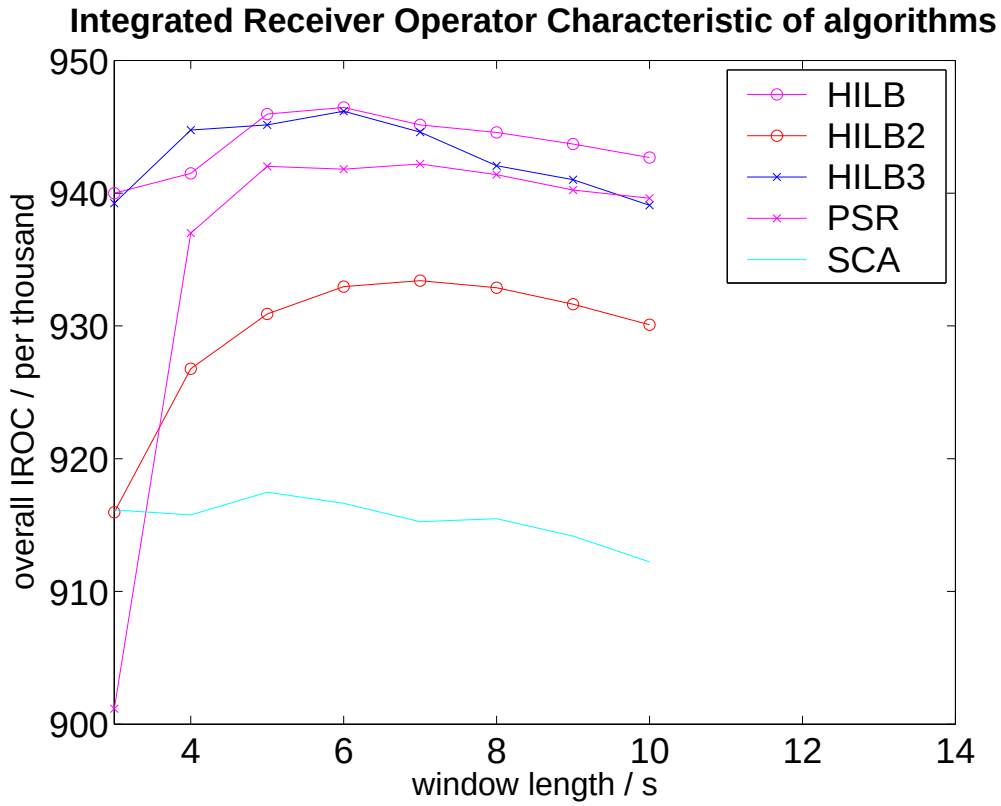

Figure 7.5: *Integrated Receiver Operator Characteristic of different algorithms from Figure 7.3: IROC in dependence on window length. The IROC range is reduced to values from 900 to 950.*

The following two figures show the sensitivity of the algorithms in dependence on the used window length. For clarity two plots are used.

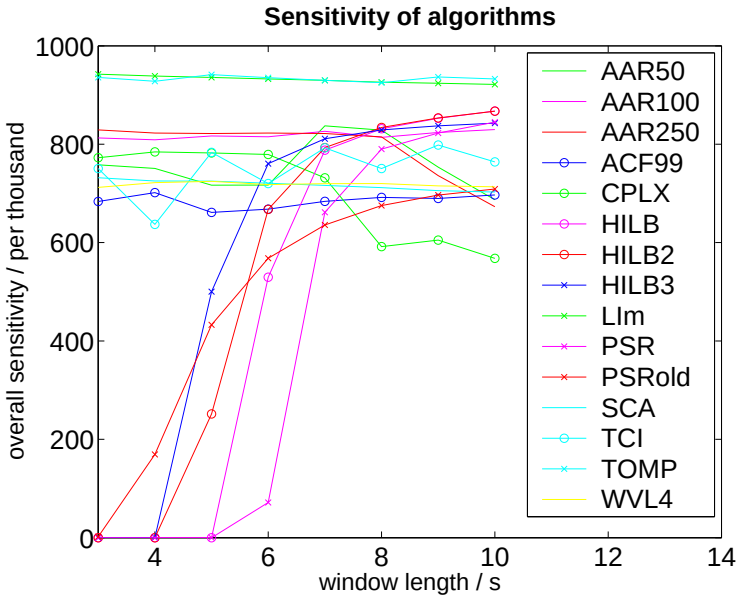

Figure 7.6: *Sensitivity of tested algorithms in dependence of the window length, one second intervals.*

From the Figures 7.6 and 7.7 it is easy to conclude that many algorithms yield good results for a window length of 8 seconds.

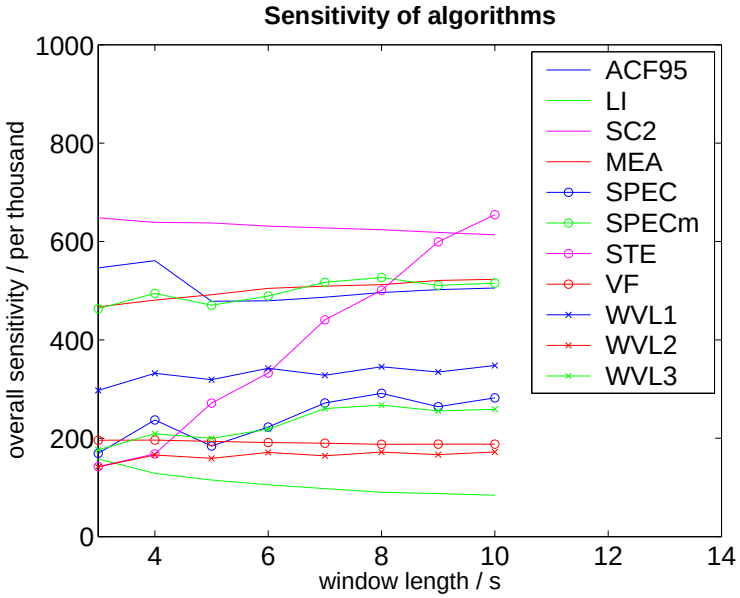

Figure 7.7: *Sensitivity of tested algorithms in dependence of the window length, one second intervals.*

The following two figures show the specificity of the algorithms in dependence on the used window length. For clarity two plots are used.

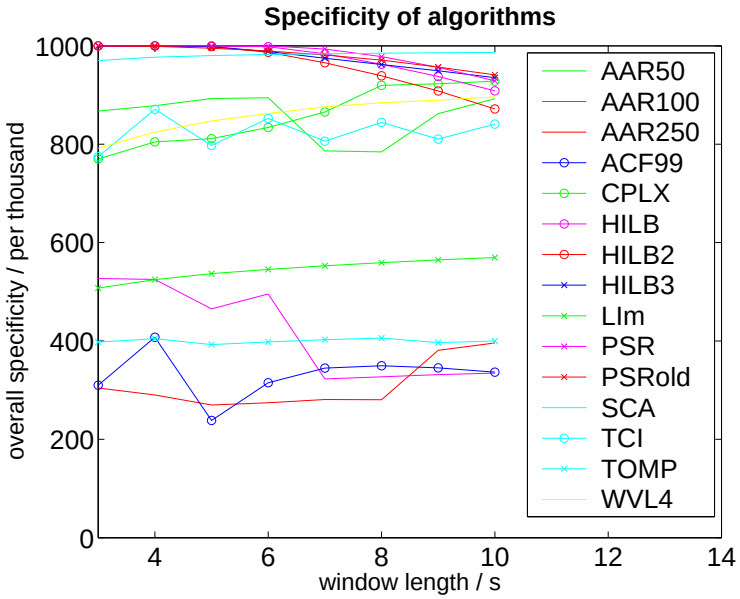

Figure 7.8: *Specificity of tested algorithms in dependence of the window length, one second intervals.*

From the Figures 7.8 and 7.9 it is easy to conclude that many algorithms yield good results for a window length of 8 seconds.

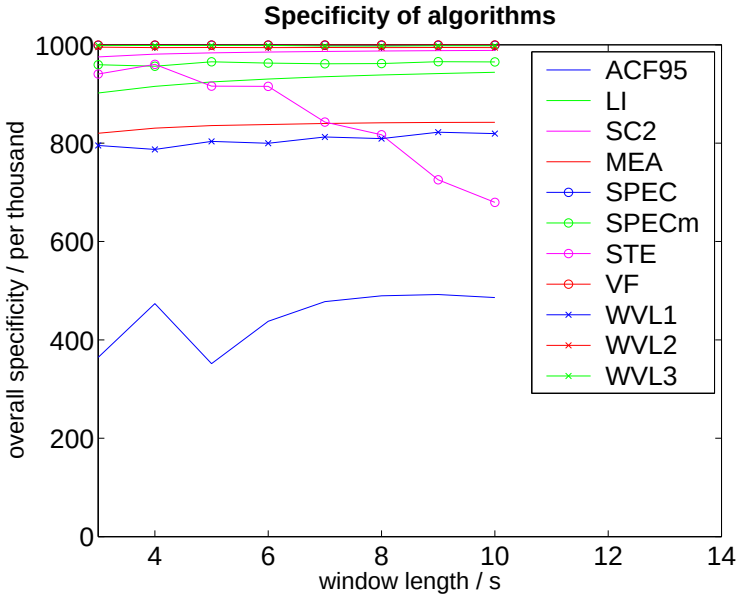

Figure 7.9: *Specificity of tested algorithms in dependence of the window length, one second intervals.*

In the following two figures the range of the specificity is limited in order to achieve a better resolution.

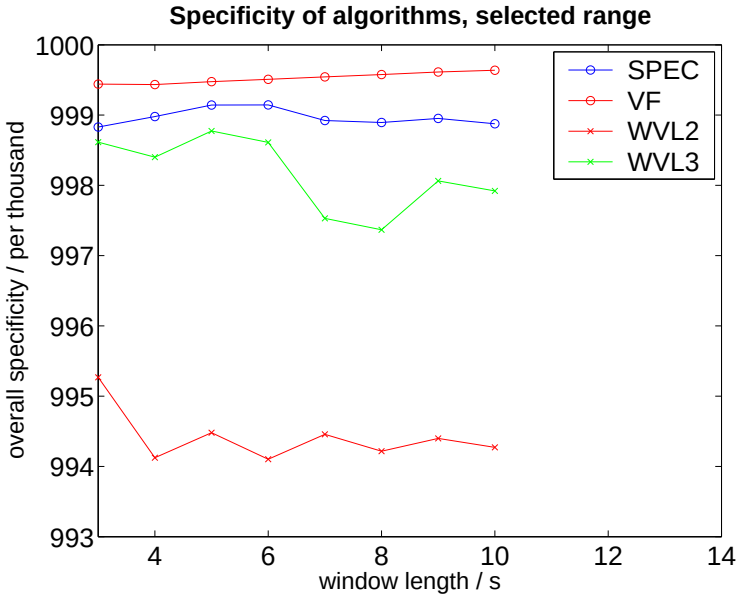

Figure 7.10: *Specificity of some tested algorithms in dependence of the window length, one second intervals. The range of the specificity is reduced to values of 993 to 1000.*

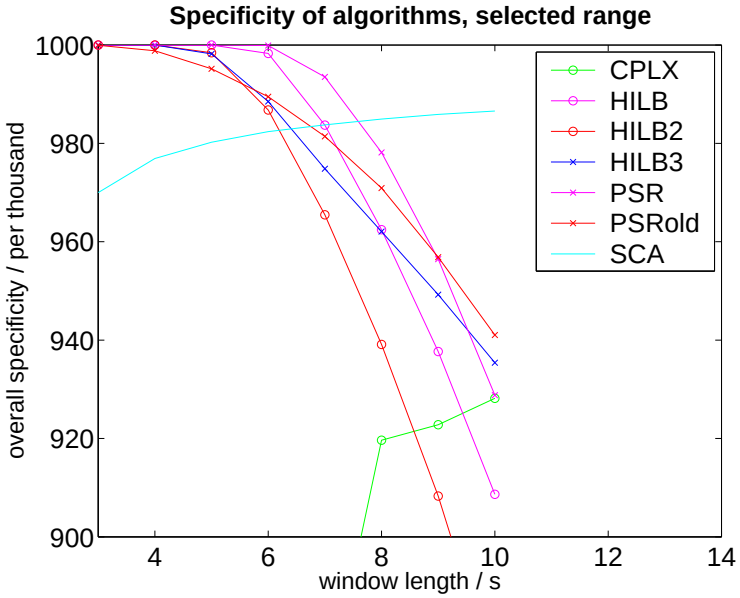

Figure 7.11: *Specificity of some tested algorithms in dependence of the window length, one second intervals. The range of the specificity is reduced to values of 900 to 1000.*

Chapter 8

Discussion

In real applications of AEDs the specificity is more important than the sensitivity, since no one should be defibrillated due to an analysis error. This would bring him into cardiac arrest. Therefore, a low number of false positive decisions should be tried to be achieved, even if this process makes the number of false negative decisions higher.

From our results it can be seen that no algorithm achieves its proclaimed values for the sensitivity or specificity. The main reason for this is the following: Whereas all other researchers made a preselection of signals, in this study it was tried to simulate the situation of a bystander, who is supposed to use an AED, more accurately. Hence, no preselection of signals was carried out.

According to the IROC values, the best algorithms are HILB, PSR, and SCA, which yield values of more than 90 per cent for the IROC value. This algorithms are new. The algorithms SPEC and WVL_3 are very good with respect to their specificities. However, the sensitivities are poor. All other algorithms yield mixed results in our simulations. We also conclude that algorithms developed for QRS detection, like LI and TOMP, are not suitable for VF detection.

Outlook: Up to now, the results were only examined with undisturbed data from the mentioned data banks. No noise or CPR were added. In the future, we plan to use data changed by addition of artifacts like noise from various sources or CPR. A CPR filter will be used to preprocess the data. Using a good CPR filter should result in only little change in quality compared to undisturbed data. The significant parameters that will be compared are again sensitivity, specificity, and IROC. Also, we want to refine and modify the algorithms to improve our results. A future aim is also the creation of a SIMULINK application to offer a very concise utilization for the different functions. Furthermore the automated detection of more subtle arrhythmias like ventricular tachycardia is planned.

Conclusion

In this thesis, sensitivity, specificity, accuracy, positive predictivity and the integrated receiver operator characteristic of different fibrillation detection algorithms are investigated. Some of the algorithms are taken from scientific literature, some are new. Different approaches for analyzing the ECG signals are used including tools like Fourier transformation, Hilbert transformation, Wavelet transformation, as well as tools which do not use a common transformation, like signal comparison, different threshold algorithms, complexity measure or phase space reconstruction. As an important parameter for the implementation in AEDs also the computational time of the algorithms is listed. The quality parameters are calculated by investigating a huge amount of data, namely the entire BIH-MIT and CU data banks, and the files 7001 - 8210 of the AHA data bank ([16], [17], [2]). As an important varying parameter we use the window length in steps of one second from 3 to 10 seconds. This equals a data amount of more than 90 hours of commented ECG data for each algorithm at each window length.

The evaluations demonstrate, that the algorithms yielding the best results are new ones rather than published ones. Especially algorithms using tools from chaos theory, like phase space reconstruction and Hilbert transformation show promising results. We think this is due to the intrinsic character of the heart, consisting of many coupled electrically active cells, that could be modeled by coupled oscillators. Depending on different conditions, this may yield a synchronized regular signal or a chaotic one. Thus this insight of the results of this thesis can be fruitful for further considerations. An advantage is also the relatively low computational effort of this methods.

Further research should be dedicated to the investigation of disturbed ECG data, like electrical signal noise, or, more important, the influences of cardiopulmonary reanimations. Nevertheless, a concise overview of many different fibrillation detection algorithms can be a very useful part in the improvement of automated external defibrillators for bystander defibrillation.

Acknowledgements

First of all, I want to thank my supervisor Karl Unterkofler. It was Prof. Unterkofler's engagement which brought me to the field of life sciences and biophysics. He managed to provide very pleasant working conditions and he was extremely helpful in many different ways. His critical reading and the following discussions proved to be invaluable. Thank you!
Then, I want to thank Anton Amann from the Universitätsklinik für Anästhesie in Innsbruck. His advices concerning detailed questions of cardiology and fibrillation detection helped me many times. His suggestions and ideas for realizing the algorithms sped up the work a lot.
Furthermore, I want to thank Ferdinand Schürrer for distinctly reading and examining the thesis.
Thanks also to Martin Fetz, who made valuable contributions to the implementation of the SPEC algorithm.
I also want to thank the University of applied sciences Vorarlberg (Fachhochschule Vorarlberg) for the financial support.
Finally, I want to thank my family and my friends who supported me in a way only they could do.

Appendix A

Filtering

For all algorithms tested in this work we used the same prefiltering algorithm. First, a moving averaging filter of order 5 is applied to the signal. This removes high frequency noise like interspersions and muscle noise. Then, a drift suppression is applied to the resulting signal. This is done by a high pass filter with a cut off frequency of one Hz. Finally, a low pass Butterworth filter with a limiting frequency of 30 Hz is applied to the signal. In our work, the filtering process is carried out in a MATLAB routine, called *filtering.m*. It uses functions from the "Signal Processing Toolbox". The algorithm *filtering.m* is displayed on the following page:

Function for prefiltering in all algorithms function Y=filtering(X,sfreq,kind);

```
% moving averaging
   b=[.2 .2 .2 .2 .2];
   a=[1];
   switch kind
      case 0
         X=X;
      case 1
         X=filter(b,a,X);
      case 2
         X=filtfilt(b,a,X);
   end;
 % drift suppression
   T=1/sfreq;              % sampling peroid [s]
   Fc=1;                   % cut-off [Hz]
   c1=1/[1+tan(Fc*pi*T)];
   c2=[1-tan(Fc*pi*T)]/[1+tan(Fc*pi*T)];
   b=[c1 -c1]; a=[1 -c2];
   switch kind
      case 0
         X=X;
      case 1
         X=filter(b,a,X);
      case 2
         X=filtfilt(b,a,X);
   end;
% Butterworth filtration
% mb order; 30 Hz lowpass;
   fh=sfreq/2;                % 1/2 sampling rate
   mb=2;                      % order of filter
   [b,a]= butter(mb,30/fh);   % 30Hz - cut-off frequency
   switch kind
      case 0
         X=X;
      case 1
         X=filter(b,a,X);
      case 2
         X=filtfilt(b,a,X);
   end;
   Y=X;
```

Bibliography

[1] P. S. Addison, *The Illustrated Wavelet Transform Handbook*, IOP Publishing Ltd, 2002.

[2] American Heart Association, AHA database: http://www.americanheart.org/

[3] S. Barro, R. Ruiz, D. Cabello, and J. Mira, *Algorithmic sequential decision-making in the frequency domain for life threatening ventricular arrhythmias and imitative artifacts: a diagnostic system*, Journ. Biomed. Eng. **11**, 320–328 (1989).

[4] S. Chen, N. V. Thakor, and M. M. Mower, *Ventricular fibrillation detection by a regression test on the autocorrelation function*, Medical & Biological Engineering & Computing, **25**, 241–249 (1987).

[5] R. H. Clayton, A. Murray, and R. W. F. Campbell, *Changes in the surface ECG frequency spectrum during the onset of ventricular fibrillation*, Proc. Computers in Cardiology 1990 (Los Alamitos, CA: IEEE Computer Society Press), pp. 515–518 (1991).

[6] R. H. Clayton, A. Murray, and R. W. F. Campbell, *Comparison of four techniques for recognition of ventricular fibrillation from the surface ECG*, Medical & Biological Engineering & Computing, **31**, 111–117 (1993).

[7] Cook-Sup So, *Praktische EKG-Deutung*, Thieme, Stuttgart, 2001.

[8] D. Ge, N. Srinivasan, and S. M. Krishnan, *Cardiac arrhythmia classification using autoregressive modeling*, BioMedical Engineering OnLine, http://www.biomedical-engineering-online.com/content/1/1/5 (2002).

[9] P. S. Hamilton and W. J. Tompkins, *Quantitative investigation of QRS detection rules using the MIT/BIH arrhythmia database*, IEEE Trans. Biomed. Eng., **BME-33**, pp. 1157–1187 (1986).

[10] I. Jekova, *Comparison of five algorithms for the detection of ventricular fibrillation from the surface ECG*, Physiol. Meas. **21**, 429–439 (2000).

[11] R. E. Kerber, L. B. Becker, J. D. Bourland, R. O. Cummins, A. P. Hallstrom, M. B. Michos, G. Nichol, J. P. Ornato, W. H. Thies, R. D. White,

and B. D. Zuckerman, *Automated External Defibrillators for Public Access Defibrillation: Recommendations for Specifying and Reporting Arrhythmia Analysis Algorithm Performance, Incorporating New Waveforms, and Enhancing Safety : A Statement for Health Professionals From the American Heart Association Task Force on Automated External Defibrillation, Subcommittee on AED Safety and Efficacy*, American Heart Association, Circulation **95**, 1677-1682 (1997).

[12] S. Kuo and R. Dillman, *Computer Detection of Ventricular Fibrillation*, Computers in Cardiology, IEEE Computer Society, 347–349 (1978).

[13] A. Lempel and J. Ziv, *On the complexity of finite sequences*, IEEE Trans. Inform. Theory **IT-22**, 75–81 (1976).

[14] C. Li, C. Zheng, and C. Tai, *Detection of ECG Characteristic Points Using Wavelet Transforms*, IEEE Trans. Biomed. Eng., **42**, 21–28 (1995).

[15] A. K. Louis, P. Maaß, and A. Rieder, *Wavelets*, Teubner, Stuttgart, 1998.

[16] Massachusetts Institute of Technology, MIT-BIH ECG database: http://www.physionet.org/physiobank/database/mitdb/

[17] Massachusetts Institute of Technology, CU database: http://www.physionet.org/physiobank/database/cudb/

[18] A. Murray, R. W. F. Campbell, and D. G. Julian, *Characteristics of the ventricular fibrillation waveform*, Proc. Computers in Cardiology 1985 (Washington, DC: IEEE Computer Society Press), pp. 275–278 (1985).

[19] A. V. Oppenheim, R. W. Schafer, and J. R. Buck, *Discrete-Time Signal Processing*, Pearson Education, 1999.

[20] J. Pan and W. J. Tompkins, *A Real-Time QRS Detection Algorithm*, IEEE Trans. Biomed. Eng., **BME-32**, 230–236 (1985).

[21] N. V. Thakor, Y. S. Zhu, and K. Y. Pan, *Ventricular Tachycardia and Fibrillation Detection by a Sequential Hypothesis Testing Algorithm*, IEEE Trans. Biomed. Eng., **37**, 837–843 (1990).

[22] Y. Yamanouchi, J. E. Brewer, A. M. Donohoo, K. A. Mowrey, B. L. Wilkoff, and P. J. Tchou, *External exponential biphasic versus monophasic shock waveform: Efficacy in ventricular fibrillation of longer duration*, Pacing and Clinical Electrophysiology (PACE), **22**, 1481–1487 (1999).

[23] X. S. Zhang, Y. S. Zhu, N. V. Thakor, and Z. Z. Wang, *Detecting Ventricular Tachycardia and Fibrillation by Complexity Measure*, IEEE Trans. Biomed. Eng., **46**, 548–555 (1999).